5-1-2015

Studies of Flerovium and Element 115 Homologs with Macrocyclic Extractants

John Dustin Despotopulos
University of Nevada, Las Vegas, despotopulos1@llnl.gov

INVESTIGATION OF FLEROVIUM AND ELEMENT 115 HOMOLOGS

WITH MACROCYCLIC EXTRACTANTS

By

John Dustin Despotopulos

Bachelor of Science in Chemistry
University of Oregon
2010

A dissertation submitted in partial fulfillment
of the requirements for the

Doctor of Philosophy -- Radiochemistry

Department of Chemistry
College of Sciences
The Graduate College

University of Nevada, Las Vegas
May 2015

UNLV | GRADUATE COLLEGE

We recommend the dissertation prepared under our supervision by

John Dustin Despotopulos

entitled

Studies of Flerovium and Element 115 Homologs with Macrocyclic Extractants

is approved in partial fulfillment of the requirements for the degree of

Doctor of Philosophy - Radiochemistry

Department of Chemistry and Biochemistry

Ralf Sudowe, Ph.D., Committee Chair

Dawn A. Shaughnessy, Ph.D., Committee Member

Ken Czerwinski, Ph.D., Committee Member

Gary Cerefice, Ph.D., Committee Member

Steen Madsen, Ph.D., Graduate College Representative

Kathryn Hausbeck Korgan, Ph.D., Interim Dean of the Graduate College

May 2015

ABSTRACT

Investigation of Flerovium and Element 115 Homologs with Macrocyclic Extractants

By

John D. Despotopulos

Dr. Ralf Sudowe, Examination Committee Chair
Associate Professor of Health Physics and Radiochemistry
University of Nevada, Las Vegas

Study of the chemistry of the heaviest elements, Z ≥ 104, poses a unique challenge due to their low production cross-sections and short half-lives. Chemistry also must be studied on the one-atom-at-a-time scale, requiring automated, fast, and very efficient chemical schemes. Recent studies of the chemical behavior of copernicium (Cn, element 112) and flerovium (Fl, element 114) together with the discovery of isotopes of these elements with half-lives suitable for chemical studies have spurred a renewed interest in the development of rapid systems designed to study the chemical properties of elements with Z ≥ 114. This dissertation explores both extraction chromatography and solvent extraction as methods for development of a rapid chemical separation scheme for the homologs of flerovium (Pb, Sn, Hg) and element 115 (Bi, Sb), with the goal of developing a chemical scheme that, in the future, can be applied to on-line chemistry of both Fl and element 115. Macrocyclic extractants, specifically crown ethers and their derivatives, were chosen for these studies.

Carrier-free radionuclides, used in these studies, of the homologs of Fl and element 115 were obtained by proton activation of high purity metal foils at the Lawrence Livermore National Laboratory (LLNL) Center for Accelerator Mass Spectrometry (CAMS): $^{nat}In(p,n)^{113}Sn$, $^{nat}Sn(p,n)^{124}Sb$, and $Au(p,n)^{197m,g}Hg$. The carrier-free activity was separated from the foils by novel separation schemes based on ion exchange and extraction chromatography techniques.

Carrier-free Pb and Bi isotopes were obtained from development of a novel generator based on cation exchange chromatography using the ^{232}U parent to generate ^{212}Pb and ^{212}Bi.

Crown ethers show high selectivity for metal ions based on their size compared to the negatively charged cavity of the ether. Extraction by crown ethers occur based on electrostatic ion-dipole interactions between the negatively charged ring atoms (oxygen, sulfur, etc.) and the positively charged metal cations. Extraction chromatography resins produced by Eichrom Technologies, specifically the Pb resin based on di-t-byutlcyclohexano-18-crown-6, were chosen as a starting point for these studies. Simple chemical systems based solely on HCl matrices were explored to determine the extent of extraction for Pb, Sn and Hg on the resin. The kinetics and mechanism of extraction were also explored to determine suitability for a Fl chemical experiment. Systems based on KI/HCl and KI/HNO_3 were explored for Bi and Sb. In both cases suitable separations, with high separation factors, were performed with vacuum flow columns containing the Pb-resin. Unfortunately the kinetics of uptake for Hg are far too slow on the traditional crown-ether to perform a Fl experiment and obtain whether or not Fl has true Hg-like character or not. However, the kinetics of Pb and Sn are more than sufficient for a Fl experiment to differentiate between Pb- or Sn-like character. To assess this kinetic issue a novel macrocyclic extractant based on sulfur donors was synthesized.

Hexathia-18-crown-6, the sulfur analog of 18-crown-6, was synthesized based with by a template reaction using high dilution techniques. The replacement of oxygen ring atoms with sulfur should give the extractant a softer character, which should allow for far greater affinity toward soft metals such as Hg and Pb. From HCl matrices hexathia-18-crown-6 showed far greater kinetics and affinity for Hg than the Pb-resin; however, no affinity for Pb or Sn was seen. This presumably is due to the fact the charge density of sulfur crown ethers does not point to the center of the ring, and future synthesis of a substituted sulfur crown ether which forces the

charge density to mimic that of the traditional crown ether should enable extraction of Pb and Sn to a greater extent than with the Pb-resin. Initial studies show promise for the separation of Bi and Sb from HCl matrices using hexathia-18-crown-6.

Other macrocyclic extractants, including 2,2,2-cryptand, calix[6]arene and tetrathia-12-crown-4, were also investigated for comparison to the crown ethers. It was noted that these extractants are inferior compared to the crown and thiacrown ethers for extraction of Fl and element 115 homologs. A potential chemical system for Fl was established based on the Eichrom Pb resin, and insight to an improved system based on thiacrown ethers is presented.

ACKNOWLEDGEMENTS

The work presented in this dissertation would not have been possible without the help and encouragement of many people. I would like to thank my graduate advisor Dr. Ralf Sudowe for his support and giving me the opportunity to work on this project. Im very appreciative of my technical advisor at LLNL, Dr. Dawn Shaughnessy, for allowing me to spend my time at LLNL performing the research, and for continued guidance support throughout the process. I would also like to thank the remaining members of my dissertation committee: Dr. Ken Czerwinski, Dr. Gary Cerefice and Dr. Steen Madsen. For his help with synthesizing the Hexathia-18-crown-6 extractant, I would like to thank William Kerlin, it would not have been possible without his help. For her help with characterizing the potential impurities in the hexathia-18-crown-6 extractant, I would like to thank Dr. Carolyn Koester. I would like to thank Kelly Kmak and Dr. Narek Gharyban for their assistance with various experiments. I would like to thank Dr. Scott Tumey and Dr. Tom Brown for their assistance with production of carrier-free radionuclides at the LLNL CAMS facility. Finally, I need to thank the rest of the LLNL heavy element group: Dr. Roger Henderson, Dr. Kenneth Moody, Dr. Patrick Grant and Dr. Julie Gostic for their support and discussions throughout this process. Thank you all.

Academic Disclaimer

The author wrote this dissertation in support of requirements for the degree Doctor of Philosophy in Radiochemistry at the University of Nevada, Las Vegas. The research is funded in part by the LLNL Graduate Scholars Program, and is not a deliverable for any United States government agency. The views and opinions expressed are those of the author, and do not state or reflect those of the United States government or Lawrence Livermore National Security, LLC.

Lawrence Livermore National Laboratory Disclaimer

Neither the United States government nor Lawrence Livermore National Security, LLC, nor any of their employees makes any warranty, expressed or implied, or assumes any legal liability or responsibility for the accuracy, completeness, or usefulness of any information, apparatus, product, or process disclosed, or represents that its use would not infringe privately owned rights. Reference herein to any specific commercial product, process, or service by trade name,

trademark, manufacturer, or otherwise does not necessarily constitute or imply its endorsement, recommendation, or favoring by the United States government or Lawrence Livermore National Security, LLC, and shall not be used for advertising or product endorsement purposes.

Lawrence Livermore National Laboratory Funding Auspice Statement

This work was performed under the auspices of the U.S. Department of Energy by Lawrence Livermore National Laboratory under Contract DE-AC52-07NA27344. This work was funded by the Laboratory Directed Research and Development Program at LLNL under project tracking code 11-ERD-011.

TABLE OF CONTENTS

LIST OF FIGURES

LIST OF TABLES

LIST OF EQUATIONS

CHAPTER 1: INTRODUCTION

The experimental investigation of the transactinide elements (Z > 103) are important tasks for both physicists and chemists. For physicists the experimental investigation offers insights to nuclear structure at the extreme edges of stability with respect to high Z nuclei. Chemists, on the other hand, can test the influence of high nuclear charge, specifically relativistic effects, on the chemical properties of the transactinides and consequently evaluate the validity of Mendeleev's theory of the periodic table. The periodic table, introduced in 1896 by Dimitri Mendeleev, arranges the chemical elements into periodic groups based on their chemical properties, providing a useful tool in predicting the chemical behavior of a given element. Experiments with the transactinides are a challenging endeavor, due to production rates as low as a single atom created per hour, day, month, or potentially even longer, and lifetimes ranging from fractions of seconds to minutes at most [1].

All elements heavier than U (Z = 92) do not occur in nature (except for trace amounts of Np and Pu in U ores formed through neutron interactions with ^{238}U as well as ultratrace amounts of ^{244}Pu), due to their half-lives being short compared to the age of the earth [2,3]. In 1932, with the discovery of the neutron by James Chadwick, new experiments began to be performed using neutrons that led to the eventual discovery of transuranic elements [4]

Enrico Fermi and Emilio Sergé were believed to have been the first to produce transuranic elements, in 1934, through neutron capture on uranium followed by β^- decay; however, they never actually characterized the new elements [5]. In 1940, Edwin McMillan *et al.* discovered ^{239}Np, the first transuranic element, by neutron bombardment of ^{238}U [6]:

$$^{238}_{92}U + n \rightarrow {}^{239}_{92}U \rightarrow {}^{239}_{93}Np + \beta^- + \bar{\nu}$$

Glenn T. Seaborg *et al.* discovered plutonium by deuteron bombardment of ^{238}U, at the University of California Berkeley's 60 inch cyclotron in 1940 [7]:

$$^{238}_{92}U + {}^{2}_{1}H \rightarrow {}^{238}_{93}Np + 2n \rightarrow {}^{238}_{94}Pu + \beta^{-} + \bar{\nu}$$

In the 1940s, ^{242}Am and ^{242}Cm were also discovered by Glenn T. Seaborg *et al.* during the Manhattan Project [8]. Seaborg introduced the actinide concept, placing the elements thorium through (not yet discovered) lawrencium in a special series within the periodic table, similar to the lanthanide series [8]. This indicated that these elements should have similar chemical behavior to each other, and led to the discovery of berkelium (Bk) and californium (Cf) through the bombardment of actinide targets with deuterons, between 1949 and 1950 [9,10]. The elements fermium (Fm) and einsteinium (Es) were discovered in the debris from the "MIKE" thermonuclear test, in 1952 [11]. The remaining three members of the actinide series, mendelevium (Md), nobelium (Nb), and lawrencium (Lr) were discovered by atom-at-a-time production methods between 1955 and 1961 [12-14]. Elements up to Fm can be produced step-wise by neutron capture followed by β^- decay in high neutron flux reactors [15]. Production of elements beyond Fm by this method encounter problems of low production rates, short half-lives, and high probability for spontaneous fission. Thus, the neutron production rate of Fm and the elements beyond is too low to create quantities large enough for target preparation, and the step-wise approach with neutron and deuteron bombardment followed by β^- decay up the periodic table ceases.

Since 1940, the periodic table has been extended to reflect the discovery of elements with atomic numbers as high as 118, Figure 1. The transactinides begin with element 104, rutherfordium (Rf), a new transition metal element.

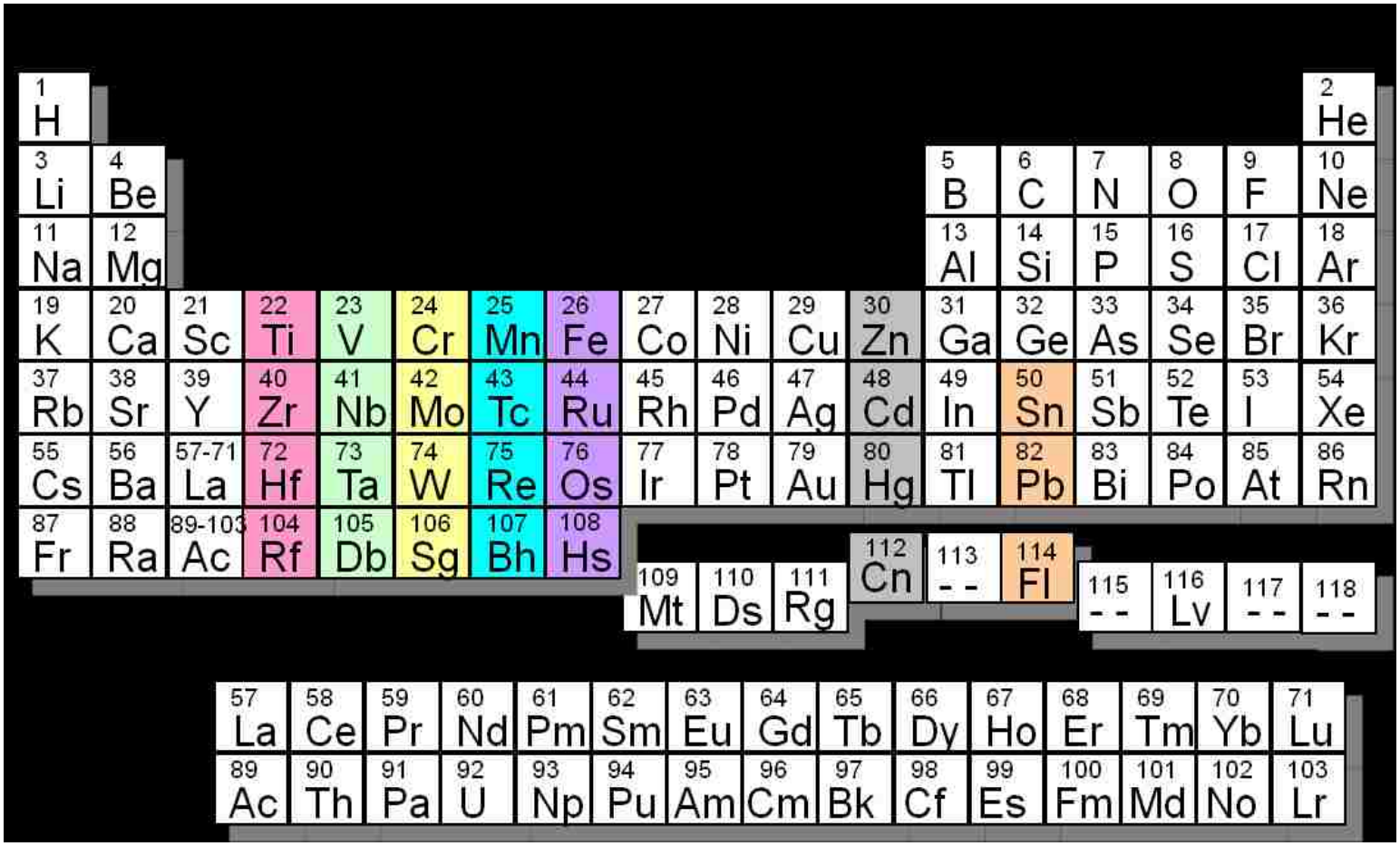

Figure 1. The modern periodic table. Elements with no experimentally known chemical properties are separated from the body of the periodic table. First attempts to characterize elements Cn, 113 and Fl have been reported.

The credit for discovery of the first two transactinides, Rf and dubnium (Db) are shared by groups at the Joint Institute for Nuclear Research (JINR) in Dubna, Russia and the group at the Berkeley Heavy Ion Linear Accelerator (HILAC) in Berkeley, California [16]. Rutherfordium was produced via the following reactions [17,18]:

$^{242}Pu + {}^{22}Ne \rightarrow {}^{260}Rf + 4n$; (Dubna, G. N. Flerov *et al.*)

$^{249}Cf + {}^{12}C \rightarrow {}^{257}Rf + 4n$; (Berkeley, A. Ghiorso *et al.*)

Dubnium was produced via the following reactions [19,20]:

$^{243}Am + {}^{22}Ne \rightarrow {}^{260}Db\ ({}^{261}Db) + 5n(4n)$; (Dubna, G. N. Flerov *et al.*)

$^{249}Cf + {}^{15}N \rightarrow {}^{260}Db + 4n$; (Berkeley, A. Ghiorso *et al.*)

In addition to Rf and Db, elements 106 to 112, 114 and 116 have been recognized by the International Union of Pure and Applied Chemistry (IUPAC) and have been named: seaborgium (Sg), bhorium (Bh), hassium (Hs), meitnerium (Mt), darmstadtium (Ds), roentgenium (Rn), copernicium (Cn), flerovium (Fl), and livermorium (Lv) [21-29]. Claims for the discovery of element 113 have been brought forward by a Japanese group and a joint American-Russian collaboration [30,31]. Claims for the discovery of elements 115, 117, and 118 have been brought forward by a join American-Russian collaboration and are awaiting confirmation [30,32-34].

1.1 Stability of the transactinides

When Meyers and Swiatecki attempted to calculate masses of nuclei from a combination of a macroscopic liquid-drop model with superimposed microscopic quantal shell corrections in 1966, they indicated that superheavy nuclei might exist far beyond the upper end of the current chart of the nuclides and owe their existence solely to shell effects [35]. Similarly to electron orbitals, the nuclear shell model describes the nucleus by placing protons and neutrons into nuclear shells. Magic numbers refer to a closed nuclear shell and occur at proton and neutron numbers of 2, 8, 20, 28, 50, and 82 and neutron number 124. At these proton and

neutron numbers the nuclei have higher binding energies per nucleon and thus greater stability against radioactive decay than nuclei with only partially filled nuclear shells. When a nucleus contains both a magic number of protons and neutrons it is referred to as doubly magic. The heaviest stable spherical nuclei, which has both a closed proton and neutron shell is ^{208}Pb (Z = 82, N = 126). Meldner predicted the next closed proton shells after Z = 82 to be at Z = 114, 164 and 182 and the next closed neutron shell after N = 126 at N = 184, and 196 therefore, the next heavier doubly-magic nucleus after ^{208}Pb was predicted to be ^{298}Fl [36,37].

Shell effects do not have a strong influence on α-decay half-lives, whereas fission half-lives are influenced to a much larger extent [38]. The calculated longest-lived heavy nucleus is ^{294}Ds with a predicted half-life of about 10^8y [38]. These predictions encouraged the search for superheavy elements (SHE) and for the investigation of their chemical properties. As a result of these calculations the idea of an unknown "island of stability" was introduced into the nuclear landscape. Experimental attempts to reach the island of stability have so far proven to be unsuccessful; however, the believed edge of the island of stability has been reached [28,33,34,39]. More recent calculations garner no agreement between theorists on the location of the next spherical shell closure [40]. The next shell closures are predicted to be in the region of Z = 114-126 and N=172 or 184 [41-45].

Calculations by Patyk *et al.* on nuclear masses at high deformation showed that nuclei were able to minimize their ground-state energy by accessing high order deformations. This led to the prediction that nuclei in the region Z = 108 and N = 162 should be relatively stable, and that ^{270}Hs would be a strongly bound deformed doubly-magic nuclide with α-particle emission half-life of about 0.1 s [46,47]. Recent calculations point to even longer half-lives, on the order of seconds. As a result the spherical superheavies on the island of stability were believed to be connected to the region near uranium by a "rock of stability" around ^{270}Hs, Figure 2.

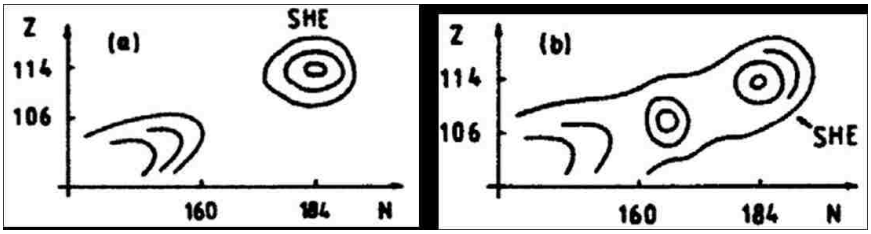

Figure 2. Schematic showing the regions of long-lived nuclei, as believed originally (a) and currently (b) [46].

Experimentally this was shown by the relatively long-lived nuclei ^{265,262,271}Sg, and further confirmed by the discovery of ^{267}Bh, and ^{269}Hs all having half-lives of seconds [27,48-51].

1.2 Production of the transactinides

Elements beyond Fm (Z > 100) can only be created synthetically by nuclear fusion reactions using heavy ions in accelerators [52]. In a heavy ion fusion reaction a heavy element target is bombarded with accelerator produced heavy ions. Most often, when a projectile hits a target only part of the constituents are exchanged in a so-called transfer reaction. The complete fusion of the two nuclei to produce a compound nucleus (CN) occurs with very low probability. For elements produced one atom-at-a-time (Z > 100) a ~0.8 mg/cm^2 target, typically an actinide, on a thin, ~2 μm thick, Ti backing is used to allow for compound nuclei to recoil out of the target to detection systems. Targets are typically bombarded with 3 x 10^{12} ions per second. A target and beam combination like this will yield transactinide production rates on the order of a few atoms per minute for Rf and Db to an atom a week or lower for the heavier transactinides [4,15,37].

Nuclear reactions have cross sections (σ) measured in barns (b), 1 b = 10^{-24} cm^2. An average nucleus has a radius on the order of 6 x 10^{-13} cm, yielding a geometric cross section (πr^2) of about 10^{-24} cm^2. The primary synthesis routes for transactinides can be assigned to either hot

or cold fusion, discussed below. Cross sections for the hot fusion production of transactinides range from about 10 nb to 1 pb, whereas production cross-sections for cold fusion reactions can be as low as 27 fb [31].

Nuclear reactions where the excitation energies of the CN at the fusion or Bass barrier is less than ~20 MeV is often referred to as cold fusion, and only one or two neutrons evaporate [53, 54]. These excitation energies occur when a spherical target nuclei, such as ^{209}Bi or ^{208}Pb, is bombarded by a medium-heavy projectile, such as ^{58}Fe or ^{62,64}Ni. These types of nuclear reactions helped lead to the discovery of elements 107-112 at the GSI [22-27,51,55]; however, due to the neutron-deficiency of these nuclei, they often have very short half-lives. There is, therefore, a serious disadvantage for performing chemical studies on nuclei produced via the cold fusion method [37].

A nuclear reaction resulting in 40-50 MeV excitation energies are considered hot fusion reactions. These reactions occur when an actinide target is bombarded by a lighter projectile, such as ^{22}Ne or ^{18}O. Hot fusion reactions often de-excite through the evaporation of 4 to 5 neutrons from the CN. Due to the neutron richness of the actinide targets, these reactions yield neutron rich and longer-lived transactinides [37].

More recently, experiments using a ^{48}Ca projectile on actinide targets have been explored. These experiments show evidence for longer-lived nuclides of elements 112-118 and their decay daughters [1,28,29,30,32,33,34,39], Figure 3. A surprising note is the relatively high reaction cross sections for these reactions, on the order of a few picobarns, which yield production rates of around one atom per day. Reasons for this phenomena are thought to be rooted in the doubly magic nature of ^{48}Ca: the ^{48}Ca nucleus has cold fusion-like properties and will lower the probability of spontaneous fission yet the target and projectile together have a hot fusion-like configuration which increase the probability of fusion [37].

Figure 3. Current chat of the nuclides populated by 48Ca +actinide target reaction products.

1.2.1 Element 114, Flerovium

For 38 days from November to December 1998, a total of 5.2 x 10^{18} $^{48}Ca^{5+}$ ions were accelerated onto a $^{244}PuO_2$ target (nine target segments in the shape of an arc, with a $^{244}PuO_2$ thickness of 0.37 mg/cm^2 on 3.5 cm^2 1.5 µm Ti foils, were mounted on a disk), by a joint JINR and LLNL collaboration at the Dubna U400 heavy ion cyclotron, leading to the discovery of element 114 [28]. The ^{48}Ca beam was incident on the ^{244}Pu target at 236 MeV giving a calculated excitation energy of the CN of about 30 MeV, which corresponded to the calculated maximum 3n-evaporation channel to form $^{289}114$. One decay chain, correlated in both time and position, consisting of an evaporation residue (EVR), α_1, α_2, α_3, spontaneous fission (SF) event, Figure 4, was observed in the reaction [28]:

$$^{244}Pu + {}^{48}Ca \rightarrow {}^{289}114 + 3n$$

The cross section for this reaction corresponded to approximately 1 pb.

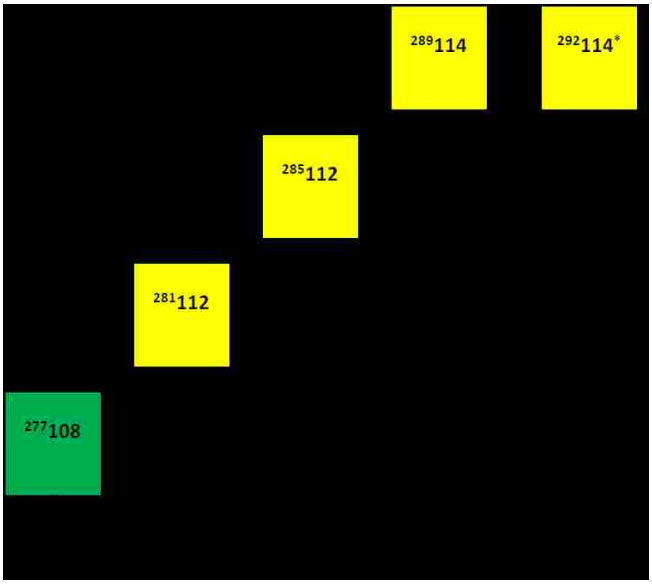

Figure 4. Observed decay chain for initial identification of element 114 [28].

The lifetimes of the decay daughters, new isotopes ^{277}112 and ^{273}110, are approximately 10^6 times longer than previously discovered isotopes [25,27]. This indicates the first experimental proof of a region of enhanced stability of superheavy elements. The same experiment was repeated in June to October 1999. The ^{292}114 CN in this experiment was estimated to have excitation energy in the 31.5-39 MeV range, corresponding to the 3n to 4n evaporation channels. Two identical decay chains, consisting of an EVR, α_1, α_2, and SF event, correlated in time and position were observed, Figure 5 [56].

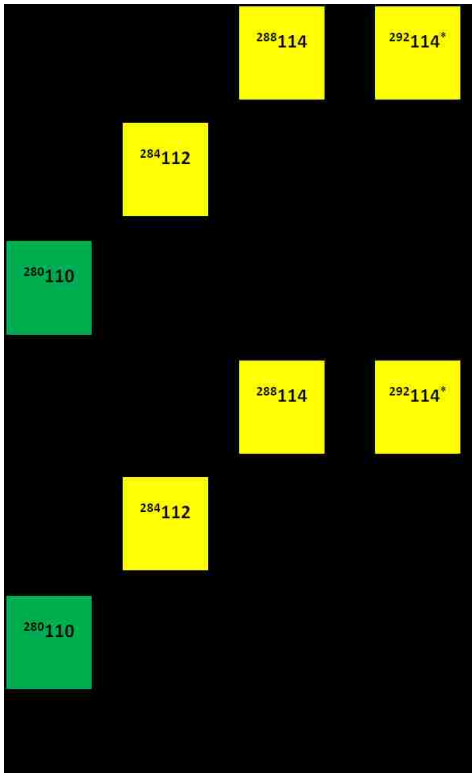

Figure 5. Two identical ^{288}114 decay chains observed in second irradiation of ^{244}Pu target [56].

The production of element 114 was independently verified by scientists at Lawrence Berkeley National Laboratory's (LBNL) 88-inch cyclotron. The LBNL ECR source produced $^{48}Ca^{11+}$ ions which were accelerated to 263 MeV onto a 9.5 cm diameter target wheel containing four

segments with 440, 340, 320, and 270 μg cm^{-1} $^{242}PuO_2$ on 2.4 μm thick Ti. Two decay chains correlated in time and position were observed. One decay chain was associated with ^{286}114 and the other ^{287}114 (3 and 4n channels), Table 1 [57].

Table 1. Events observed by LBNL group.

Interpretation	E (MeV)	Δt (s)	Position (mm)	Bρ (Tm)	σ (pb)
EVR-strip 14	11.55	--	13.0(2)	2.28	$1.4^{+3.2}_{-1.2}$
^{286}114 α decay	10.23(4)	0.3009	12.9(3)	--	
^{282}112 SF	214.5	0.0036	13.1(15)	--	
EVR-strip 7	7.73	--	-2.8(4)	2.25	$1.4^{+3.2}_{-1.2}$
^{287}114 α decay	3.86(4)[a]	0.8149	-3.3(7)	--	
^{283}112 α decay	9.65(10)[b]	1.9208	10.1(64)	--	
^{279}110 SF	176	0.1854	-2.9(15)	--	

[a]Escape α particle depositing only partial energy.
[b]Reconstructed from 382 keV in focal plane and 9271 keV in upstream detector.

The LBNL group synthesized ^{285}114 through the reaction ^{244}Pu(^{48}Ca,5n)^{285}114, with a cross section of $0.6^{+0.9}_{-0.5}$ pb. The decay chain observed: ^{281}Cn, ^{277}Ds, ^{273}Hs, and ^{269}Sg, followed by ^{265}Rf SF, all consisted of new isotopes [58]. Oganessian *et al.* measured the excitation functions for the reaction ^{244}Pu(^{48}Ca,xn)$^{292-n}$114 where n = 3-5 to be σ_{3n} = 2 pb σ_{4n} = 5 pb, and σ_{5n} = 1 pb [59].

1.2.2 Element 115

From July 14 to August 10, 2003 the Dubna U400 heavy ion cyclotron bombarded a $^{243}AmO_2$ target (same design as the $^{244}PuO_2$ target used for element 114 discovery mentioned in section 1.2.1 above) with 4.3 x 10^{18} ^{48}Ca ions at both 248 MeV and 253 MeV. These energies corresponded to a ^{191}115 CN with excitation energies 38.0-42.3 MeV and 42.4-46.5 MeV, corresponding to the 3n and 4n evaporation channels, respectively [30]. Three similar decay chains with five consecutive α-decays followed by a spontaneous fission event were observed at the lower beam energy. At the higher beam energy, one decay with four consecutive α-decays

followed by a spontaneous fission event was observed. Figure 6 summarizes the decay chains observed [30].

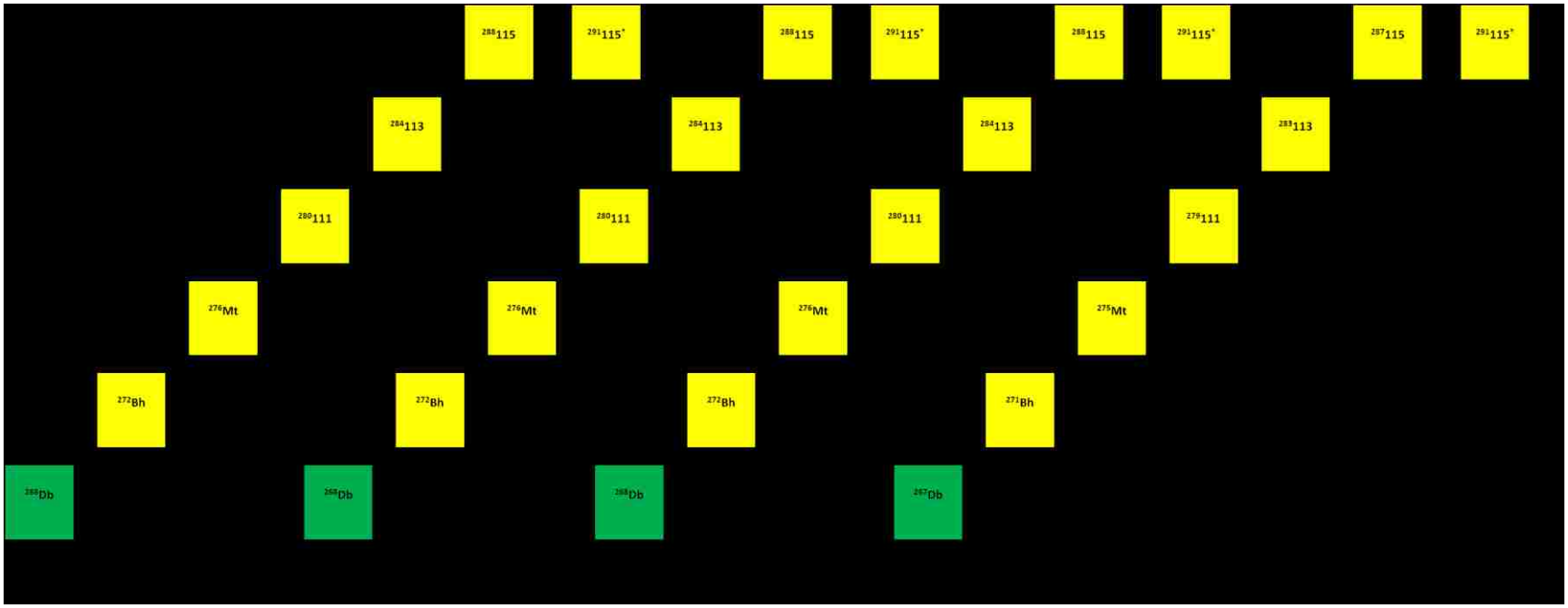

Figure 6. Observed element 115 decay chains. A. E_L = 248 MeV. B. E_L = 253 MeV [30].

The nuclear reaction corresponding to the above decay chains is:

$$^{243}\text{Am} + ^{48}\text{Ca} \rightarrow ^{291}115^{*} \rightarrow ^{(287\text{-}288)}115 + (3\text{-}4)\text{n}$$

The calculated cross sections for the 3n and 4n evaporation channels were $\sigma_{3\text{n}} = 2.7^{+4.8}_{-1.6}$ pb and $\sigma_{4\text{n}} = 0.9^{+3.2}_{-0.8}$ pb, respectively. The isotopes $^{289}115$ and $^{290}115$ were identified as decay daughters of the recently discovered element 117 [32].

1.3 Chemistry of the transactinides

The primary interest in transactinide chemistry is to correctly place new elements in the periodic table by evaluating their chemical similarity to the expected homologs (elements from the same chemical group). Without validating the chemical behavior the transactinides, the arrangement of the current periodic table places elements Rf through Cn in the d-block below Hf through Hg, and elements 113 to 118 are expected to be p-block elements located beneath Tl through Rn. The placements of the transactinides are solely based on their proton numbers not their chemical behavior. Quantum mechanical calculations have concluded that this arrangement may not be entirely accurate due to relativistic effects on the valence electrons potentially causing variations in the group chemical trends [60,61].

Relativistic effects occur when the inner-most s- and p-orbital electrons approach the speed of light, c. The s electrons, which have no angular momentum, approach the nucleus most closely, and thus gain the greatest velocity [62]. Einstein's theory of relativity describes how mass increases as velocity approaches the speed of light [63]:

$$m = \frac{m_o}{\sqrt{\left(1-\left(\frac{v}{c}\right)\right)}} \qquad \text{(Eqn. 1)}$$

Where m_o is the rest mass and v is the speed of the electron. From this equation the effective Bohr radius becomes [63]:

$$a_o = \frac{(4\pi\epsilon_o)}{\left(\frac{\hbar^2}{me^2}\right)} \qquad \text{(Eqn. 2)}$$

Therefore, as the electron speed increases, the Bohr radius for the inner shell electrons decreases. Figure 7 shows the relativistic and hypothetical non-relativistic distribution of the 7 s valence electrons in Db.

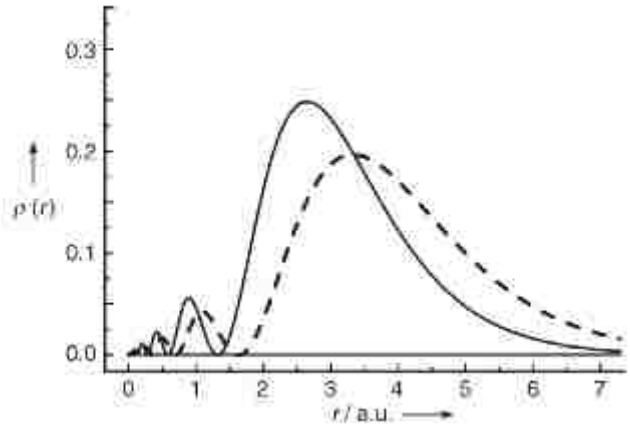

Figure 7. Relativistic (solid line) and non-relativistic (dashed line) distribution of the 7 s valence electrons of Db [37].

For p electrons, which do have an angular momentum, this mass-velocity effect is close to that of the s electrons but of smaller magnitude. However, there is a spin-orbit effect which divides the three p-orbitals into one $p_{1/2}$ and two $p_{3/2}$ orbitals [62,63]. For the $p_{1/2}$ electrons the mass-velocity and spin-orbit effect yield contractions and energy stabilization on the same order as the s electrons; however, for the $p_{3/2}$ electrons these effects cancel [62-64]. The contraction of the spherical s and $p_{1/2}$ electrons is known as the "direct relativistic effect" [37]. This contraction of the s- and $p_{1/2}$-orbitals provides sufficient screening of the nuclear charge to allow the outer d- and f-orbitals to expand, also known as the "indirect relativistic effect" [37,62-64]. The third and final relativistic effect occurs when electrons in levels with $l > 0$ (p, d, f,… electrons) undergo spin-orbit splitting into $j = l \pm ½$ states. This effect originates near the nucleus and therefore, for

orbitals with the same l values the spin-orbit splitting decreases with increasing number of subshells. Each of these effects grows in magnitude proportional to Z^2 [37].

Chemical studies of transactinide elements are difficult due to the nature of their production, which is one atom-at-a-time. Since transactinide element production is atom-at-a-time questions as to the statistical validity of experimental results are raised. Both thermodynamic and kinetic views of this problem must be explored. In the macroscopic world chemical equilibrium is represented through the law of mass action:

$$\mathrm{K} = \frac{\boldsymbol{a^c(C)a^d(D)}}{\boldsymbol{a^a(A)a^b(B)}}; \quad \text{For} \quad \mathrm{aA} + \mathrm{bB} \leftrightarrow \mathrm{cC} + \mathrm{dD} \qquad \text{(Eqn. 3)}$$

Where K is the equilibrium constant. Assuming a metal ion is a constituent of both A and C, at equilibrium the metal ions A and C exchange at a constant rate. If only a single atom of a metal is present, however, it cannot exist in both A and C simultaneously and therefore, an equilibrium constant cannot be defined since either the activity of A or C is zero. Guillaumont *et al.* proposed a law of mass action in which the concentrations are substituted with the probabilities of finding an atom in a given phase, thus deriving an equilibrium formulation valid for atom-at-a-time studies [65-67].

For the reaction, $\mathrm{MA} + \mathrm{B} \leftrightarrow \mathrm{MB} + \mathrm{A}$, there is a forward and reverse rate. The rate at which this reaction proceeds is based on the activation energy barrier. The higher this energy the slower the reaction rate and slower equilibrium will be established. Therefore, for transactinide chemistry, the chemical system must have extremely fast kinetics due to the short half-lives of the transactinide elements. Activation energy less than 60 kJ will allow for equilibrium to be established quickly compared with the half-life of the transactinide element [68].

Prior to performing a transactinide chemistry experiment, the chemical system must be thoroughly studied with the homologs and pseudo-homologs of the desired transactinide

element. Due to the short half-lives of the transactinide elements, fast and efficient separations are necessary to evaluate their properties, such as ionic radii and chemical speciation, by comparison to their lighter homologs. For liquid-phase studies, this is accomplished through batch and dynamic column studies to assess the uptake on the chromatographic column system. The kinetics of these experiments must also be tested to ensure the system can be performed on the required short time scale. Finally, on-line studies of accelerator produced short-lived isotopes of the homolog and pseudo-homolog elements need to be performed to assess the experimental set-up in similar conditions to a transactinide experiment. The on-line studies provide the only means to truly test the kinetics of the chemical system as well as the chemical species present after the nuclear reaction and transport to the chemical apparatus.

The chemical system must be extremely selective for the desired element. During the production of a transactinide element many reaction products other than the desired atom (from partial transfer of nucleons between target and projectile) will reach the chemical system. The production rates of these transfer products are orders of magnitude higher than the production of the transactinide [15]. The reaction transfer products can interfere with identification of the transactinide element of interest.

Magnetic pre-separators, such as the TransActinide Separator and Chemistry Apparatus (TASCA) at Gesellschaft für Schwerionenforschung (GSI), and the Berkeley Gas-filled Separator (BGS) at Lawrence Berkeley National laboratory (LBNL) can be used as an alternative to chemical separations and separate the unwanted transfer products by their magnetic rigidities [69,70]:

$$B\rho = \frac{mv}{q} \qquad \text{(Eqn. 4)}$$

Where Bρ is the magnetic rigidity of a particle of mass, m, velocity, v, and charge, q. If the separator (see Figure 8) is filled with a dilute gas medium (like H or He), moving ions will change their energy, direction, and charge due to collisions with the gas. After entering the gas as a

homogeneous ion beam, the beam will split into components with different charge values, eventually reaching an equilibrium mean charge after interaction with a large number of gas atoms. The equilibrium of the charges can be approximated by a Gaussian distribution centered at $\bar{q}$:

$$\bar{q} \approx \frac{v}{v_o} Z^{1/3} \qquad \text{(Eqn. 5)}$$

Where Z is the ion atomic number and v_o= 2.19 x 10^6 m/s (Bohr velocity). Combining Equations 4 and 5 yeilds:

$$B\rho = 0.02267 \frac{A}{Z^{\frac{1}{3}}} (Tm) \qquad \text{(Eqn. 6)}$$

Using these gas-filled physical pre-separators can yield large background suppression, removing a substantial amount of the unwanted co-produced reaction products. Figure 8 shows a diagram of the Dubna Gas-filled Recoil Separator (DGFRS).

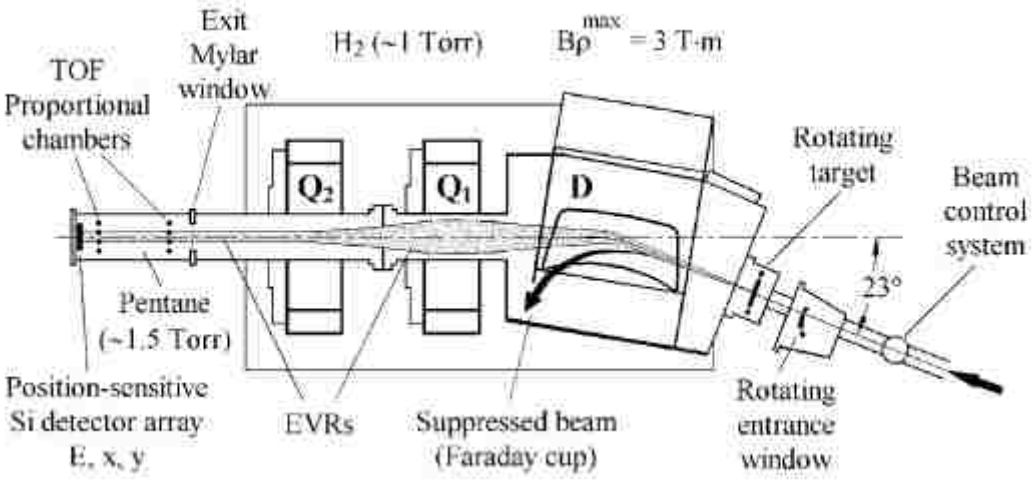

Figure 8. Schematic of the Dubna Gas-filled Recoil Separator (DGFRS) [70].

Chemical experiments themselves can be performed in two ways. The first, a static method, is to measure the distribution coefficient of a single atom between two phases by

repeating the same experiment hundreds of times. The earliest experiments of this form were liquid-liquid extraction experiments, where hundreds of chemical extractions were done to determine if the atom, identified by alpha spectroscopy, resided in the organic or aqueous phase. A continuous experiment with no interruptions, liquid-liquid extraction system SISAK (Short-lived Isotopes Studied by the AKUFVE technique), has been used in the study of transactinide elements [71]. A dynamic experiment, the second method, involves a process such as column chromatography experiments where atoms in solution undergo hundreds of exchange steps as they travel through the column, which results in hundreds of successive static experiments being performed in a single step. Both methods can be performed in a discontinuous or continuous manner; ideally experiments should be as continuous as possible to avoid missing a transactinide event. However, with systems such as ARCA (Automated Rapid Chemistry Apparatus), an extraction chromatography system, a discontinuity is introduced into the experiment due to the need to make modifications or perform maintenance to the chemical system [72,73].

The first transactinide studied was Rf (Z =104) as a tetrachloride in the gas-phase in Dubna by Zvara *et al.* [74]. Following this study many other gas-phase experiments were performed on Rf [75-81]. Experiments on Rf in the liquid-phase with ion exchange resins were performed as well [82-91]. The next transactinides, Db (Z = 105) and Sg (Z = 106) were also studied in the gas- and liquid-phases [72,78,92-109]. Gas-phase experiments of Bh (Z= 107) and Hs (Z = 108) were also performed [110,111]. Most recently gas-phase experiments have been performed on Cn (Z = 112) element 113 (Z = 113) and Fl (Z = 114) in the elemental state in the gas phase [112-117].

In some of the chemical systems mentioned above, Rf and Db showed some deviations from the chemical trends expected based on their lighter homologs, a possible result of

relativistic effects. These deviations have not been observed for Sg, Bh and Hs. These observations as well as the similarities between the transactinides and their lighter homologs gave strong support for assigning these elements to groups 4 through 7 of the periodic table. Flerovium and element 115 belong to group 14 and 15 of the periodic table, respectively, indicating that Fl is homologous to Pb, Sn, and Ge and element 115 is homologous to Bi, Sb, and As, with both elements belonging to the p-block. Predictions, however, have indicated vastly different chemical properties for these elements, with Fl ranging from a metal to even a potential noble gas. The investigation of these unique elements, which should have exceedingly strong relativistic effects, forms the basis for this work.

1.4 Predicted properties of Flerovium

With the exception of two experiments by Eichler *et al.* and Yakushev *et al*., discussed below, only theoretical predictions of the chemical behavior of Fl have been performed. These predictions fall into two categories: early efforts based on periodic trends, and relativistic quantum mechanical calculations. The electronic ground state of Fl is predicted to be closed shell $7s^2 7p_{1/2}^2$, due to large spin-orbit splitting of the 7p orbital and relativistic stabilization of the $7p_{1/2}$ orbital. Therefore, Fl's chemistry should be based on the $7p_{1/2}^2$ orbital, and thus relatively inert and volatile, due to the fact the electrons in this $7p_{1/2}$ orbital are relativistically stabilized and act as another inert-pair. The primary oxidation state for Fl is predicted to be Fl^{2+} (most stable of group 14), due to the large 7s orbital stabilization. The sp^3 hybridization energy needed for the Fl^{4+} state makes it very unstable [118].

Keller, O. L. *et al.* in the 1970s predicted many chemical properties of Fl by periodic table extrapolation. For example, Table 2 shows the predicted ionization potentials for group 14 [119].

Table 2. Ionization potentials for group 14 elements.

Isotope	HFS (rel) (eV), I	Experimental (eV), I	Δ (eV), I	HFS (rel) (eV), II	Experimental (eV), II	Δ (eV), II
Ge	6.44	7.88	1.44	14.63	15.93	1.30
Sn	6.14	7.34	1.20	13.54	14.63	1.09
Pb	6.46	7.42	0.96	14.07	15.03	0.96
114	7.77	(8.49)	(0.72)	15.97	(16.75)	(0.78)

From Table 1-2 the predicted Fl ionization potential is much higher than the other elements in group 14 indicating it should be the least reactive element in the group. Figure 9 shows the ionization potentials of the sixth and seventh row elements [120,121].

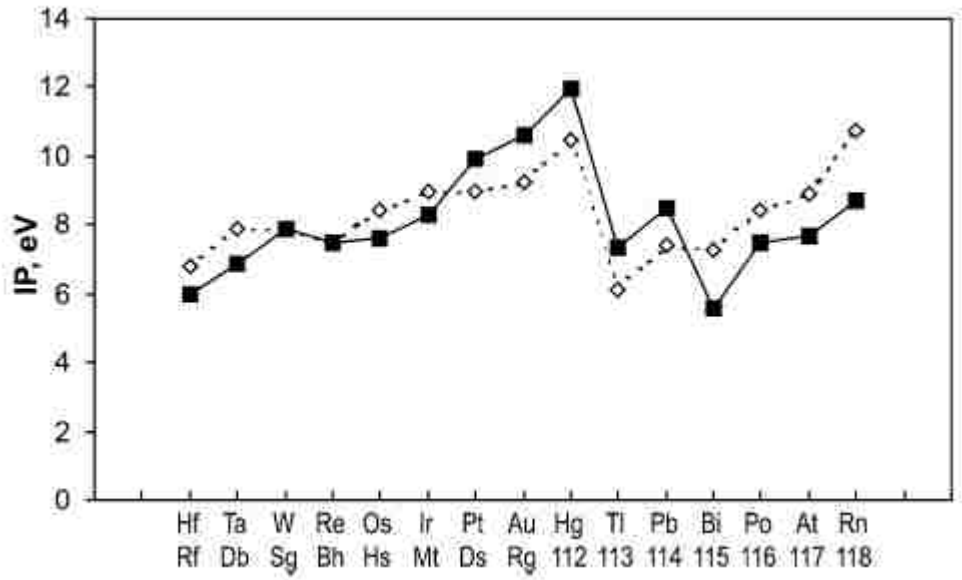

Figure 9. Ionization potentials of the sixth row elements (dashed line, experimental) and seventh row (solid line, calculated).

Predictions by Eichler *et al*. in the 1970s, showed a correlation for ΔH_f vs. Z with a Fl ΔH_f value of 71.5 ± 15 kJ/mol, the lowest among the group 14 elements [121]. These predictions support the notion that Fl should be relatively inert. The predicted standard electrode potential of $E^{\circ}(Fl^{2+}/Fl)$

= +0.9 V strengthens the idea that Fl should be relatively inert compared to its lighter homologs [118]. A well-known prediction based on atomic calculations by K. S. Pitzer indicated Fl may be as inert as a noble gas [122]. These predictions indicate that the relativistic effects on the $7p_{1/2}$ electrons cause a diagonal relationship introduced into the periodic table. Therefore, Fl^{2+} is expected to behave as if it were somewhere between Hg^{2+}, Cd^{2+}, and Pb^{2+} [121,123].

Examining the bonding in homonuclear dimers is an indication about bonding in the solid state. Many calculations based on different methods have been performed [124-129]. The calculations agree that Fl_2 is a stronger bound than a typical van der Waals system. The calculations also show that it is more strongly bound than Cn_2, but weaker than Pb_2. Theory shows that the $7p_{1/2}$ and $7p_{3/2}$ orbitals take part in bond formation, the HOMO of the σ character is composed of 98% $7p_{1/2}$ and 2% $7p_{3/2}$ [118].

Volatility of Fl can be studied by its adsorption on a metal surface. Calculations indicate that the $7p_{1/2}$(Fl) orbital forms a double-occupied σ bonding molecular orbital and one single-occupied σ^* anti-bonding molecular orbital with the 6s(Au) orbital [118]. Modern fully relativistic calculations indicate Fl interacts with a Au surface through the formation metal-metal bonds and is a volatile metal [130-132].

Eichler *et al.* performed experiments at the FNLR Dubna U400 heavy ion cyclotron with Fl in the gas phase to determine its adsorption on a thermochromatography column with gold covered detectors. Three atoms of Fl were identified, and their deposition pattern on a gold surface detector with a varying temperature gradient was examined. Results indicate that Fl is at least as volatile as the simultaneously investigated Hg, At, and Cn. Experiments indicate that Fl has increased stability compared to Pb. Lead being the least volatile element of group 14 deposits on a gold surface at 800-1000 ^{o}C, 1000^{o}C higher compared to the three identified atoms of Fl [116].

A second Fl experiment performed at GSI by Yakushev *et al.* observed two atoms of Fl which indicated that Fl is less reactive than Pb. The results also indicated that Fl had a metallic character upon adsorption to a Au surface through formation of metal-metal bonds [117]. These results were consistent with fully relativistic calculations of Fl on an Au surface [130-132], but disagreed with the Eichler *et al.* result that its absorption was only due to physisorption [116]. Yakushev *et al.* indicated that Fl was a volatile metal, and the least reactive of group 14; however, not as inert as a noble gas.

1.5 Predicted properties of Element 115

The chemistry of element 115 has had very little investigation theoretically and no experimental attention. Predictions indicate that one electron is located in a relativistically destabilized $7p_{3/2}$ orbital and it is loosely bound. The two electrons located in relativistically stabilized $7p_{1/2}^2$ orbital act as an inert pair. This leads to the predicted primary oxidation state for element 115 of 115^{1+}. This is supported by the prediction that element 115 has the smallest ionization potential of the group 15 elements, Table 3 [133].

Table 3. Ionization potentials of group 15 elements.

Isotope	HFS (rel) (eV), I	Experimental (eV), I	Δ (eV), I	HFS (rel) (eV), III	Experimental (eV), III	Δ (eV), III
As	8.00	9.81	1.8	27.0	28.34	1.4
Sb	7.05	8.639	1.6	24.1	25.3	1.2
Bi	6.09	7.287	1.2	24.5	25.56	1.1
115	4.70	(5.2)	(0.5)	26.5	(27.4)	(0.9)

Element 115 predicted standard electrode potential ($E^o(115^+/115)$ = -1.5V), suggests that element 115 should be quite reactive. Predictions indicate that the properties of element 115 should be similar through a diagonal relationship to Tl as well as to Bi. The same predictions

indicate that 115^{3+} should be somewhat stable and should have chemical properties between Tl^{3+} and Bi^{3+} [133]. There were 4c-BDF (van Wüllen *et al.*) and SO ZORA (Liu, W. *et al.*) calculations performed with $(115)_2$ and Bi_2 homonuclear dimers [126,134]. The element 115 dimer was bound more weakly than the Bi dimer: D_e (115_2) = 0.83 eV and R_e = 3.08 Å, and D_e (Bi_2) = 2.45 eV and R_e = 2.69 Å, respectively. These results also indicate that bonding should be stronger in element 115 than in element 114.

1.6 Chemical properties of group 12, 13, 14 and 15

1.6.1 Group 12 chemical properties, the homologs of Cn and pseudo-homolog of Fl

As early as 1970 from extrapolation of periodic trends, Fl (discussed further in section 1.4), was believed to potentially behave similar to mercury and cadmium, which are therefore, the pseudo-homologs of Fl. Mercury exists primarily as Hg^{2+} in aqueous solutions. In the presence of sulfates (such as from H_2SO_4) and halides (such as from HCl), mercury readily forms sulfate and halide complexes. In the presence of excess NO_3^- ions the aqueous complex ion $[Hg(NO_3)_4]^{2-}$ forms [135].

Cadmium, like mercury, exists primarily as Cd^{2+}. Cadmium halide species readily form and are highly soluble due to the formation of complex ions ($[MX_3]^-$) in solutions with high halide concentrations; however, Cd^{2+} does not form stable fluoro-complexes [136]. Cadmium is readily hydrolyzed in solution and can form species such as: $[Cd(OH)(H_2O)_x]^+$, and $[M_2(OH)(H_2O)_x]^{3+}$. Table 4 summarizes the atomic properties of the group 12 elements [135].

Table 4. Atomic properties of group 12 elements.

Property	Zn	Cd	Hg
Atomic number	30	48	80
Number of naturally occurring isotopes	5	8	7
Atomic weight	65.38	112.41	200.59(±0.03)
Electronic configuration	$[Ar]3d^{10}4s^2$	$[Kr]4d^{10}5s^2$	$[Xe]4f^{14}5d^{10}6s^2$
Electronegativity	1.6	1.7	1.9
Metal radius (pm)	134	151	151
Effective ionic radius (pm) II	134	151	151
I	74	95	102
Ionization energy (kJ/mol), 1st	906.1	876.5	1007
2nd	1733	1631	1809
3rd	3831	3644	3300
$E^o(M^{2+}/M)$ (V)	-0.7619	-0.4030	0.8545
MP (°C)	419.5	320.8	-38.9
BP (°C)	907	765	357
ΔH_{fus} (kJ/mol)	7.28 (±0.01)	6.4 (±0.2)	2.30 (±0.02)
ΔH_{vap} (kJ/mol)	114.2 (±1.7)	100.0 (±2.1)	59.1 (±0.4)
$\Delta H_{mon.\ gas}$ (kJ/mol)	129.3 (±2.9)	111.9 (±2.1)	61.3
Density (25 °C) (g cm^{-3})	7.14	8.65	13.534 (1)
Electric resistivity (20 °C), (µohm cm)	5.8	7.5	95.8

Due to the filled d block, mercury and cadmium do not to show normal properties of the transition metals. There is also an increasing polarizing power and covalency in compounds formed by mercury and cadmium in the order, $Cd^{2+}<Hg^{2+}$, which is a reflection of lessening nuclear shielding and increasing power of the distortion of the filled p shell < filled d shell < filled f shell [135].

1.6.2 Group 13 chemical properties, the homologs of element 113 and pseudo-homologs of element 115

The predicted properties of element 115, discussed in section 1.5, indicate that thallium and indium are pseudo-homologs. The stability of the M^+ state compared to the M^{3+} state

increases in the order Al < Ga < In < Tl, with the reason having to do with the inert pair effect as in the homologs of Fl and 115 and the Fl pseudo-homologs. Thallium has been shown to form complex ions and or neutral species, $TlCl^{+}$, $TlCl_2$, and $TlCl_3^{-}$ (similar species for nitrate and sulfate ions) [137,138].

Indium, like thallium, exists primarily as In^{3+} with In^{+} also occurring. In aqueous solution the In^{3+} ion is the only stable oxidation state [139]. The chloride, nitrate, and sulfate salts of indium are all soluble. Very little information as to complex ion formation exists in literature; however, the existence of $InCl_6^{3-}$ and $InCl_4^{-}$, is the basis of its anion-exchange behavior [140,141]. These ions are only stable in high hydrochloric acid concentrations (greater than 8 M). Positive fluoride complexes of In have been reported, InF^{2+} and InF_2^{+} [142]. It has also been shown that in dilute halide solutions In readily forms $InOH^{2+,}$ InX^{2+} (X a halide), and In^{3+} [143]. Table 5 summarizes the atomic trends of the group 13 elements [135].

Table 5. Atomic trends of group 13 elements.

Property	B	Al	Ga	In	Tl
Atomic number	5	13	31	49	81
Number of naturally occurring isotopes	2	1	2	2	2
Atomic weight	10.81	26.98154	69.72	114.82	204.383
Electronic configuration	$[He]2s^2 2p^1$	$[Ne]3s^2 3p^1$	$[Ar]3d^{10} 4s^2 4p^1$	$[Kr]4d^{10} 5s^2 5p^1$	$[Xe]4f^{14} 5d^{10} 6s^2 6p^1$
Ionization energy (kJ/mol), I	800.5	577.4	578.6	558.2	589.1
II	2426.5	1816.1	1978.8	1820.2	1970.5
III	3658.7	2744.1	2962.3	2704.0	2877.4
Metal radius (pm)	(80-90)	143	135	167	170
Ionic radius (pm) M^{III}	27	53.5	62.0	80.0	88.5
M^{I}	--	--	120	140	150

1.6.3 Group 14 chemical properties, the direct homologs of Fl

The group 14 elements (homologs of Fl) Ge, Sn, and Pb show an increasing stability of the M^{2+} compared to the M^{4+} when moving down the group towards Pb. This can be attributed to the inert-pair effect, or tendency of ns electrons to remain unionized [135]. The group is also characterized by increasing metallic character with increasing atomic number, Z [144]. Thus far, with the exception of generator studies by Guseva et al. (discussed below), no chemical studies of the homologs and pseudo-homologs of Fl have been performed with the goal of developing a chemical system for Fl itself.

Lead has the primary oxidation state of Pb^{2+} with Pb^{4+} being possible but less stable in aqueous systems [145]. In hydrochloric acid solutions, Pb tends to exist as: Pb^{2+}, $PbCl^{+}$, $PbCl_2$, $PbCl_3^{-}$, and $PbCl_4^{2-}$ at 25 $^{\circ}$C (with Pb^{2+} and $PbCl_2$ being most probable). In nitric acid lead has been

shown to readily form $PbNO_3^+$ and $Pb(NO_3)_2$. There is no evidence for polynuclear Pb species; however, once the concentration of Pb exceeds 0.5 M, Pb can form polyatomic and homopolyatomic species [135, 145, 146]. The ion-exchange behavior of lead has been extensively studied by Guseva *et al.* for use in obtaining Pb tracers for Fl homolog studies. Guseva *et al.* showed that Pb could be continually eluted from a Ra, Th, or Ac solution sorbed onto a Dowex 50x8 cation exchange column in hydrochloric acid matrices, Figure 10 [147,148].

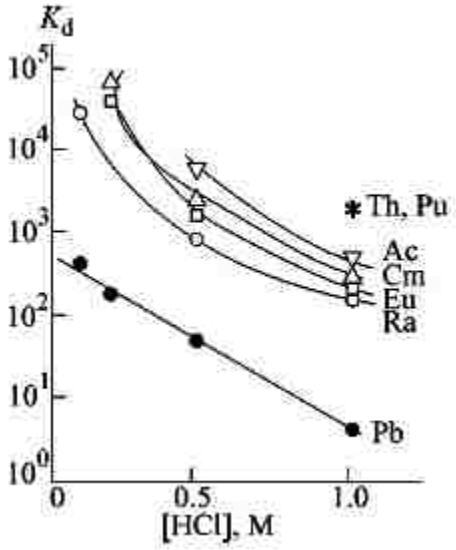

Figure 10. Distribution coefficients for Pb, Ra, Ac, actinides, and Eu on Dowex 50x8 as a function of [HCl] [147].

While noting a generator from a pure HCl matrix was possible Guseva *et al.* indicated the optimal elution conditions for Pb were found to be with 0.5 M HCl containing 90% CH_3OH. Guseva has also proposed a Pb generator based on an HBr matrix, Figure 11.

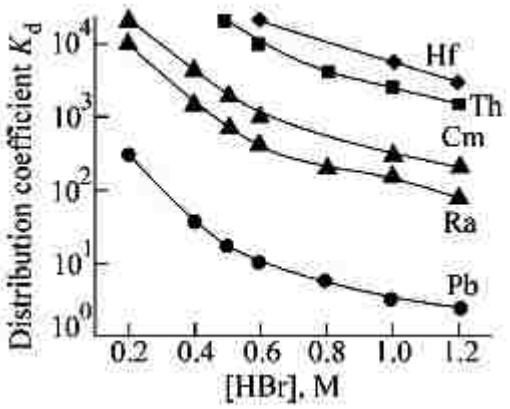

Figure 11. Distribution coefficients for various metals on Dowex 50x8 as a function of [HBr] [148].

A final generator was based on first removing Th and Ac from Ra using a Dowex 1x8 anion-exchange resin and 1 M HNO_3 in 90% CH_3OH, then preparing a Pb generator by loading the Ra onto a Dowex 50x8 cation-exchange resin by the methods mentioned above [149,150].

Tin, like Pb, exists as both Sn^{2+} and Sn^{4+}; however, with the Sn^{4+} being the more stable oxidation state [145]. In aqueous solutions Sn has been shown to easily hydrolyze. In concentrations above 10^{-3} M tin has the ability for form polynuclear species. Tin forms halide compounds easily in low pH and high halide concentrations (greater than 10^{-3} M). The most prevalent Sn^{4+} halide species are the hexacoordinated complex anions (e.g. SnF_6^{2-}, $SnCl_6^{2-}$, and $SnBr_6^{2-}$) [151,152]. In hydrochloric acid concentrations above 0.7 M, Sn^{4+}, almost exclusively forms $SnCl_6^{2-}$, an extremely stable anion [151-153]. Table 6 summarizes the atomic properties of group 14 elements [135].

Table 6. Atomic properties of the group 14 elements.

Property	C	Si	Ge	Sn	Pb
Atomic number	6	14	32	50	82
Electronic structure	[He]$2s^2 2p^2$	[Ne]$3s^2 3p^2$	[Ar]$3d^{10} 4s^2 4p^2$	[Kr]$4d^{10} 5s^2 5p^2$	[Xe]$4f^{14} 5d^{10} 6s^2 6p^2$
Number of naturally occurring isotopes	2+1	3	5	10	4
Atomic weight	12.011	28.00(±3)	72.59(±3)	118.69(±3)	207.2
Ionization energy (kJ/mol), I	1086.1	786.3	761.2	708.4	715.4
II	2351.9	1576.5	1537.0	1411.4	1450.0
III	4618.8	3228.3	3301.2	2942.2	3080.7
IV	6220.0	4354.4	4409.4	3939.3	4082.3
R^{iV} (covalent), (pm)	77.2	117.6	122.3	140.5	146
R^{iV} (ionic), (pm)	(15)(CN 4)	40	53	69	78
R^{II} (ionic), (pm)	--	--	73	118	119
Pauling electronegativity	2.5	1.8	1.8	1.8	1.9

The similarities in the ionization potentials from Table 6 between Si and Ge can be related to the filling of the 3d shell and between Sn and Pb can be attributed to the filling of the 4f shell [135].

1.6.4 Group 15 chemical properties, the direct homologs of element 115

Group 15 elements are characterized primarily by M^{3+} and M^{5+} states. The elements of the group vary drastically as the group is descended, with the lighter elements being non-metals, the heavier elements being metallic in character, and elements in the middle exhibiting semi-metallic character. As in the group 14 elements, the tendency of the heavier group members to show increasing stability of the lower oxidation state can be attributed to the inert-pair effect [154]. At this time, with the exception of generator studies by Guseva *et al.*

(discussed below), no chemical studies of the homologs and pseudo-homologs of element 115 have been performed with the goal of developing a chemical system for element 115 itself.

Bismuth is the heaviest element with a stable isotope. In aqueous systems, Bi is most often found in the Bi^{3+} state; however, Bi^{5+} is also a stable oxidation state, and is extremely oxidizing. In solution Bi^{3+} shows no tendency to disproportionate into the Bi^{5+} state. Due to relativistic effects, there is a possibility for a stable Bi^{+} oxidation state due to the splitting of the p-orbitals and the development of a double inert pair effect, Bi^{+}: $6s^2 6p_{1/2}^2 6p_{3/2}^0$. However, due to the fact relativistic effects are small for Bi, the Bi^{+} state is not apparently chemically stable [154]. In aqueous solutions Bi is shown to only form mononuclear species. In acidic halide solutions the common species are of the form BiX_n^{3-n}, where n = 1,…,6, and X = F, Cl, Br, I [155]. In nitric acid solutions metallic Bi tends to form a nitrate complex ($Bi(NO_3)_3$) as well as has the possibility of complex ion formation for high nitric acid concentration. However, a $Bi(NO_3)_3 \cdot 5H_2O$ species can crystallize out easily [154]. For tracer levels of Bi^{3+} (less than 10^{-7} M) in 1M HNO_3, $Bi(NO_3)_n^{3-n}$, $Bi(OH)(NO_3)_n^{2-n}$, $Bi(OH)_2(NO_3)_n^{1-n}$, and $Bi(OH)_3(NO_3)_n^{n-}$ form [155]. Unless it is kept in very acidic media (below pH 1-2) Bi tends to hydrolyze, often forming the hydroxy cations $BiOH^{2+}$ and $Bi(OH)_2^{+}$ [155]. Guseva *et al.* has published papers on the ion-exchange behavior of Bi, and preparation of generators to continually elute Bi for tracers in element 115 homolog studies. These generators are prepared the exact same way as the lead generators mentioned in Section 1.6.3; however, the eluant is changed to elute Bi from the generator.

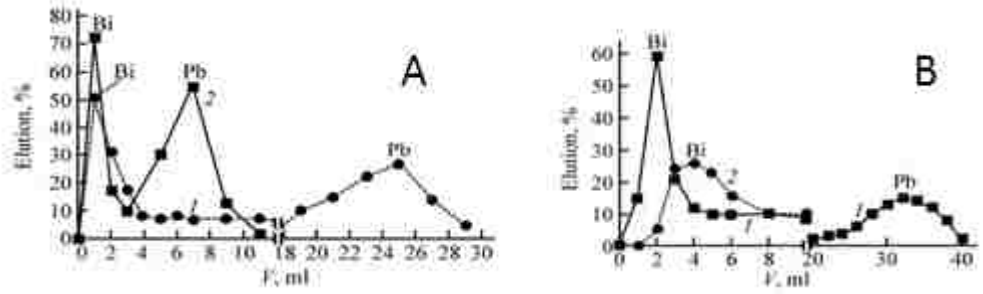

Figure 12. A. Elution of Bi and Pb from Dowex 50x8 with 0.3 M HBr (dotted line) and 0.25 M HBr (solid line). B. Elution of Bi and Pb from Dowex 50x8 with 0.3 M HCl (dotted line) and 0.25 M HCl (solid line) [156].

Figure 12 shows the elution behavior used demonstrated by Guseva *et al.* to turn the lead generators into Bi generators.

Antimony has stable Sb^{3+} and Sb^{5+} states, with the Sb^{3+} state being slightly more stable. Antimony is less metallic than Bi [157]. In nitric acid solution under 2 M the primary species in solution is $Sb(OH)_2^+$ [158]. Antimony is not attacked by dilute aqueous acids, even in concentrated nitric acid, and there is a tendency for antimony to form $Sb^{3/5+}$ oxides instead of the nitrates. In sulfuric acid, Sb forms Sb^{3+} sulfates [157]. Antimony shows no evidence of forming polynuclear species [137]. In solution Sb tends to hydrolyze in more dilute acid concentrations, and even at high acid concentrations is reluctant to form halide and nitrate complexes [157]. Table 7 shows the atomic trends of group 15 elements [135].

Table 7. Atomic trends of group 15 elements.

Property	N	P	As	Sb	Bi
Atomic number	7	15	33	51	83
Atomic weight	14.0067	30.97376	74.9216	121.75 (±3)	208.9804
Electronic configuration	$[He]2s^2 2p^3$	$[Ne]3s^2 3p^3$	$[Ar]3d^{10}4s^2 4p^3$	$[Kr]4d^{10}5s^2 5p^3$	$[Xe]4f^{14}5d^{10}6s^2 6p^3$
Ionization energy (MJ/ mol), I	1.402	1.012	0.947	0.834	0.703
II	2.856	1.903	1.798	1.595	1.610
III	4.577	2.910	2.736	2.443	2.466
Sum (I+II+III), (MJ/mol)	8.835	5.825	5.481	4.872	4.779
Sum (IV+V), (MJ/mol)	16.920	11.220	10.880	9.636	9.776
Electronegativity (χ)	3.0	2.1	2.0	1.9	1.9
R_{cov} (M^{III}), (pm)	70	110	120	140	150
R_{ionic} (M^{III}), (pm)	(16)	44	58	76	103
R_{ionic} (M^{V}), (pm)	(13)	38	46	60	76

1.7 Macrocycles

Macrocyclic compounds are defined by IUPAC as “a cyclic macromolecule or a macomolecular cyclic portion of a molecule,” more commonly thought of by coordination chemists as a cyclic molecule which has three or more donor atoms for coordination to metal centers [159]. In 1967 the crown ether dibenzo-18-crown-6 (DB18C6) was accidentally discovered by C. J. Pederson during synthesis of a bisphenol from catechol and dichlorodiethylether [160]. This discovery combined with the discovery of cryptands by C. J. Lehn in 1977 and calyx[n]arenes by D. C Gutsche in 1989 kick-started the field of coordination chemistry with the use of macrocyclic compounds [161,162]. The 1987 Nobel Prize in Chemistry was shared by C. J. Pederson, J. M. Lehn and D. J. Cram for the development of macrocycles [163].

1.7.1 Crown ethers

Crown ethers form very stable metal-crown complexes. Complexation depends on the relative size of the cation compared to that of the crown cavity. The complexes are formed by ion-dipole interactions between the cations and the negatively charged donor atoms (oxygen, sulfur, etc.) on the ring, Figure 13 [164].

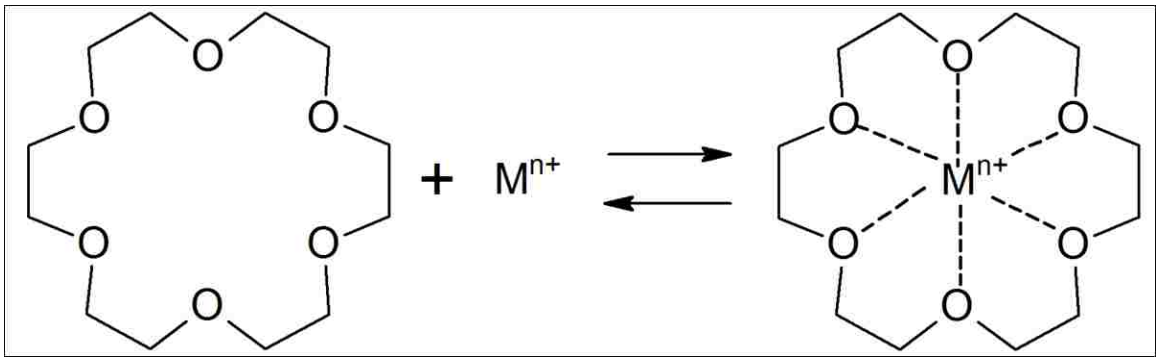

Figure 13. Mechanism for typical crown ether extraction of metal cation.

The stability of the crown complexes are governed by the following parameters [165]:

- Size of the cation and cavity of the crown ether;
- Number of donor atoms (more gives higher stability);
- Arrangement of the donor atoms (planar structures are more stable);
- Symmetry of the oxygen atom arrangement (more symmetrical means more stable);
- Basicity of the donor atom (i.e. oxygen) (the more basic the donor atom the more stable the complex);
- Steric hindrances in the polyether ring (more hindrances present the less stable the complex);
- Electrical charge of the cation (high importance to stability)

Table 8 shows the relative cavity diameters for various crown ethers.

Table 8. Cavity size of crown ether and sulfur crown ethers [165].

Compound (sulfur and oxygen crown)	Cavity Diameter (Å)
12C4	1.2-1.5
14C4	1.2-1.5
15C5	1.7-2.2
18C6	2.6-3.2
21C7	3.4-4.3
24C8	> 4.0

Typically crown ethers form 1:1 complexes with the metal in the cavity of the crown ether, provided the cation diameter and crown cavity diameter are compatible. When the cation is slightly larger than the crown ether cavity, it is possible for 2:1 or 3:2 complexes to form as a sandwich in which the cation is located slightly off from the plane of the oxygen donor atoms. In cases where the cation is much smaller than the crown ether cavity, 1:2 complexes can form where oxygen atoms are located as close to the cation as possible [164]. Other well-known 2:1 sandwich complexes have been known to form with crown ethers extracting anionic complexes by formation of ion-association complexes [166]. Crown ethers, specifically 18-crown-6 (18C6) are known to form positively charged complexes by coordination with the hydronium ion, H_3O^+, which can then be used to extract anionic metal complexes [167,168]. The stability of crown ether-metal complexes can be best explained by the macrocyclic effect, or an increase in the binding stability of metal cations by a cyclic polyether compared to that of the open ring, Figure 14 [169].

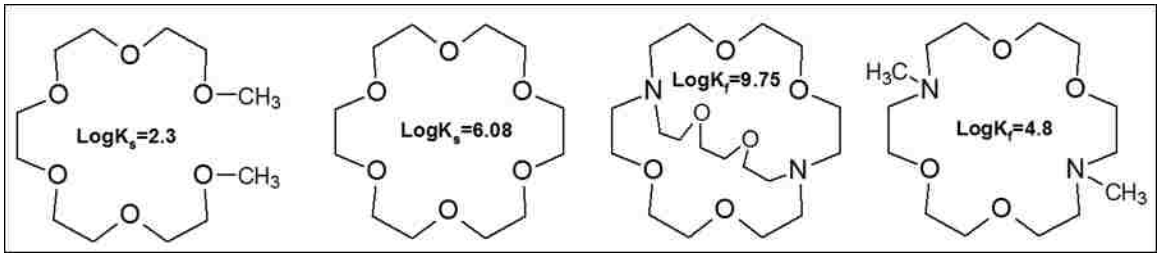

Figure 14. Illustrated macrocyclic effect for binding of K^+ in shown macrocycles.

As illustrated in Figure 14, a vastly increased stability is seen for the K^+ ion between the macrocyclic and non-macrocyclic compound. A 6000 fold increase in stability is seen between 18-crown-6 and the non-macrocyclic ligand, whereas the cryptand showed an even larger increase in stability by the addition of a pocketed coordination site [164,169].

1.7.2 Thiacrown ethers

Synthetically it is possible to replace the oxygen donor atoms in crown ethers with other donor atoms. This was first achieved accidentally by Meadow and Reid in 1934 by replacing the oxygen atoms with sulfur atoms in 18C6 [170]. This discovery was more than 30 years before the work of Pederson on crown ethers and the first work by Rosen and Busch on macrocyclic thioethers [171]. In the case of thiacrown ethers the replacement of oxygen atoms with sulfur atoms allows them to act as softer Lewis bases compared to traditional crown ethers [172]. This unique property should make them better extractants than traditional crown ethers for soft metals such as Hg and Pb. Extensive studies have been performed by Baumann *et al.* using a thiacrown ether to extract Hg, showing its high extractability and quick kinetics [173-177]. One large difference between traditional oxygen containing crown ethers and thiacrown ethers is the conformational preference. Thiacrowns tend to have their sulfurs oriented in an exodentate manner; whereas crown ethers take an endodentate conformation [178]. Therefore, thiacrowns do not have the pocket of charge density oriented toward the center of a ring. In order for a

thiacrown to bond with a metal cation, it is required that it first distort into an endodentate conformation to permit multiple sulfur metal interactions [179,180]. Due to the fact this costs an energetic penalty, thiacrowns generally form bridged or sandwich complexes [181-184]. Synthesis of thiacrowns with substituents attached to the ring can force the default conformation to become endodentate and thus have similar properties to that of the traditional crown ether.

1.8 Dissertation overview

Chapters 1 through 3 give a detailed literature review of macrocyclic extractants and transactinide chemistry. The predicted chemical properties of Fl and element 115 as well as the known chemical properties of the homologs and pseudo-homologs are presented. Also described in these chapters are the experimental techniques used and the facilities where experiments were performed. The synthesis and characterization of a novel macrocyclic compound hexathia-18-crown-6 is described in Chapter 4. Short lived radionuclides of the homologs and pseudo-homologs of Fl and element 115 were produced at the Lawrence Livermore National Laboratory (LLNL) Center for Accelerator Mass Spectrometry (CAMS). These radionuclides combined with Pb and Bi isotopes generated from the ^{232}U decay chain were used as tracers for chemistry development. These experiments are described in Chapter 5. Chemistry development experiments for the homologs and pseudo-homologs of Fl are described in Chapter 6 and 7 (Eichrom Pb resin experiments) and Chapter 8 (thiacrown experiments). Experiments to develop a chemical system for element 115 are presented in Chapter 9. A comparison of results with different macrocycles is discussed in Chapter 10, and concluding remarks on the possibility of an on-line system for Fl is presented in Chapter 11. The raw data of the results as presented in figures can be found in the Appendix.

1.9 Project Goals

The development of a system to assess the chemical properties of both Fl and element 115 is the primary goal of this work. More specifically, a chemical system with full control of the chemical forms present during separations is desired for the homologs and pseudo-homologs of Fl and element 115. Therefore, an on-line experiment with the transactinides would allow for extrapolation of their chemical properties by comparison to the lighter homologs, and help to assess the role relativistic effects play on chemical properties of the heaviest elements. These separations must be fast, highly efficient, and simple enough to be automated.

CHAPTER 2: BACKGROUND

2.1 Ion Exchange Chromatography

A chromatographic separation based on the exchange of ions is known as ion exchange chromatography (IXC). This process is a reversible interchange of ions between an insoluble (but permeable) inert material which carries exchange sites of opposite charge, and a mobile phase containing ions of interest [185]. Materials with this capability are known as ion exchangers, and can be classified as either a cation or anion exchanger (depending on the type of ion exchanged). For anion exchange, the ionic group is typically a quaternary ammonium group, Figure 15.

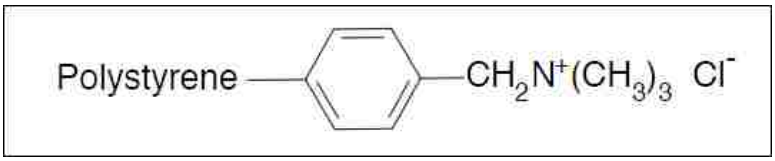

Figure 15. Typical anion exchanger with associated counter ion.

For cation exchange, the ionic group is typically a sulfonic acid group, Figure 16.

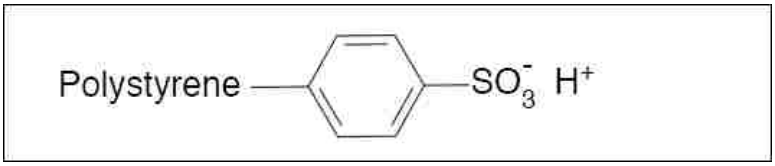

Figure 16. Typical cation exchanger with associated counter ion.

As shown in Figures 15 and 16, these exchanger groups are covalently bound to an inert polystyrene support and contain counter ions of the opposite charge. Resin permeability is controlled by the degree of cross-linking within the resin. Cross-linking is the bonding across the

polymer chains, linking them together; these bonds are controlled during the synthesis of the ion exchange resin. The magnitude of cross-linking has an influence on the capacity, equilibrium rate, and hydration of the resin. Higher cross-linking results in lower permeability, moisture content, and equilibrium rates. However, while the ability to incorporate larger ions at exchange sites decreases, the overall capacity increases. The opposite is true for lower cross-linking. Another important, tunable, property of ion exchange resins is the particle size. Particle size has the ability to affect the equilibrium and flow rates: increasing the particle size leads to an increase in equilibrium rates and an increase in the flow rate due to a decrease in flow resistance [185-187]. The particle size is also the most sensitive parameter when determining the theoretical plate height or elution band width, this height is decreased by the largest magnitude by decreasing the particle size radius [188].

Separations are performed based on the relative strengths of attraction between the ions in solution and exchange sites on the resin. In general, a separation is performed using a column packed with an ion exchange resin to which a sample is added containing a mixture of ions. Equilibrium is established between the exchanges of ions in solution with the exchange sites on the resin. Once equilibrium is established, a selectivity coefficient, the ratio of ions in solution to ions on the resin, can be determined for the ion exchange resin. As ions travel down a column, they will exchange with the counter ions and bind to the resin, Figure 17.

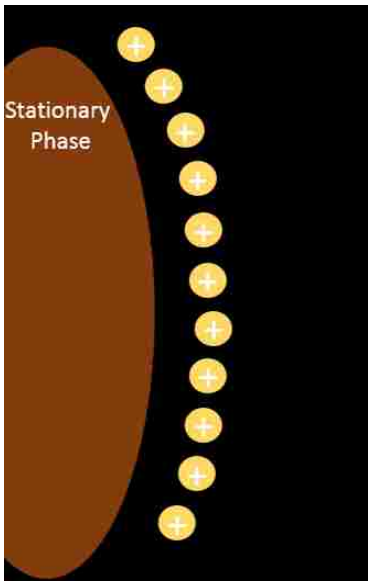

Figure 17. Ion exchange concept (X- is the ion of interest).

The magnitude of their binding strength is determined by their selectivity coefficients. Mixtures of ions will separate as they move down the column. Ions that are more tightly bound with a higher selectivity coefficient will elute later than ions that are less tightly bound with a lower selectivity coefficient.

Two different methods for separation exist in ion exchange: one based on the affinity differences between ions and another through the use of complexing agents. A system which is based only on affinity relies on the differences in the selectivity coefficients of the ions being significantly large enough to achieve a separation. This coefficient can be affected by many different factors such as ionic strength of the mobile phase and temperature. When two ions have similar selectivity coefficients it is often possible to add a complexing agent into the mobile phase, which will alter the ions selectivity coefficients based on their complex formation in the mobile phase [185,189].

Ion exchange resins are easily regenerated for reuse. Due to the fact the exchange of ions is a reversible stoichiometric process, unwanted ions can be removed by the addition of a

high concentration of ions with lower selectivity. Thus, the resin can easily be regenerated and reused [185].

2.2 Solvent Extraction

Also known as liquid-liquid extraction, solvent extraction (SX), is based on the principle that a solute has different distributions in two immiscible solvents, Figure 18.

Figure 18. Diagram of SX where a solute would be distributed between two immiscible solvents. In this example an organic phase, such as toluene, is on the top, and an aqueous phase, such as hydrochloric acid, is on the bottom (color added for clarity).

In general an organic and aqueous solvent are used for separations, when the solute of interest has a different solubility in each phase. A separation is achieved when the solute has distributed itself into one phase or the other. The distribution ratio of a SX system is given by:

$$\mathrm{D} = \frac{[\mathrm{Org}]}{[\mathrm{Aq}]} \qquad \text{(Eqn. 7)}$$

Where [Org] and [Aq] are the concentrations of a solute in the organic and aqueous phases respectively. The distribution ratio, D from Equation 7, is calculated after sufficient mixing time has passed so that the net change of the concentration of the solute amongst the phases remains constant. The distribution ratio can be converted to a percent extracted, %E, by:

$$\%\mathrm{E} = \frac{100D}{(1+\mathrm{D})} \qquad \text{(Eqn. 8)}$$

Where a distribution ratio of 1 indicates even distribution between phases (or 50 % extracted) and a distribution ratio of 10 indicates 90.9 % extraction [190].

Extractions are highly dependent on the organic solvent chosen. Initially the solute is present in the aqueous phase; therefore the organic solvent chosen must have high solubility for the solute or extractant molecule used. Polarity is also of concern since a non-polar solvent is used to extract a non-polar substance and vice versa. Temperature affects solubility as well, so the temperature of the system must be chosen to increase solubility of solutes if possible.

The extraction in a SX system takes place at the phase boundary. By mixing the two phases vigorously the surface area of the phase boundary increases, and consequently the time it takes for the system to reach equilibrium decreases. In order for a sufficient separation to be achieved, the distribution ratio for a given solute must be large. In order to increase the distribution ratio, an extractant molecule that forms complexes with the solute (such as a crown ether) is often added to the organic phase. This enables tuning of a system to selectively select one solute over another if the extractant molecule preferentially forms complexes with one solute and not another.

To separate two different solutes with SX, one solute is selectively extracted over the other. This occurs when the distribution ratios between each solute are significantly different for the given system. The extraction can occur one of two ways: the solute of interest is extracted into the organic phase, or the contaminants are extracted into the organic phase leaving the solute of interest in the aqueous phase. The efficiency of a separation performed using SX is determined by the separation factor:

$$\mathrm{SF} = \frac{\mathrm{D_A}}{\mathrm{D_B}} \qquad \text{(Eqn. 9)}$$

Where D_A and D_B are the distribution ratios for two different solutes A and B [190].

2.3 Extraction Chromatography

Extraction chromatography (EXC) is a form of SX in which the organic phase is the stationary phase and the aqueous phase is the mobile phase [191,192]. Extraction chromatography resins can be prepared by taking an extractant commonly used for SX experiments (such as a crown ether) and coating it onto resin beads. This is accomplished by dissolving the extractant in a volatile solvent (such as dichloromethane) and mixing it with the resin beads (such as an insoluble aliphatic polymer), allowing the solvent to slowly evaporate while mixing. Once the solvent has evaporated, the resin beads remain and are coated with the desired extractant [193]. The resins can be packed into columns and used similarly to other chromatographic techniques (Figure 19).

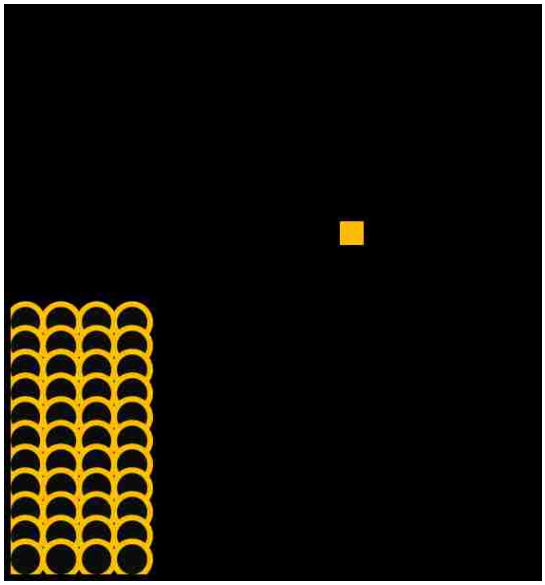

Figure 19. Cross section view of an EXC column with a coated resin being the stationary phase.

The main advantage of EXC is the combination of column chromatography performance and solvent extraction selectivity. The organic phase from SX is also eliminated thus removing the concern of producing mixed waste [194].

The height equivalent to a theoretical plate (HETP) is the efficiency of an EXC column, and is given by:

$$\mathrm{HETP} = \frac{(\mathrm{L})(\mathrm{W}^2)}{8(\mathrm{V}_{\mathrm{max}}^2)} \qquad \text{(Eqn. 10)}$$

In Equation 10, L is the length of the column bed, W is the width of the peak at 1/e times the maximum value and V_{max} is the elution volume to peak maximum [195]. A theoretical plate is the concept that represents the point at which equilibrium is established between the mobile and stationary phase with respect to solute distribution. In the case of solvent extraction, a theoretical plate represents a single stage in the extraction process. The HETP can be converted to number of theoretical plates by dividing by the length of the column, L.

Parameters such as particle size of the inert support, extractant weight loading, temperature, cross section of the column, elution rate, and the column bed length can affect the HETP value according to studies performed by Horwitz and Bloomquist [195]. Changing HETP will result in changes to the elution fraction for a given solute. For example, lower HETPs lead to higher retention times and thus larger elution volumes. Extraction by a theoretical plate in the stationary phase prevents a solute from eluting. Given a distribution ratio, Equation 7, a solute will travel down the column interacting with each plate till it elutes. The volume it requires to elute a given solute is known as the elution volume, and this can be affected by the HETP value [194,195].

Like with solvent extraction, the separation of two solutes can be accomplished through their different distribution ratios in a given system. In the case of EXC the most common way to

represent elution volumes is through the number of free column volumes to peak maximum, k', which is calculated by:

$$k' = \frac{V_{max} - v_m}{v_m} \quad \text{(Eqn. 11)}$$

Where V_{max} is the elution volume to peak maximum and v_m is the column void volume (or space within the column not occupied by the stationary phase) [195]. Due to the fact k' is independent of the column parameters, it is a very useful value. Using k' the separation factor between two solutes can be determined:

$$SF = \frac{k'_A}{k'_B} \quad \text{(Eqn. 12)}$$

To determine the width of an elution band a separation resolution must be defined:

$$SR = \frac{1}{4}\left(1 - \frac{1}{SF}\right)\left(N^{1/2}\right)\frac{k'_2}{1+k'_2} \quad \text{(Eqn. 13)}$$

Where SF is the separation factor and N is the number of theoretical plates [196].

Extraction chromatography resins can be characterized for parameters such as k' through batch experiments where free resin is used instead of a column. Radiotracers are often used in trace level studies due to the ease of which they can be detected using radioanalytical techniques. A weight distribution ratio can be measured for a given solute in batch studies using:

$$D_w = \left(\frac{A_o - A_s}{A_s}\right)\left(\frac{mL}{g}\right) \quad \text{(Eqn. 14)}$$

Where A_o-A_s is the activity sorbed on a known weight of resin, g, and A_s equals the activity in a known volume of solution, mL. To calculate k', D_w must be first converted to the volume distribution ration:

$$D_v = D_w \times \frac{d_{extr}}{w_{load}} \quad \text{(Eqn. 15)}$$

Where d_{extr} is the density of the extractant and w_{load} is the extractant loading in grams of extractant per gram of resin. It is then possible to convert D_v to k':

$$k' = D_v \times \frac{v_s}{v_m} \quad \text{(Eqn. 16)}$$

Where v_s is the volume of the stationary phase and v_m is the volume of the mobile phase. It is possible to convert from D_w directly to k':

$$k' = D_w \times F_c \quad \text{(Eqn. 17)}$$

Where F_c is the resin factor, which is a constant for a given resin and provided by the manufacturer, that accounts for the various parameters mentioned in the calculation of D_v and k' in Equations 15 and 16 [192,194].

2.4 Experimental facilities, CAMS

The production of carrier-free radionuclides for extraction studies were performed at the model FN tandem Van-de-Graaff accelerator at the LLNL Center for Accelerator Mass Spectrometry (CAMS) facility, Figure 20.

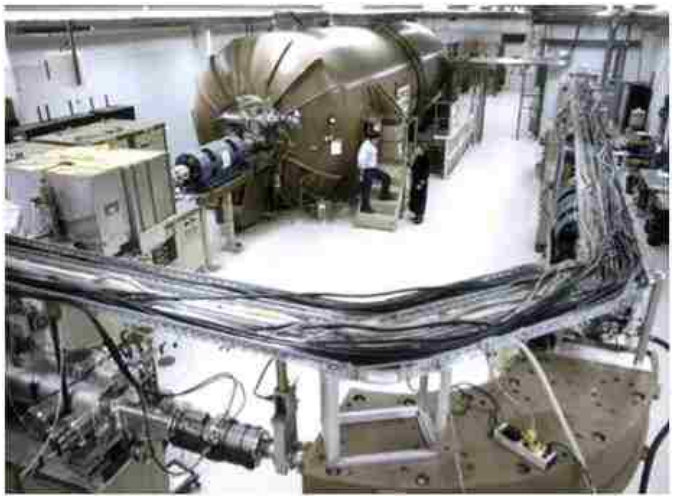

Figure 20. Lawrence Livermore National Laboratory Center for Accelerator Mass Spectrometry.

This 10 MV accelerator can typically produce up to 15 MeV protons at beam currents of 100-400 nA. A cesium-sputter ion source was utilized for production of negatively charged hydrogen ions which were introduced to the tandem accelerator at ~40 keV energy and accelerated through a

stripper gas to produce the 12-15 MeV positively charged protons for irradiation of the target materails. This energy range is suitable for proton induced production of carrier-free radionuclides. The reactions of interest for this work are: $^{124}Sn(p,n)^{124}Sb$, $^{197}Au(p,n)^{197}Hg$, and $^{113}In(p,n)^{113}Sn$, each of which have peak cross-sections in the 10-15 MeV range [197-199].

CHAPTER 3: ANALYTICAL TECHNIQUES

Solvent Extraction (SX), ion exchange chromatography (IXC), extraction chromatography (EXC), and high purity germanium (HPGe) gamma spectroscopy were the techniques in the investigation of Fl and element 115 homologs. In this chapter the general experimental procedures for each technique, and where applicable, the theory behind them are presented. An explanation for the data analysis used for each technique is also presented.

3.1 Ion exchange chromatography

Ion exchange chromatography with both anion and cation exchange was the main method used for separation of carrier-free radioisotopes. This section will describe the methods used for cleaning resin, preparing columns, and general column procedures used for these separations. Data analysis methods are also presented.

3.1.1 Resins and Preparation of Columns

For the purpose of this work, the anion-exchange resin AG 1x8 and cation-exchange resin AG 50Wx8 (both DOWEX and Bio-Rad, 100-200 mesh) were used in the separation of carrier-free activities for homolog studies (see Chapter 5). These commercial resins contain impurities both organic and inorganic from the manufacturing process. Therefore, prior to use the following conditioning procedure was used on each resin from Ref. [188]:

1. Approximately 200 g of resin was added to a 500 mL Nalgene bottle.
2. The resin was rinsed twice with 200 mL of de-ionized (DI) water (18.2 MΩ·cm).
3. The resin was then rinsed twice with 200 mL of 1 M NaOH.
4. The resin was then rinsed twice with 200 mL of DI water.
5. The resin was then rinsed twice with 200 mL 1 M HCl.
6. The resin was then rinsed twice with 200 mL DI water.
7. The resinw as then rinsed with 200 mL ethanol (95 %).
8. The resin was then rinsed twice with 200 mL DI water.
9. Finally a dilute 0.1 M HCl solution was placed over the resin to store.

When applicable the capacity of the resin was calculated from the manufacturer supplied number of ionic sites per unit volume of the resin (milliequivalents per mL) to determine the

amount of resin needed for the given separation [200]. For the majority of separations the only analytes retained by the resin were fundamentally massless (carrier-free), and therefore, a bed volume of 2 mL was chosen. All elution volumes were chosen based on the relative free column volumes for the resin used (Table 9), using several free column volumes for each elution fraction [188].

Table 9. Relative free column volumes for various commercial resins.

Resin Type	Crosslinking	Free column volume (V/V_b)	Standard deviation
Dowex 50	2	0.304	0.010
	4	0.327	0.017
	8	0.379	0.010
	16	0.395	0.016
Dowex 1	2	0.351	0.022
	4	0.350	0.012
	8	0.390	0.015
	10	0.396	0.024

Columns were first filled with water and then the resin was added drop wise (previously in 0.1 M HCl slurry, from above) was added to the column and allowed to settle by gravity. This was repeated until the desired bed volume was obtained, before either a thin layer of purified sand or a PTFE frit was added to the top of the resin, Figure 21.

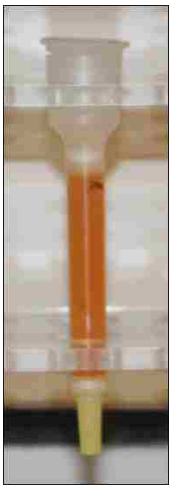

Figure 21. Column packed with 2-mL bed volume AG 50Wx8, with PTFE frit on top.

3.1.2 Column Experimental Procedure

Column procedures were loosely based on procedures described in the literature [200, 188]. Prior to use resins were conditioned by flowing 5-20 free column volumes of a solution matching the acid type and concentration of the sample load solution. In general, a sample was prepared in 1-4 mL of solution in a 15 mL PTFE centrifuge tube and counted by HPGe gamma spectroscopy to determine initial activity. This sample was loaded onto a column by gravity and the resulting fraction collected as the load fraction. Two rinses, in the same concentration and volume of the load solution, were collected as rinse fractions one and two. Then several free column volumes in fractions of the same volume as the load fraction were passed through the column to elute a desired analyte. If more than one analyte was present several free column volumes of a different acid composition was passed through the column to elute the second analyte, still in the same volume as the load fraction. In each case, the fractions were collected in a 15 mL centrifuge tube to maintain counting geometry, and analyzed by HPGe gamma spectroscopy to determine elution curves for the given separations.

3.1.3 Data Analysis

Since the counting geometry of the sample and all elution fractions were kept consistent, relative activity measurements by HPGe gamma spectroscopy could be directly compared due to equivalent counting geometries. The fractional percent eluted was calculated for each fraction by comparison to the load solution activity:

$$\text{Elution Fraction} = \frac{A_F}{A_{LS}} \qquad \text{(Eqn. 18)}$$

Where A_F is the activity (cps) of a given analyte in the elution fraction, and A_{LS} is the activity (cps) of the analyte in the initial load solution. Elution curves were constructed by plotting the elution fraction as a function of volume eluted. Error was calculated by standard error propagation techniques.

3.2 Extraction Chromatography

EXC grants the selectivity of a SX system, through the use of organic extractants, with the multi-stage extraction processes associated with chromatography. This technique was used to study the homologs of Fl and element 115, with the commercially available Eichrom Pb resin which is based on 4',4"(5")-di-tert-butyldicyclohexano-18-crown-6 (DtBuCH18C6) extractant [201]. EXC was also used for separation of carrier-free Hg from irradiated Au foils (Chapter 5). In this section the general EXC procedures and data analysis techniques for both batch and column studies are presented.

3.2.1 Procedure: Batch Studies

The experimental method for batch studies was adapted from a variety of different literature procedures [193,194,201-204]. A known amount of resin (10-20 mg) was placed into a 1.5 mL centrifuge tube and preconditioned with 1 mL of a desired acid concentration by shaking with a Grant-bio Multi-Tube Vortex Mixer, Figure 22.

Figure 22. Grant-bio Multi-tube Vortex Mixer.

Radiotracers from 20-100 µL were added to the centrifuge tube and allowed to equilibrate with the preconditioned resin by shaking. During this equilibration process each sample was taken and counted by HPGe gamma spectroscopy to determine initial activity. The sample was filtered into a new centrifuge tube using a 0.45 µm, Whatman polytetrafluoroethylene (PTFE) filter attached to a polypropylene syringe, Figure 23.

Figure 23. Removal of loose resin by 0.45 µm Whatman PTFE filter.

A 700 µL aliquot of the filtered solution was added to another centrifuge tube along with enough DI water to make the solution volume identical to the pre-filtered sample. The aliquot was taken due to the fact 50-150 µL of solution was lost during the filtration process. The samples were then counted by HPGe gamma spectroscopy to determine post-extraction sample activity.

3.2.2 Data Analysis: Batch Studies

The tracer activities before, A_o, and after, A_s, equilibration with free resin were used to determine the weight distribution ratio, D_w, as shown in Equation 14. With the A_s being calculated by multiplying the ratio of total volume to aliquot volume for the measured post-extraction sample activity. The number of free column volumes to peak maximum, k', was calculated from D_w according to Equation 17. Errors were calculated by standard deviations of replicates or from propagation of counting errors if only one replicate was performed.

3.2.3 Procedure: Column Studies

All columns for EXC were performed with 2 mL pre-packed (from Eichrom) vacuum flow columns with a 24-hole polycarbonate vacuum box (Eichrom Inc.) set to approximately 4 mmHg vacuum gauge reading which corresponded to a 1-2 mL/min flow rate, Figure 24.

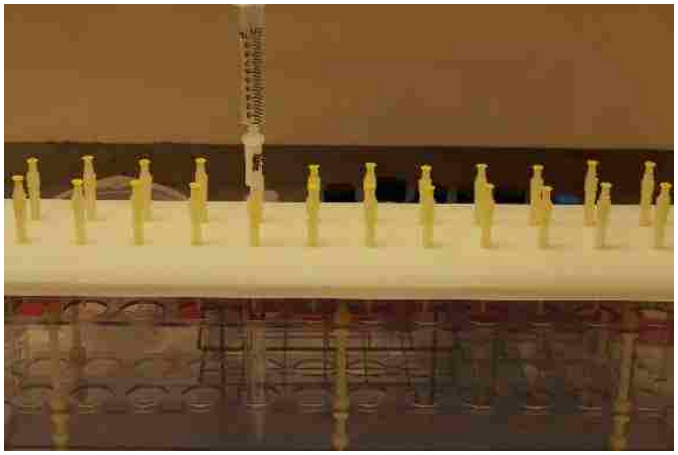

Figure 24. 24-hole polycarbonate vacuum box with vacuum flow column and reservoir.

This procedure was adapted from similar experiments reported in literature [204,205]. A 2 mL pre-packed column was placed on the vacuum box with a 10 mL syringe reservoir on top. The resin cartridge was conditioned with 10 free column volumes (FCV, ~10 mL) of an appropriate HCl load solution for the column study. A sample was prepared in 1 mL of a desired load matrix by evaporation and reconstitution (Figure 25) in a 15 mL centrifuge tube and counted by HPGe gamma spectroscopy to determine initial activity.

Figure 25. Evaporator for changing sample matrices.

The solution was loaded on to the column and sequential 1 mL fractions were collected in separate 15 mL centrifuge tubes. Care was taken to stop the column flow just as liquid was about to reach the top-frit so the column never dried and each elution fraction was a consistent 1 mL. Fractions were counted by HPGe gamma spectroscopy.

3.2.4 Data Analysis: Column Studies

The tracer activities in each elution fraction were compared to that of the load solution, and the fractional elution percentage was calculated the same way as for IXC, Equation 18. Elution curves were constructed by plotting the elution fraction against total volume. Error was calculated by propagation of counting errors in both the load solution and fractions.

3.3 Solvent Extraction

SX enables extraction of a given solute in an aqueous phase by its chemical interaction with an organic extracant present in the organic phase. For this work, SX was used to explore the extraction properties of various thiacrowns as well as to test the chemical speciation of solutes when extracted by DtBuCH18C6 (the extractant on Eichrom's Pb resin).

3.3.1 Sample Preparation and Measurement

Methods for SX experiments were adopted from similar studies presented in literature [206]. To a VWR 1.5-mL high spin centrifuge tube 480 µL of an organic phase (typically dichloromethane) with desired organic extractant was brought together with 500 µL of acid, Figure 26.

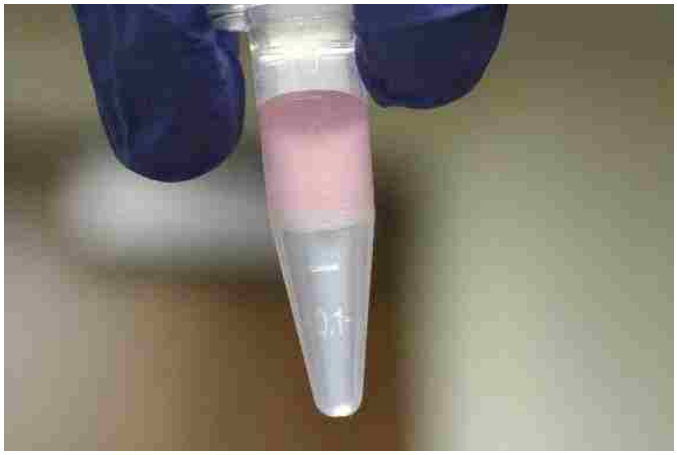

Figure 26. Organic phase (dichloromethane) and aqueous phase in VWR 1.5-mL high spin centrifuge tube (pink color of aqueous phase added for visual purposes only).

Samples were mixed for 30 minutes on a Grant-bio Multi-Tube Vortex Mixer (Figure 22, above) to allow for pre-equilibration. A 20 µL spike containing radioisotopes of interest was added to the centrifuge tubes and phases were mixed for varying amounts of time to allow equilibration. After mixing, the phases were separated by centrifuging with a RevSci micro-centrifuge, Figure 27, for 30 seconds each at 10000 rpm.

Figure 27. RevSci micro-centrifuge.

A direct displacement pipette was used to remove 300 µL of each phase and place into separate 1.5 mL centrifuge tubes, which were counted by HPGe gamma spectroscopy to determine the analytes activities in each phase.

3.3.2 Data analysis

Once activities for the desired tracer were determined in both the aqueous and organic phases by HPGe gamma spectroscopy, Equation 7 and 8 were used to determine the distribution ratio and percent extracted for each analyte. These were generally plotted as a function of acid concentration to show extraction properties.

3.5 High Purity Germanium Gamma Spectroscopy

Gamma spectroscopy is a commonly used technique for radionuclide activity and identity determination. Germanium gamma-ray detectors (HPGe) have significantly improved the ability to detect gamma-rays when compared with the traditional NaI(Tl) detector. Ultrapure germanium detectors have a much higher active volume than a low-purity detector would. This allows for a much larger region for electron hole-pairs to be created and collected. HPGe detectors must be operated at liquid nitrogen temperatures to limit the number of thermal electrons promoted to the conduction band from the valence band (limit false signals). Unlike the scintillator based NaI(Tl) gamma-ray detector, the HPGe detector detects electron-hole pairs (semiconductor) created by recoil electrons produced when a gamma-ray interacts with the detector. These electron-hole pairs create the pulses in the gamma-ray spectrum. Resolution with the HPGe detector is on average a factor of 30 better than that of a NaI(Tl) detector [207]. For the purpose of this work, HPGe gamma spectroscopy was used for activity determination for all SX, EXC, and IXC experiments performed.

3.5.1 Theory of Operation

Detection of gamma-ray photons by HPGe detectors is based on the way in which they interact with the semiconductor Ge material. These interactions occur by three main pathways: the photoelectric effect, the Compton effect, and pair production.

The photoelectric effect is an interaction in which the gamma-ray photon completely disappears by transferring all of its energy to a photoelectron from one of the Ge electron shells (usually the K-shell). The energy of the electron is given by:

$$E_e = h\nu + E_b \quad \text{(Eqn. 19)}$$

The recoil electron produces electron-holes pairs within the detector that create the detector pulse through their collection. Pulses created by the photoelectric effect are proportional to the full energy of the gamma-ray, and thus show up as the photopeaks in the spectrum [207].

Compton scattering is an interaction where a gamma-ray photon interacts with an electron creating a scattered gamma-ray photon of lower energy and a recoil electron. With the energy of the scattered electron being given by:

$$h\nu' = \frac{h\nu}{1+\left(\frac{h\nu}{m_0c^2}\right)(1-cos\theta)} \quad \text{(Eqn. 20)}$$

Where hν is the incident photon energy and θ is the angle of interaction. The maximum Compton recoil energy between incident gamma-ray energy occurs at a θ=π interaction gives rise to a simplified Equation 20:

$$h\nu' = \frac{E_\gamma}{1+4E_\gamma} \quad \text{(Eqn. 21)}$$

A gamma-ray scattered in this manner, gives rise to a backscatter peak (the γ' is scattered directly back) with energy, hν'. A pulse generated at the maximum kinetic energy for the Compton electron (recoil electron in which energy is imparted during the 180 degree Compton interaction) produces the Compton edge, which is given by [207]:

$$E_e = h\nu - h\nu' \quad \text{(Eqn. 22)}$$

Pair production occurs near the protons of the absorbing nuclei and is the creation of an electron-positron pair and the disappearance of the incident gamma-ray. Due to the fact $2m_0c^2$ (rest mass of a positron-electron pair) is required to create an electron-positron pair at least 1.02 MeV gamma-ray photons must interact to make the process energetically favorable. The kinetic energy of the positron and electron are given by:

$$E_{e^-} + E_{e^+} = h\nu - 2m_0c^2 \quad \text{(Eqn. 23)}$$

The energy deposited in the detector will be the original gamma-ray energy minus 1.02 MeV assuming both 0.511 MeV positron annihilation photos escape the crystal (double escape peak). If only one annihilation photon escapes a single escape peak will form, and if both are absorbed the energy will equal the total absorption peak energy [207].

3.5.2 HPGe Systems

Two different HPGe detectors were used for this work. A Canberra up-looking planar BEGe (broad energy germanium) detector and an Ortec side-looking coaxial detector, Figure 28 and 29 respectively.

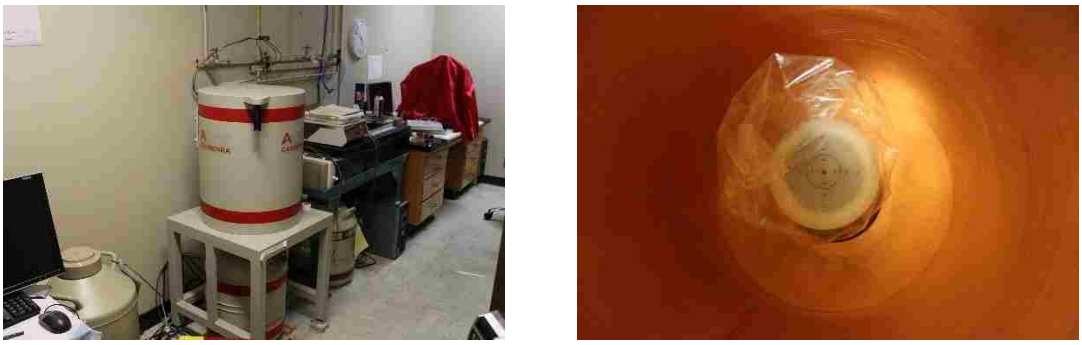

Figure 28. (Left) Canberra BEGe detector, (Right) detector sample stage.

Figure 29. (Left) Ortec HPGe detector, (Right) detector sample stage.

The Canberra detector was controlled with Genie 2000 software and the Ortec detector was controlled with the MAESTRO software.

3.5.3 Detector Calibration

Due to the fact all measurements in this work were relative measurements taken in the same exact geometry before and after separations, efficiency calibrations were not required. Periodically throughout experiments the peak resolution and energy was checked for drift, and no observed drifts were seen. Energy calibration was performed by with the respective software by counting a ^{152}Eu source for five minutes 5 cm from each detector face, then performing an energy calibration using 10 gamma lines ranging from 0-1.6 MeV, Table 10.

Table 10. ^{152}Eu gamma-rays used for detector calibration [208].

Energy (keV)	Intensity (%)
121.78	28.58
244.70	7.58
344.28	26.5
411.12	2.23
867.38	4.25
964.08	14.61
1085.87	10.21
1089.74	1.727
1299.14	1.62
1408.01	21.01

3.5.4 Sample Analysis

Samples for HPGe measurement were prepared with 1 mL to 1.1 mL of solution in either a 1.2, 1.5 or 15-mL centrifuge tube. In the case of the Canberra detector a sample holder was placed directly on the carbon entrance window, Figure 28, and the ORTEC detector had sample holders that could be fit into various distances, Figure 29. In each case the sample distance and geometry was held constant between pre-separation and post-separation samples.

Each sample was counted until at least 100 counts were obtained for very low activity samples, but in general 1000 counts (or 3 % error) were desired.

3.5.5 Data Analysis

Data analysis was performed by placing regions of interest (ROI) a few channels to the left and right of the desired photopeaks from Table 11, and using the Genie 2000 or MAESTRO reported peak areas for each peak.

Table 11. Gamma energies used for analysis of desired radionuclides [208].

Isotope	Gamma Energy (keV)	Intensity (%)
^{212}Pb	238.6	43.3
^{212}Bi	727.33	6.58
^{207}Bi	596.70	97.74
^{113}Sn (^{113m}In)	391.69	64.2
^{124}Sb	602.73	98.26
^{120m}Sb	197.3	87.0
^{197m}Hg	133.99	33
^{197}Hg	191.44	0.63
^{196}Au	355.68	87
^{198}Au	411.80	96

There was no observed detector energy drift, therefore, the same ROI was used for each experiment. Due to the fact each samples geometry was kept consistent for a given experiment direct comparisons before and after separations were possible without taking into account detector efficiency.

CHAPTER 4: SYNTHESIS OF HEXATHIA-18-CROWN-6

This chapter describes the detailed synthesis of the hexathia-18-crown-6 extractant, Figure 30.

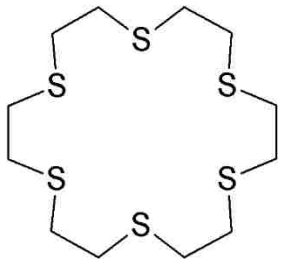

Figure 30. Hexathia-18-crown-6.

The synthesis was based on following the procedure by R. E. Wolf, Jr. *et al.* [209]. Though this synthesis is not novel, it is presented here to show the process used as well as the estimated purity of the product used for experiments performed.

4.1 Materials and Reagents

The 2,2'-thiobis(ethanethiol) (≥ 90 %) was purchased from Alfa Aesar and purified by vacuum distillation prior to use. Sodium metal (99.95 %) was purchased from Alfa Aesar and cut into small pieces under oil prior to use. Small bottles of 2-chloroethanol (≥ 99 %) were purchased from Alfa Aesar and used immediately upon opening. Dichloromethane (DCM, ≥ 99.6 %) was purchased from Acros Organics and used as received. Thionyl chloride (≥ 99 %) was purchased from Alfa Aesar and vacuum distilled prior to use. Acetone (≥ 99.5 %) was purchased from BDH and used as received. Methanol (≥ 99.8 %) was purchased from Alfa Aesar and used as received. Dimethylformamide (DMF, ≥ 99.8 %) was purchased from J.T. Baker and always used from a freshly opened bottle without further purification.

4.2 Experimental

4.2.1 Step 1: Synthesis of 2,2'-[Thiobis(2,1-ethanediylthio)]bis(ethanol).

The experimental set up is depicted in Figure 31.

Figure 31. Experimental set up showing reaction vessel, rotary evaporator and distillation apparatus.

Under a nitrogen atmosphere, to a 1 L three neck round bottom flask equipped with a reflux condenser and addition funnel, approximately 11 g of Na metal was added slowly to 500 mL ethanol, Figure 32.

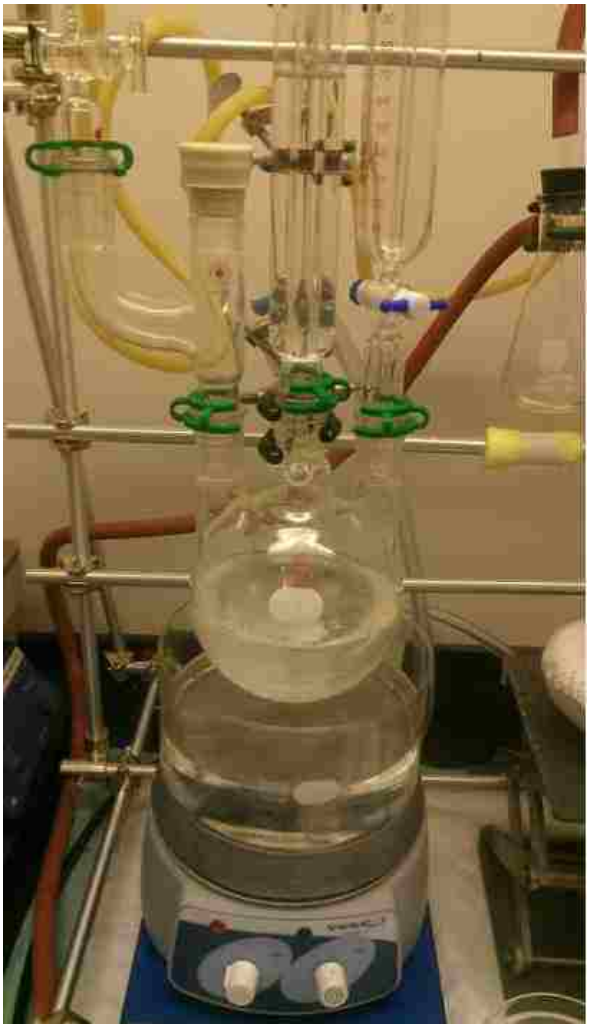

Figure 32. Addition of Na metal under nitrogen atmosphere to ethanol.

After complete reaction approximately 39 g of 2,2'-thiobis(ethanethiol) was added via the addition funnel, and the solution brought to reflux in an oil bath (round bottom flask wrapped with tinfoil to allow for uniform heating), Figure 33.

Figure 33. Reflux of 2,2'-thiobis(ethanethiol) with NaOEt.

The solution was allowed to reflux for 10 hours before being cooled and then dissolved in 500 mL hot acetone and filtering to remove crystalized NaCl that formed, Figure 34.

Figure 34. 2,2'-[Thiobis(2,1-ethanediylthio)]bis(ethanol) product with NaCl prior to dissolving in hot acetone and filtering.

Upon evaporating the acetone approximately 45 g of 2,2'-[Thiobis(2,1-ethanediylthio)]bis(ethanol) was formed, confirmed by NMR spectroscopy in $CDCl_3$. The reaction for the above procedure is:

$$HS(CH_2)_2S(CH_2)_2SH + 2NaOEt + 2Cl(CH_2)_2OH \rightarrow HOCH_2(CH_2SCH_2)_3CH_2OH$$

4.2.2 Part 2: Synthesis of 1,1'-[Thiobis(2,1-ethanediylthio)]bis[2-chloroethane].

Approximately 8 g of the 2,2'-[Thiobis(2,1-ethanediylthio)]bis(ethanol) product from step one was added to a 500 mL round bottom flask with a three neck adapter on top along with 200 mL distilled DCM. Attached the round bottom flash was a Drierite drying tube, a pressure equalizing addition funnel and a valve blocking the third neck, Figure 35.

Figure 35. Drierite drying tube during reaction.

From the addition funnel 8.0 mL distilled $SOCl_2$ dissolved in 25 mL DCM was added drop wise to the reaction vessel. Vigorous gas evolution occurred and the solution was allowed to stir for 6 hours before being quenched with 5 mL methanol. The resulting solution was rotary evaporated to dryness (a pasty solid), Figure 36.

Figure 36. 1,1'-[Thiobis(2,1-ethanediylthio)]bis[2-chloroethane] product during rotary evaporation.

Care was taken to not bump the solution due to the low boiling point of DCM, the final product after evaporation is shown in Figure 37.

Figure 37. 1,1'-[Thiobis(2,1-ethanediylthio)]bis[2-chloroethane] product after evaporation.

After rotary evaporation the resulting solution was pumped on overnight with 0.5mmHg vacuum to remove excess HCl residue. The reaction for the above procedure is:

$$\mathrm{HOCH_2(CH_2SCH_2)_3CH_2OH + 2SOCl_2 \rightarrow\ ClCH_2(CH_2SCH_2)_3CH_2Cl + 2SO_2 + 2HCl}$$

4.2.3. Step 3: Synthesis of Hexathia-18-Crown-6.

The 1,1'-[Thiobis(2,1-ethanediylthio)]bis[2-chloroethane] obtained previously was dissolved in 150 mL of DMF, from a fresh bottle, along with approximately 5 g of 2,2'-thiobis(ethanethiol). The resulting solution was placed in a 250 mL Hirschberg constant addition funnel, Figure 38.

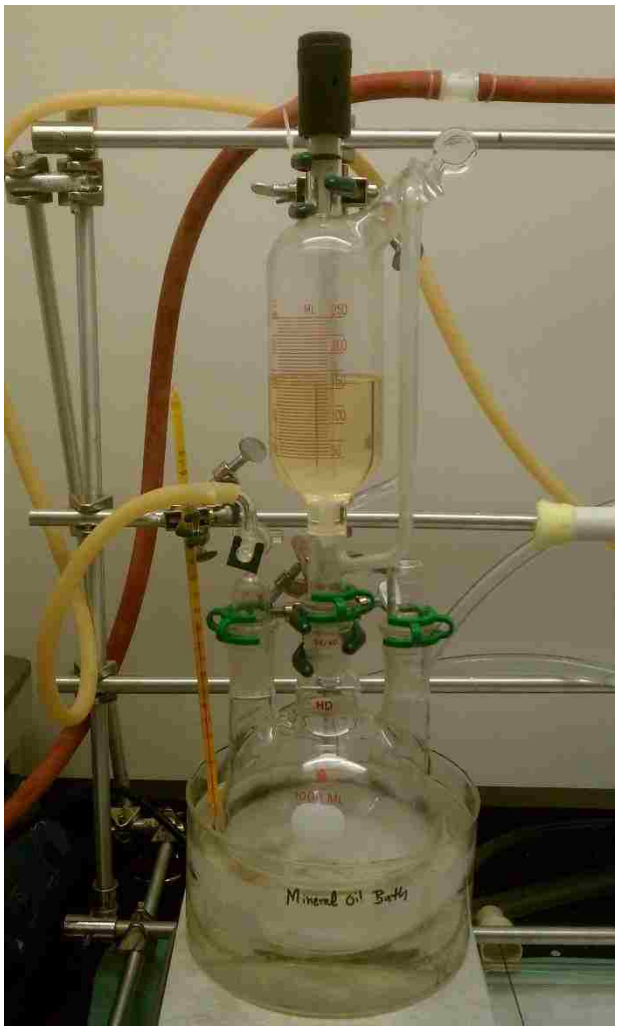

Figure 38. Hirschberg constant addition funnel with reaction products.

The Hirschberg constant addition funnel was used to add the solution over a 36 hour period to a round bottom flask containing approximately 13 g of Cs_2CO_3 in a suspension with 350 mL DMF at

50-55 °C . After complete addition stirring was continued for 1 hour, before removing the solvent by vacuum distillation (1 mmHg), Figure 39.

Figure 39. Removal of solvent from formed HT18C6.

The residue was stirred with 300 mL DCM and filtered. The filtrate was washed three times with 80 mL 1 M NaOH, followed by one time with 100 mL water and then was dried over Na_2SO_4. The dried solution was evaporated by vacuum, like in Figure 39, before being recrystallized from a 4:1 hexane-acetone solution. The product was analyzed with NMR spectroscopy. The reaction for the above procedure was:

$$HS(CH_2)_2S(CH_2)_2SH + ClCH_2(CH_2SCH_2)_3CH_2Cl + Cs_2CO_3 \rightarrow HT18C6 + 2CsCl + H_2O + CO_2$$

4.3 Results and Discussion

The primary focus of this chapter was to describe the synthesis of the HT18C6 used in experiments throughout this dissertation. Figure 40 shows a vial containing the final synthesized product.

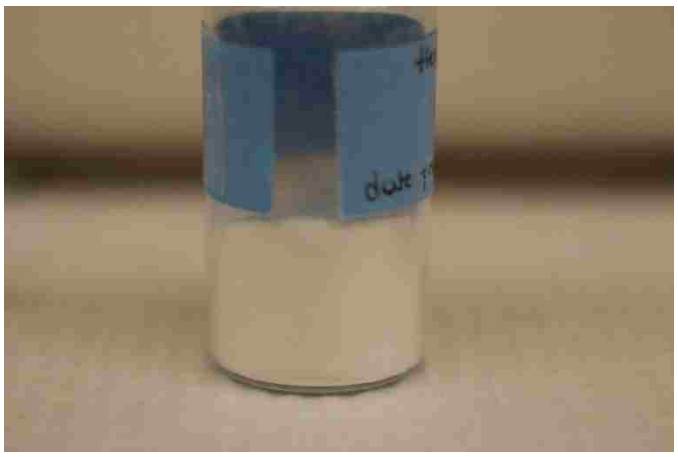

Figure 40. HT18C6 product.

Conformation of the product and its purity was confirmed by NMR spectroscopy from $CDCl_3$, Figure 41.

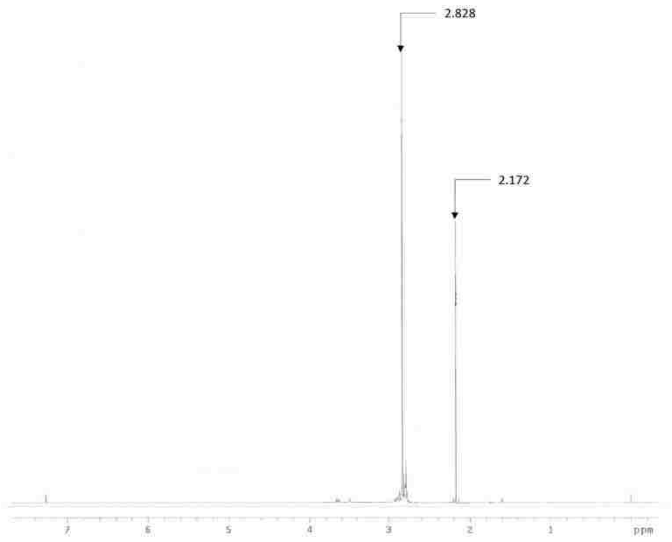

Figure 41. ^{1}H NMR spectra of HT18C6 product in CDCl3.

As can be seen in Figure 41, a singlet at 2.828 is prominent in the spectra with the other singlet at 2.172 being from ethanol present in the sample. The singlet at 2.828 is consistent with the literature expected singlet at 2.82 [209]. From the magnitude of the other peaks in the spectrum, the purity of the synthesized HT18C6 is ≥ 90 %. From GC-MS analysis (Performed by Dr. Carolyn Koester, LLNL) potential impurities found are summarized in Table 12.

Table 12. GC-MS analysis of potential impurities (Performed by Dr. Carolyn Koester, LLNL).

Tentative Identification	Retention Time (min)
dithiolane	9.90
dithiane	11.77
sulfur mustard	13.87
dimethylbenzaldehyde	14.64
trithiepane	17.47
di-tert-butylphenol	19.45
bis(chloroethylthio)ethane	22.22
unknown aromatic compound	25.41
tetrathiacyclododecane	28.54
unknown sulfur-containing compound (MW=360?)	32.95
unknown sulfur-containing compound (MW=300?)	35.00

Most of the impurities in Table 12 are either incomplete cyclization products, trace starting materials, or impurities picked up from DCM in the plastic centrifuge tubes samples were kept in.

4.4 Conclusions

From the brief results described above, it can be seen that HT18C6 was synthesized in rather high purity. For the purpose of experiments performed below, HT18C6 was used without further purification, as the goal was to test its suitability for further investigation.

CHAPTER 5: PRODUCTION OF CARRIER-FREE RADIONUCLIDES

As mentioned in Chapter 1, the chemical investigation of the transactinides is performed one atom-at-a-time. Therefore, it is impossible for a transactinide to interact with another atom of the same element [15], so homolog studies must approximate this condition as close as possible. As a result, homolog studies of transactinides must, therefore, be carried out on-line (atom-at-a-time) or with carrier-free (low concentration, massless) ultratrace radionuclides.

Carrier-free radionuclides can be readily produced in charged particle reactions since the target and the product are different elements and can be subsequently separated from one another [210]. Typical tracers produced for this work utilized proton-bombardment reactions on stable target materials; however, heavier charged particles such as helium can also be used. The Fl homolog, Sn, and pseudo-homolog, Hg, as well as the element 115 homolog, Sb, were produced by proton reactions on stable foils. The other homologs of Fl and element 115, Pb and Bi respectively, were obtained carrier-free by separation from the natural decay chain of ^{232}U (see section 5.6) [211]. Although excitation functions for the ^{124}Sn(p,n)^{124}Sb, ^{197}Au(p,n)^{197}Hg, and ^{113}In(p,n)^{113}Sn reactions have been reported in literature, separation methods of carrier-free activity from the Sn, Au, and In target materials are lacking [197-199].

The production methods of carrier-free Sn isotopes in literature are based on the isolation of ^{113,110}Sn in the production of ^{113m,110}In generators for radiopharmaceutical applications [212,213]. The production of carrier-free Hg has been described from high energy reactions designed to produce a packet of different radionuclides through the bombardment of Au targets with ^{7}Li and ^{12}C beams and subsequent separation of the carrier-free products from the excess Au [214]. The production of ^{124}Sb is often not carrier-free, and it is commonly used as a gamma-ray calibration source and in radiopharmaceutical production methods [215].

High purity natural In, Sn, and Au foils were irradiated at the LLNL CAMS facility (described in Chapter 2.4) to produce the carrier-free ^{124}Sb, ^{113}Sn, and $^{197m/g}$Hg radionuclides for the homolog studies of Fl and element 115. In this chapter the production routes as well as methods for rapidly separating the carrier-free activities from bulk target materials is described. New methods for preparation and use of a ^{212}Pb generator are also described.

5.1 Experimental Production of ^{124}Sb, ^{113}Sn and $^{197m/g}$Hg

Natural Sn (0.05 mm thick, 99.999%) and In foils (0.05 mm thick, 99.999%) were obtained from Goodfellow and Au foils (0.025 mm thick, 99.95%) were obtained from Alfa Aesar and used as received. Reagents for the separations were prepared from trace-metal grade acids and de-ionized (DI) water (18.2 MΩ·cm). Eichrom TEVA resin (50-100 µm, 40 % w:w), BioRad AG 1x8 (100-200 mesh) and AG 50Wx8 (100-200 mesh) were cleaned prior to use (procedure described in Chapter 3).

Foils were cut into 8x8 mm squares weighing 20-50 mg and placed in a target chamber (Figure 42). Foils of different types were separated by 0.01 mm Ta catcher foils. Separate irradiations were performed with various different foil stacks consisting of Au, In, and Sn foils. The foil stacks were irradiated for 6-8 h with 12-15 MeV protons at a current of 100-400 nA at the tandem Van-de-Graaff accelerator at CAMS (further described in Chapter 2.4). The foils were allowed to cool for 8-12 h at the end of the irradiation before being removed from the target chamber.

Figure 42. CAMS target chamber for irradiations of stable metal foils: copper cooling block with aluminum clamp to hold foil stack in place (left) and the irradiation chamber as installed at the CAMS beamline (right).

5.2 Isolation of ^{113}Sn

5.2.1 Experimental

The procedure for the isolation of ^{113}Sn from the irradiated ^{nat}In foil is based on results presented in Ref. [188,213]. The ^{nat}In foil was dissolved in 4 mL of concentrated HCl and set to evaporate to dryness at 90 °C, with the low temperature chosen to prevent volitalization of Sn [151]. The dry residue was reconstituted in 4 mL of 1 M HCl plus 0.5 mL of 30 % H_2O_2 in order to oxidize the Sn to the Sn^{4+} state. A 2-mL bed volume of AG 1x8 (100-200 mesh) anion-exchange column was prepared and conditioned with 10 mL of 1 M HCl. The solution containing the dissolved foil was loaded onto the column, running under gravity, and the empty container was rinsed twice with 4 mL of 1 M HCl. Under these conditions the ^{nat}In target material was expected to pass through the column and the carrier-free ^{113}Sn would be retained . An additional four 4-mL fractions of 1 M HCl were passed through the column to ensure all ^{nat}In foil was eluted, and each 4-mL fraction was collected and analyzed individually by HPGe gamma spectroscopy for ^{113m}In content. The ^{113}Sn was then eluted with five 4-mL fractions of 3 M HNO_3, which were analyzed for ^{113m}In content initially and after one day had passed to allow for the ^{113m}In to reach secular equilibrium with its parent, ^{113}Sn. The ^{nat}In fractions were also counted one day later to

ensure that all of the ^{113m}In had decayed out and the samples were at background, indicating the absence of ^{113}Sn. Separations were performed approximatelly one day after irradiation to ensure ^{113m}In was in equilibrium with ^{113}Sn.

5.2.2 Results and Discussion

The speciation of In in the 1 M HCl column load solution should be dominated by the neutral $InCl_3$ complex which is not retained on the anion-exchange resin [188]. However, Sn^{4+} in 1 M HCl forms a stable anion complex, $SnCl_6^{2-}$, which is strongly retained on the column [151,188]. Since ^{113}Sn ($t_{1/2}$=115.1 days) has no characteristic gamma-rays, its activity is measured by the daughter, ^{113m}In (E_γ=391.69 keV, $t_{1/2}$=1.658 h), once in secular equilibrium. The ^{nat}In is also traced through the ^{113m}In activity by counting early before its ingrowth from ^{113}Sn, and counting later to see if the ^{113m}In has decayed out (indicating no ^{113}Sn contamination). Figure 43 shows the gamma spectrum of the activated ^{nat}In foil.

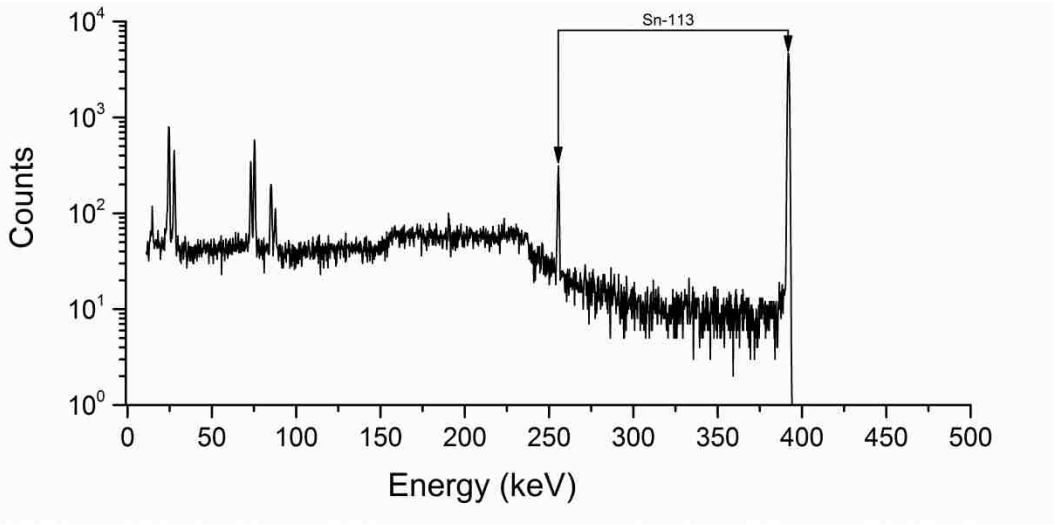

Figure 43. Gamma spectrum of activated ^{nat}In containing ^{113}Sn.

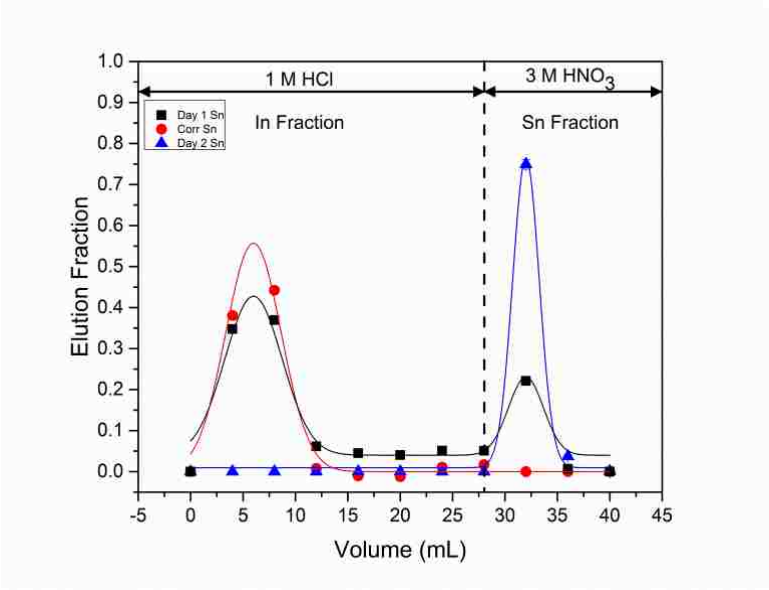

Figure 44. Elution curves for ^{nat}In/^{113}Sn separation, ^{nat}In fraction from initial day counts of ^{113m}In, with ^{113}Sn fraction from day two counts after equilibration of ^{113m}In. Errors presented are calculated from counting statistics.

The “Day 1 Sn" in Figure 44 shows the counts immediately following the elution of ^{nat}In and ^{113}Sn. As mentioned above, since ^{113}Sn has no gamma-rays associated with its decay, the ^{113}Sn elution is shown by the "Day 2 Sn" curve when ^{113m}In has reached secular equilibrium with ^{113}Sn. The corrected day one curve, "Corr Sn," takes into consideration both the growth of ^{113m}In in the presence of ^{113}Sn on the column and decay of ^{113m}In in the ^{nat}In fraction based on the count times and elution times. From this curve it is apparent that all of the ^{nat}In as traced by the ^{113m}In activity is in the ^{nat}In fraction, and the ^{113}Sn fraction is clean of any ^{nat}In. After the evaporation of the ^{113}Sn fraction, it was noted that no visible residue was present while the ^{nat}In fraction contained the solid ^{nat}In when it was evaporated to dryness. The total recoveries of In and Sn were: 100 ± 20 % and 78.7 ± 1.4 % respectively. The losses of Sn are attributed to the amount remaining on the column, presumably due to slow elution kinetics. It was not possible to quantify the In in the ^{113}Sn fraction due to the ingrowth of ^{113m}In during the slow elution process,

which also made accurate decay correction of the ^{113m}In in the In fraction difficult leading to the large error on In recovery.

5.3 Isolation of $^{197m/g}$Hg

5.3.1 Experimental

The separation of ^{197}Hg from Au target material was based on the Aliquot 336 liquid-liquid extraction described in Ref. [214]. Eichrom's TEVA resin, which contains 40% w:w Aliquot 336 as an extractant, was chosen for this separation with Aliquot 336 acting as a selective anion exchanger. Initial batch experiments were performed to establish the uptake of Hg and Au on Eichrom's TEVA resin. To a 1.5-mL centrifuge vial, 5-10 mg TEVA resin were weighed and added along with appropriate amounts of HNO_3 with varying concentrations from 0.001 M to concentrated was added. The resin and acid were placed on a rotary mixer for 1 hour to precondition the resin. A 20 µL spike containing either carrier-free ^{195}Au or ^{197}Hg tracer in 2.0 M HNO_3 was added to the wet resin. The solutions were each equilibrated for 3 hours on the mixer, counted with a HPGe detector for 120 to 900 seconds (≥1000 counts for the desired photo-peak), and then filtered through a 0.45 µm polytetrafluoroethylene (PTFE) filter to completely separate the resin from the solution. A 700 µL aliquot of each filtered solution was added to 320 µL de-ionized water in a 1.5 mL centrifuge vial (to maintain initial counting geometry) and counted for 300 to 84600 seconds (depending on activity) with an HPGe detector. The experimental parameters for the column study were then established based on the results from this batch study. The Au foil was dissolved in 800 µL of aqua regia and evaporated to approximately 300 µL in total volume. This solution was diluted to 2 mL by adding 1.7 mL of 1 M HNO_3. Two pre-packed, 2-mL vacuum flow Eichrom TEVA columns were stacked on top of each other, to accommodate the excess Au mass. A 24-hole polycarbonate vacuum box (Eichrom, Darien, IL, USA) with a pressure regulator was used to accelerate the elution

process by maintaining a flow rate of ~1 mL/min. The columns were conditioned with 10 mL of 1 M HNO_3 prior to use. The Au foil solution was added to the column, and two 2-mL rinses with 1 M HNO_3 were performed. The ^{197}Hg was stripped off the column with 12 mL of 12 M HNO_3. This fraction was analyzed by HPGe gamma spectroscopy to ensure the ^{197}Hg had been eluted and no ^{198}Au (produced via neutron capture by the scattered neutrons produced during the irradiation) was present in this fraction. Under these conditions the Au foil was expected to remain on the column.

5.3.2 Results and Discussion

The extractant Aliquot 336, on the Eichrom TEVA resin, is an anion-exchanger [216]. In a 1 M HNO_3 column load solution, it is expected that the majority of the Hg will be in the form $Hg(NO_2)_2$; however, a small amount (accounting for the 10-15% loss, discussed below) forms a kinetically slow to reverse $[Hg(NO_2)_4]^{2-}$ complex which is retained by the column. Under the same conditions, Au forms species strongly absorbed by the resin, as observed in other anion-exchange resins [214,217]. The Hg behavior was assessed by gamma spectroscopy of the ^{197m}Hg (E_γ=133.99 keV, $t_{1/2}$=23.8 h) isotope [208]. Due to the scattered neutrons (produced in the (p,n) reaction) at the target chamber, ^{198}Au (E_γ=411.80 keV, $t_{1/2}$=2.70 d) was also produced via the ^{197}Au(n,γ)^{198}Au reaction which yielded a convenient tracer for quantifying the Au content in the elution fractions [208]. Figure 45 shows the gamma spectra of the irradiated Au foil and the ^{197}Hg elution fraction.

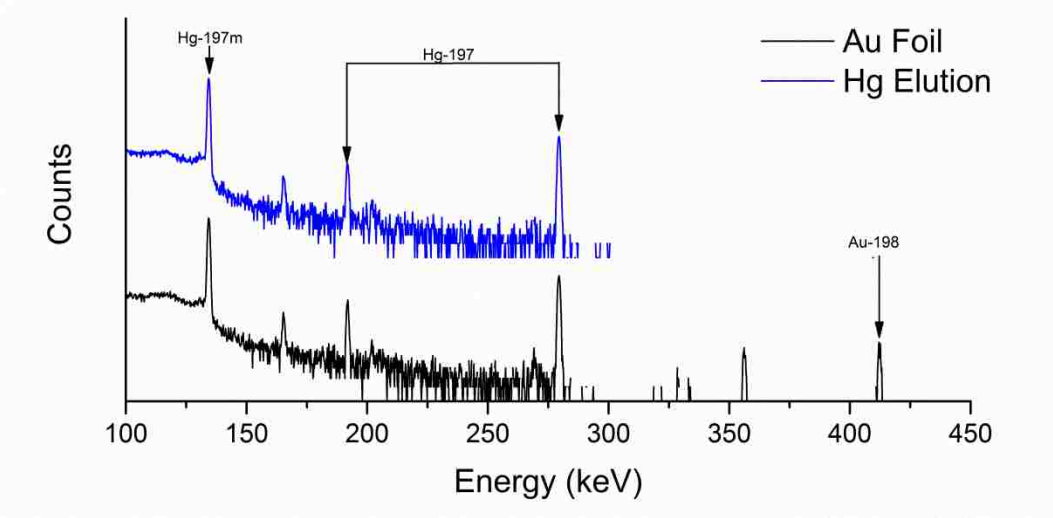

Figure 45. Gamma spectra of the irradiated Au foil (bottom line) and the ^{197}Hg elution fraction (top line).

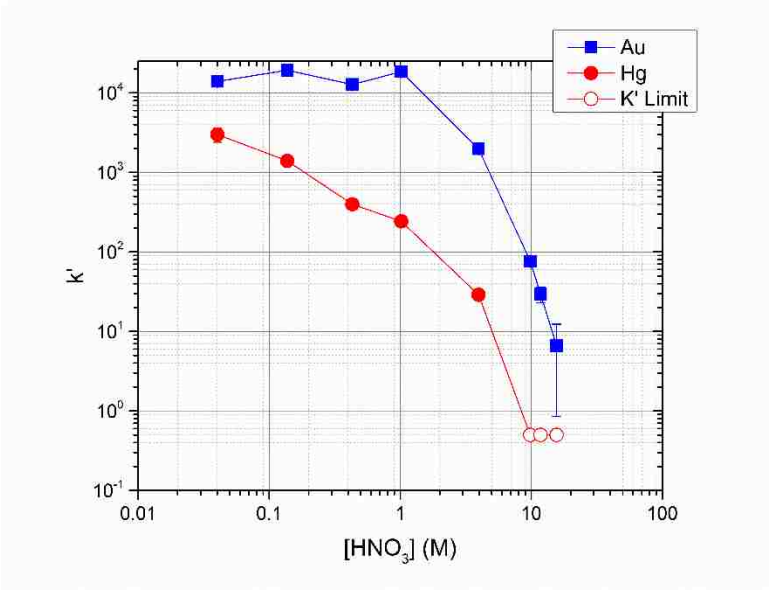

Figure 46. The batch uptake (k') of ^{195}Au and ^{197}Hg as a function of nitric acid media on TEVA resin (50-100 µm) with a 3 hour equilibration time. Errors represent counting statistics.

As can be seen in Figure 46, both Au and Hg have strong uptake at the load condition of 1 M HNO_3, but Hg extraction is negligible above 10 M HNO_3 while Au is still strongly sorbed up to ~13 M HNO_3. Due to the fact the Au foil was left on the TEVA columns, no elution curve was

obtained; however, the Au band, which was visible on the columns, moved to about 1/3rd (4 cm of the total 6 cm column height) of the way down the second TEVA column. Table 13 summarizes the results from three individual Au foil separations.

Table 13. Summary of Au/Hg separation on Eichrom's TEVA resin

Au Foil	Au in Hg Fraction (%)	Hg Recovery (%)
Au1	<<< 3.2	85.8 ± 0.6
Au2	<<< 4.7	87.1 ± 0.6
Au3	<<< 3.9	87.8 ± 0.6

In each ^{197}Hg fraction no detectable ^{198}Au was observed indicating a complete separation of Hg from Au. The "Au in Hg fraction" column from Table 13 is a calculated limit based on the minimum detectable activity [207]. Upon evaporation of the Hg fraction no visible residue was observed.

5.4 Isolation of ^{124}Sb

5.4.1 Experimental

The isolation of ^{124}Sb from ^{nat}Sn was based on distribution ratios presented in Ref. [218,219]. The ^{nat}Sn foil was dissolved in 1 mL of concentrated HCl and 20 µL of 30 % H_2O_2 was added to ensure the oxidation to Sb^{5+} and Sn^{4+}. A 2 mL bed volume AG 50Wx8 cation-exchange column was prepared and conditioned with 10 mL of concentrated HCl. The solution containing the dissolved ^{nat}Sn foil was added to the column and ten 1 mL fractions of concentrated HCl were collected. Under these conditions the Sn was expected to pass through the column, while the Sb would be retained. The Sb was stripped off the column by collecting ten, 1 mL fractions consisting of concentrated HCl and 0.05 M HI.The Sb activity was monitored by HPGe gamma spectroscopy of ^{124}Sb, where as the Sn was monitored by ^{117m}Sn from the decay of produced

^{117}Sb ($t_{1/2}$=2.80 h). The separations were performed approximately one day after irradiation allowing the ^{117m}Sn daughter to reach equilibrium with the ^{117}Sb parent nucleus. A second experiment was performed in order to produce elution curves, with an activated Sn foil which had been allowed to decay until only the ^{124}Sb activity remained before undergoing the same separation mentioned above with an aliquot of ^{113}Sn (from the above purification) added to trace the Sn foil.

5.4.2 Results and Discussion

Speciation of Sb^{5+} in concentrated HCl is presumably $SbCl_6^-$, which, contrary to common thought, has high retention on the cation exchange-resin AG 50Wx8 as described in the literature [219]. Tetravalent tin, however, forms the stable $SnCl_6^{2-}$ in HCl concentrations above 0.7 M as mentioned above, and passes through the column under the concentrated HCl load solution [151]. Figure 47 shows an HPGe gamma spectrum of an activated Sn foil soon after irradiation and after Sb separation, with Sn activity monitored by ^{117m}Sn (E_γ=156.0 keV, $t_{1/2}$=13.60 d) and Sb activity from ^{120m}Sb (E_γ=1171.3 keV, $t_{1/2}$=5.76 d) and ^{124}Sb (E_γ=602.8 keV, $t_{1/2}$=60.20 d) [208].

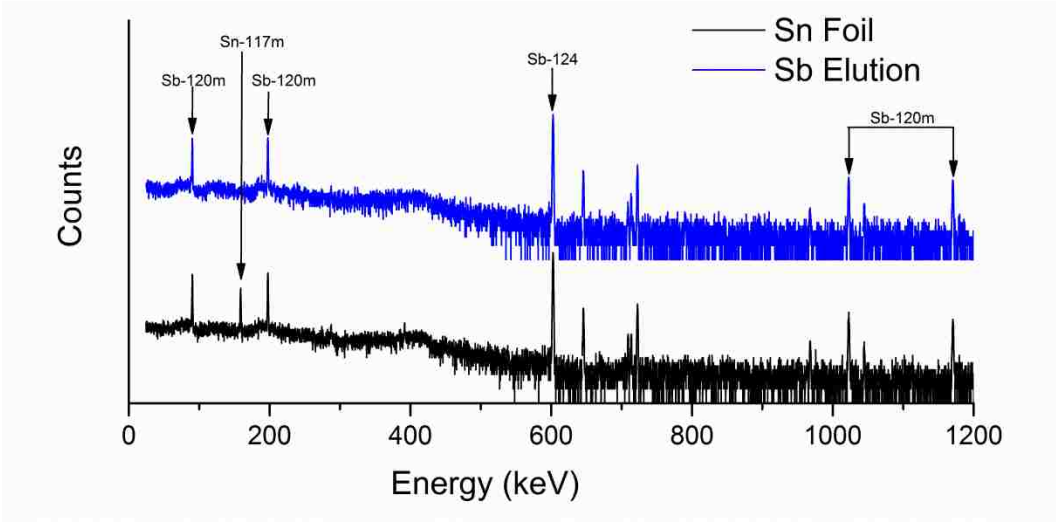

Figure 47. Gamma spectra of the irradiated ^{nat}Sn foil (bottom line) and the Sb combined elution fraction (top line).

The elution cures presented in Figure 48 are from a separation of an activated Sn foil performed long after decay of all short lived Sb products and ^{117m}Sn with only ^{124}Sb remaining, using a small aliquot of ^{113}Sn to trace the Sn foil.

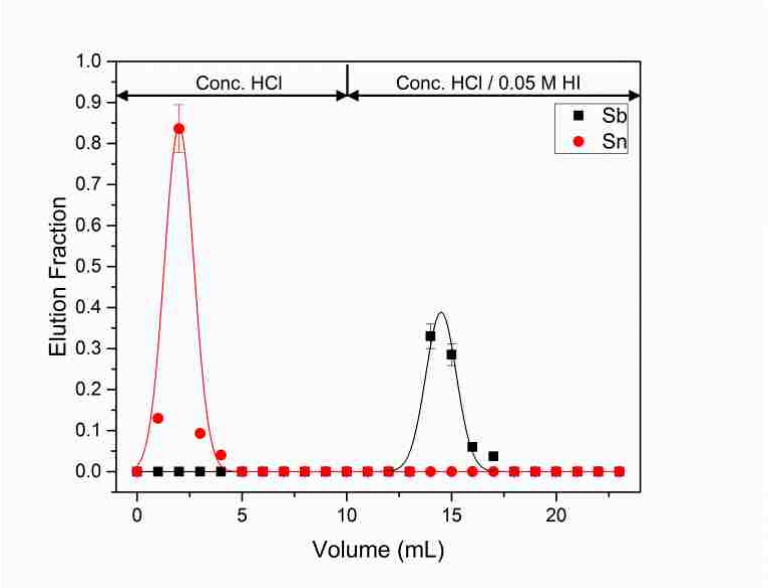

Figure 48. Elution curves for Sn and Sb. Errors represent counting statistics.

As shown in Figure 47 and 48, an efficient separation of ^{124}Sb from the irradiated ^{nat}Sn foil is obtained. Due to the slow Sb elution kinetics and the desire to obtain as small of an elution volume as possible since evaporating extremely volatile ^{124}Sb fractions was needed to change the solution matrix, no more than 10 mL of the concentrated HCl and 0.05 M HI solution was used [220]. As a result, only 71.2 ± 7.7 % ^{124}Sb was recovered while the rest presumably remained on the column.

5.5 Additional Sb and Sn Separations

The above separations presented in sections 5.2 and 5.4 for the isolation of ^{113}Sn and ^{124}Sb were the same procedures used to obtain carrier-free activity for all experiments involving Sn and Sb. However, prior to settling on these separation procedures, other procedures were used to isolate ^{113}Sn and ^{124}Sb that were deemed less efficient. These procedures are briefly presented in this section.

5.5.1 Additional ^{113}Sn Separation Experimental and Results and Discussion

The isolation of ^{113}Sn from ^{nat}In was based on distribution ratios presented in Ref. [221,222] The ^{nat}Sn foil was dissolved in 6 mL of concentrated HCl, and a 1 mL aliquot was diluted with DI water to 2 mL making the solution 6 M in HCl. An additional 150 µL of 30 % H_2O_2 was added to ensure oxidation to Sn^{4+}. A 7-mL bed volume AG 1x8 (100-200 mesh) anion-exchange column was prepared and conditioned with 12 mL of 6 M HCl. This column is large enough to retain the In target mateiral. The solution containing the dissolved ^{nat}In foil was added to the column and rinsed with two, 4-mL 6M HCl fractions (both Sn and In should be retained by the column under these conditions). Six, 4-mL fractions of 0.6 M HF were collected to elute the ^{nat}In target material while the ^{113}Sn is retained on the column, and each fraction was analyzed individually by HPGe gamma spectroscopy for ^{113m}In content. An additional three, 4-mL 6 M HCl

fractions were collected to remove excess flourides from the system. Finally, ^{113}Sn was eluted with eight, 3 M HNO_3 fractions, which were analyzed for ^{113m}In content initially and after one day had passed to allow for the ^{113m}In to reach secular equilibrium with its parent, ^{113}Sn. The ^{nat}In fractions were also counted one day later to ensure that all of the ^{113m}In had decayed out and the samples were at background, indicating the absence of ^{113}Sn.

The speciation of In in the 6 M HCl column load solution should be dominated by the neutral $InCl_3$ complex, which is not retained on the anion-exchange resin [188]. As mentioned in section 5.3.2, Sn^{4+} in 6 M HCl forms a stable anion complex, $SnCl_6^{2-}$, which is strongly retained on the column [151,188].

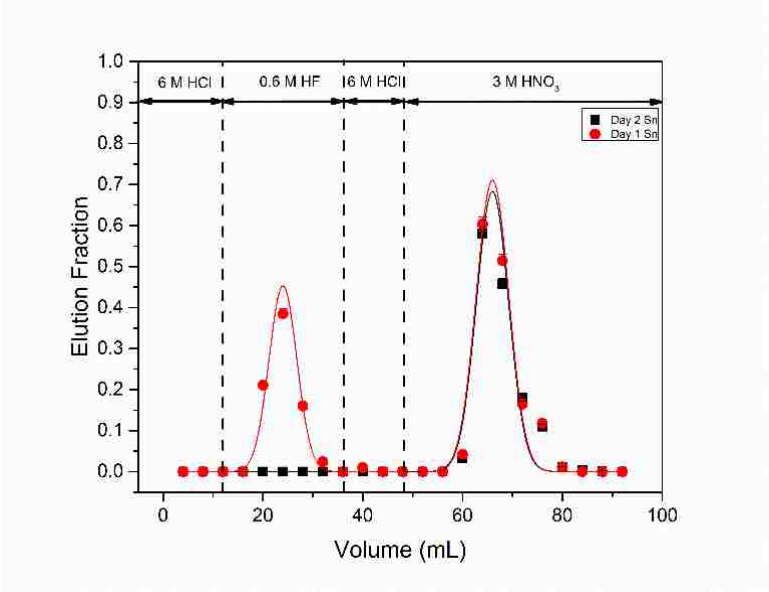

Figure 49. Elution curves from the initial attempt to separate ^{113}Sn from ^{nat}In, errors from counting statistics.

The day 1 counts in Figure 49 represent the counting data collected immediately after elution and the In fraction is not decay corrected due to lack of time information (time between beginning to collect each fraction and counting each fraction was not recorded) on this

particular separation. The reason that the day 2 counts show nearly the same ^{113}Sn activity is because several half-lives had passed before the Sn fraction was counted on day one, allowing for most of the ^{113m}In activity to have grown in. However, as expected, the In fraction returns to background levels after a day has passed, indicating all ^{113m}In has decayed due to the absence of ^{113}Sn. After the evaporation of the ^{113}Sn fraction, it was noted that no visible residue was present while the ^{nat}In fraction contained the solid ^{nat}In when it was evaporated to dryness (the HF fractions also had no visible residue). Due to differences in counting geometry, accurate recoveries were impossible to determine. This separation was not used for future studies due to the large elution volumes and the fact that the simpler 2 step separation described above without the use of HF was found to give similar or better results (section 5.2).

5.5.2 Additional ^{124}Sb Separation Experimental and Results and Discussion

The isolation of ^{124}Sb from ^{nat}Sn was based on distribution ratios presented in Ref. [87]. The ^{nat}Sn foil was dissolved in 10 mL of concentrated HCl and a 3 mL aliquot was taken and diluted to 6 mL with DI water resulting in a final concentration of 6 M HCl. To this, 0.7 mL of 30 % H_2O_2 was added to ensure the oxidation to Sb^{5+} and Sn^{4+}. A 7-mL bed volume AG 1x8 (100-200 mesh) anion-exchange column was prepared and conditioned with 10 mL of 6 M HCl. The solution containing the dissolved ^{nat}Sn foil was added to the column and rinsed with two, 4-mL fractions of 6 M HCl. Under these conditions the Sn and Sb were expected to remain on the column. The Sb was stripped off the column by collecting five 4-mL fractions of 0.8 M HCl effluent on the first day, capping the column to avoid evaporation, and eluting four more 4-mL 0.8 M fractions the second day. The column was capped again and two more 4-mL 0.8 M HCl fractions were eluted on the third day.The Sb activity was monitored by HPGe gamma spectroscopy of ^{124}Sb, where as the Sn was monitored by ^{117m}Sn from the decay of produced

^{117}Sb ($t_{1/2}$=2.80 h). The separations were performed approximately one day after irradiation allowing the ^{117m}Sn to reach equilibrium with the ^{117}Sb.

Due to the fact the Sn was left on the column, no elution curves were produced from this separation method. However, there was no detectable ^{117m}Sn in the Sb fractions and >80 % of the Sb was recovered during the separation.

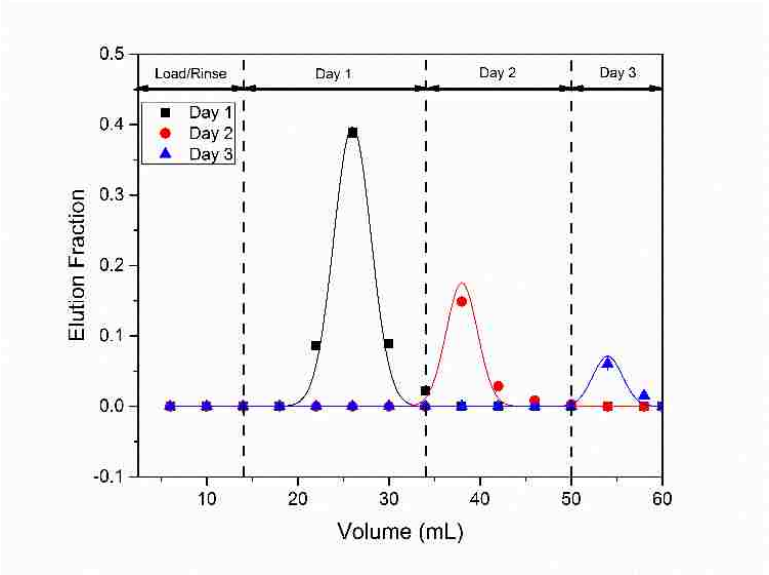

Figure 50. Elution curves for separation of ^{124}Sb from ^{nat}Sn, initial attempt, error from counting statistics.

As seen in Figure 50, all the Sn remained sorbed to the column as a dark band on the upper 1/3rd of the column and most of the Sb was eluted. The reason for the three days worth of elutions was due to the observation that only about 50% of the Sb elutes initially due to very slow elution kinetics. After the third day, >90% of Sb recovery was obtained. Upon evaporation of the combined Sb fractions, no visible Sn foil residue was observed. The ^{117m}Sn gamma line (see Figure 47) was not observed in the Sb fractions, indicating a clean separation. This method was

not used for final separation of future Sb from Sn foils infavor of the method described above in section 5.4, due to the length of separation and excessivly large elution volumes in comparison.

5.6 Radionuclide generators for Pb and Bi isotopes

As mentioned above a convenient way to obtain carrier-free Pb and Bi isotopes is through the preparation of an isotope generator based on the natural decay chains, Figure 51. For the purpose of this work, a generator for elution of ^{212}Pb (E_γ=238.63 keV, $t_{1/2}$=10.64 h) (and if desired ^{212}Bi (E_γ=727.33 keV, $t_{1/2}$=60.55 m)) was prepared from ^{232}U (legacy material, LLNL) [208].

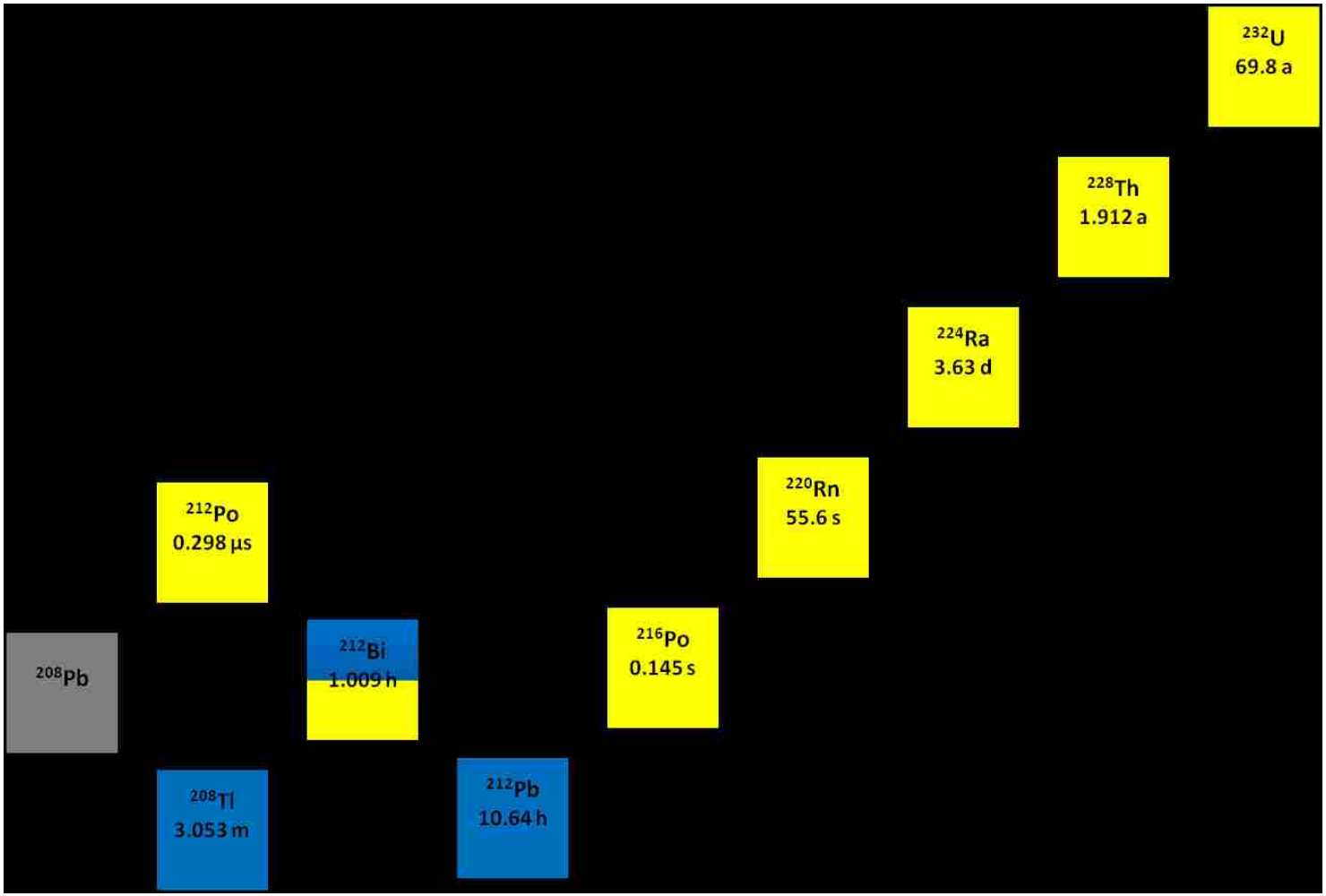

Figure 51. ^{232}U decay chain

5.6.1 Experimental

An AG 50Wx8 (100-200 mesh) cation exchange column, approximately 2 mL bed volume, slurry packed, was cleaned and prepared as mentioned in Chapter 3.1. The column was conditioned with 10 mL of 1 M HCl. To this, a 1 mL stock solution of ^{232}U containing all daughters in secular equilibrium was added, after being counted by HPGe gamma spectroscopy to determine its initial activity. Under these conditions all radionuclides from ^{212}Pb to ^{232}U on the decay chain are strongly retained by the column. The column was then converted to an appropriate condition for longer-term storage by adding of 2 mL 0.4 M HCl, before being capped, Figure 52.

Figure 52. ^{232}U generator, capped for storage.

After allowing approximately 7 half-lives of ^{212}Pb to pass (74.5 hr, time it takes for > 99% of activity to grow to equilibrium), the generator was eluted with 10, 1-mL fractions of 2 M HCl, each collected in a 15 mL centrifuge tube (same geometry as the stock solution). These solutions were monitored by HPGe gamma spectroscopy to determine the elution behavior of Pb from the generator. The solutions were stored for one month, allowing any ^{228}Th to reach secular equilibrium with its daughters, before counting each sample again to look for Th breakthrough.

For the purpose of performing the experiments presented in this dissertation, legacy ^{207}Bi material from LLNL was used as a source of Bi, however, it is possible to change the elution concentration on the generator to 0.5 M HCl and elute ^{212}Bi while leaving ^{212}Pb on the column.

The general usage procedure for obtaining ^{212}Pb for experiments presented in this dissertation is as follows. The column was stored in a small amount of 0.4 M HCl. Upon opening, 1 mL of 2.0 M HCl was allowed to pass through the column and then discarded. An additional 2 mL of 2 M HCl was used to elute ^{212}Pb and was collected as the Pb elution fraction (stock solution). To place the column in its storage state, 2 mL of 0.4 M HCl was passed through the column and it was capped and sealed with a small amount of solution remaining above the frit.

5.6.2 Results and Discussion

Under the operating conditions of the generator, the ^{232}U will eventually bleed off the column; however, ^{228}Th and the daughters with higher Z ^{212}Pb remain strongly sorbed, Table 14.

Table 14. Distribution ratios for elements in the ^{212}U decay chain for various concentrations of HCl on AG 50Wx8 [223].

Element	0.2 M HCl	0.5 M HCl	1.0 M HCl	2.0 M HCl
U	860	102	19.20	7.3
Th	$>10^5$	$\sim10^5$	2049	239
Pb	1420	183	35.66	9.8
Bi	Ppt.	<1	1	1

Due to the 69.8 year half-life of ^{232}U and the long 1.912 year half-life of ^{228}Th the bleeding of the ^{232}U, even if all in one 2 mL ^{212}Pb elution, will be unable to grow enough ^{212}Pb into solution to be detected over the approximately 3 hour experimental time frames. However, if ^{228}Th were to breakthrough, the generator would slowly degrade and detectable amounts of ^{212}Pb would grow into the experimental solutions during the 3 hour time frames.

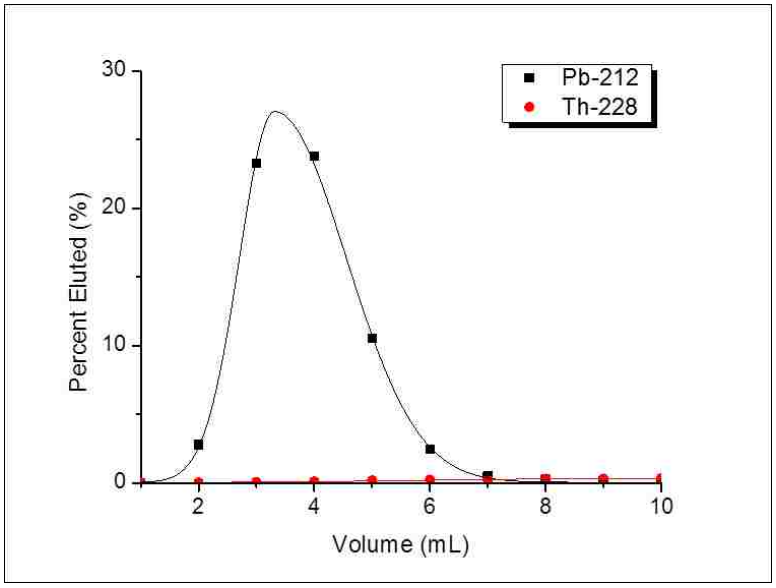

Figure 53. ^{212}Pb elution curve with ^{228}Th breakthrough.

From Figure 53, it can be seen that initial counts of a ^{212}Pb elution show an as expected elution curve. By counting these same solutions one month later and looking for the ^{212}Pb gamma-lines, any detectable ^{212}Pb would be due to ^{228}Th bleeding through the column. As seen in Figure 53 no ^{212}Pb was detected one month later, indicating no detectable breakthrough of ^{228}Th. Periodically over the 1.5 year usage time of the generator the eluted ^{212}Pb stock solutions were counted a month later and in each case no detectable ^{212}Pb was seen, indicating a very stable generator that can be used for greater than 1.5 years without issue. The 3.63 day half-life of the ^{224}Ra parent of ^{212}Pb is the most important element to retain on the column during ^{212}Pb elutions. If this isotope was to elute with ^{212}Pb, a large amount of ^{212}Pb would grow into the stock solution during the experimental time frames. The presence of^{224}Ra is easy to detect via its 241.0 KeV gamma-line, and each ^{212}Pb elution was checked for ^{224}Ra, Figure 54 [208].

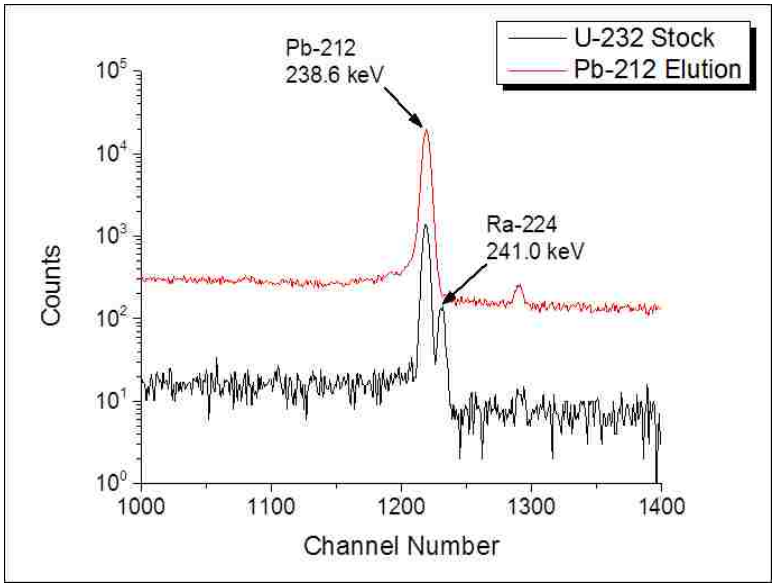

Figure 54. Gamma spectrum showing the ^{212}Pb and ^{224}Ra gamma lines for the ^{232}U stock solution and an eluted ^{212}Pb fraction.

As seen in Figure 54 there is no detection of the ^{224}Ra gamma-line in the ^{212}Pb elution, indicating ^{224}Ra is retained by the column during ^{212}Pb elution. Each ^{212}Pb stock solution prepared from the generator for all experiments described later in this dissertation were checked for the breakthrough of ^{224}Ra before use, and this gamma-line was not detected over the 1.5 year usage of the generator.

5.7 Conclusions and Future Work

Carrier-free radionuclides of the Fl and element 115 homologs and pseudo-homologs Sn, Hg and Sb, were produced at the LLNL CAMS facility through the bombardment of stable foils with 12-15 MeV protons for 6-10 hours at beam currents of 100-400 nA . The following reactions were used for production: ^{nat}Sn(p,n)^{124}Sb, ^{197}Au(p,n)^{197}Hg, and ^{nat}In(p,n)^{113}Sn.

Separation procedures for the rapid isolation of the carrier-free activities were established. An anion-exchange based separation from hydrochloric and nitric acid matricies was used to separate the ^{113}Sn radiotracer from ^{nat}In. A cation-exchange based separation from

hydrochloric and mixed hydrochloic/hydroiodic acid matrices was used to isolate the ^{124}Sb radionuclide from ^{nat}Sn. A separation based on Eichrom TEVA resin, which uses Aliquot 336 as the extractant, was used to separate the ^{197}Hg radiotracer from Au. Batch studies were performed to establish the uptake of Au and Hg on the TEVA resin and these results were used to develop the separation procedure. In all cases, carrier-free radionuclides were obtained and confirmed by HPGe gamma spectroscopy.

A novel ^{212}Pb and ^{212}Bi generator was developed by loading ^{232}U onto a cation-exchange column. Elution of carrier-free Pb and Bi was achieved by simply changing concentrations of HCl. The generator was characterized and shown to provide usable radionuclides without breakthrough of the parents for an on-going duration of 1.5 years.

The 10 MV tandem Van-de-Graaff accelerator at the LLNL CAMS facility was shown to be adequate in producing carrier-free radionuclides for transactinide homolog studies. The target chamber used in this experiment can be filled with a vast array of metal foils for production of various carrier-free radionuclides. This can be useful for the study of other transactinides or for the production of tracers to be used for yielding chemical procedures in other radiochemistry experiments.

CHAPTER 6: EICHROMS PB RESIN WITH Fl HOMOLOGS AND PSEUDO-HOMOLOGS IN HYDROCHLORIC ACID

This chapter deals with the development of chemistry for Fl homologs (Pb and Sn) and pseudo-homologs (Hg) using a commercially available extraction chromatography resin. The resin, Eichrom's Pb resin (50-100 μM particle diameter), is coated with DtBuC18C6 (Figure 55), which as mentioned above separates analytes based on their size as well as their charge and complexation [164,201]. This resin was developed for the specific application of separating Pb from other analytes; however, no research into the behavior of Sn or Hg has been performed.

Figure 55. Pb resin extractant 4',4''(5'')-di-tert-butyldicyclohexano-18-crown-6.

Batch experiments were conducted to determine the extraction efficiency of the Pb resin for both Pb(II), Sn(IV) and Hg(II) from HCl. In acidic solution, Pb tends to stay in the +2 oxidation state, Sn in the +4 oxidation state and Hg in the +2 oxidation state [151,211,224-226]. The extraction kinetics were investigated, and column separation schemes were developed for the separation of the homologs Pb(II) and Sn(IV) alone as well as for the homologs and pseudo-homolog, Hg(II), combined. To assess the speciation of Pb(II) and Sn(IV), liquid-liquid extraction experiments were performed with varying DtBuC18C6 concentrations. The primary focus of this chapter is to establish a separation scheme for Fl that gives insight into the chemical form of the extracted homologs and pseudo-homologs, with appropriate kinetics for a future application to a Fl chemistry experiment. Proposed potential Fl experiments are discussed at the end.

6.1 Experimental

6.1.1 Reagents and Materials

The Pb resin (50-100 µm, 40 % w:w, Eichrom Industries, Inc.) was used for both batch and column studies. The extractant 4',4"(5")-di-*tert*-butyldicyclohexano-18-crown-6 (90 %) was purchased from Sigma Aldrich and used as received. Dichloromethane (99.9 %, un-stabilized, Fisher) was used without further purification. Acids were prepared by volumetric dilution from trace-metal grade acids and de-ionized water (18 MΩ·cm). A total of 12 different hydrochloric acid concentrations were used for experiments, Table 15.

Table 15. Acid solutions for various studies.

Acid	Concentration (M)
HCl	0.001, 0.01, 0.1, 0.2, 0.4, 0.8, 1.0, 2.0, 4.0, 8.0, 10.0, Conc.

The tracer solutions of ^{212}Pb and ^{113}Sn and ^{197m}Hg were prepared with activity concentrations ranging from 2 to 10 cps. Tracers were obtained from an isotope generator (^{212}Pb) or from ^{197}Au(p,n)^{197}Hg and ^{113}In(p,n)^{113}Sn production reactions at CAMS as described in further detail in Chapter 5.

6.1.1 Batch study

General procedures for batch studies are described in Chapter 3. The uptake parameters for Pb^{2+}, Sn^{4+} and Hg^{2+} on Pb resin in HCl solutions were determined by batch extraction experiments. To a 1.5 mL centrifuge vial, 10-20 mg of Pb resin were added along with 1 mL of HCl ranging from 0.001 M to concentrated as listed above. The resin was placed on a rotary mixer for 1 hour for the preconditioning of the resin. A 20 µL spike containing either ^{212}Pb (eluted from the generator with 2.0 M HCl), ^{113}Sn (oxidized to Sn^{4+} with a drop of H_2O_2) or ^{197m}Hg

in 2.0 M HCl was added to the wet resin. The solutions were equilibrated for 3 hours (for Pb and Sn) or 5 hours (Hg) hours on a vortex mixer. Each sample was counted with a HPGe detector for 120 to 900 seconds (≥1000 counts in the desired photo-peak), and then filtered through a 0.45 µm PTFE filter to completely separate the resin from the solution. A 700 µL aliquot of each filtered solution was added to 320 µL de-ionized water in a 1.5 mL centrifuge vial for consistent geometry and counted for 300 to 900 seconds, depending on activity, with a HPGe detector. All experiments were performed in triplicate and the reported errors are based on the standard deviation of the replicates. The Pb resin capacity factor (k') was calculated as described in Chapter 3. Reported values for each HCl concentration tested were calculated from the combination of the 1 mL of initial acid and 20 µL of tracer solution in 2 M HCl.

6.1.2 Speciation study

Solutions containing DtBuC18C6 in un-stabilized dichloromethane were prepared in volumetric flasks with volumes and masses as described for Pb and Sn speciation in Tables 16 and 17, respectively.

Table 16. Sample masses and volumes for Pb speciation studies.

[DtBuC18C6]	Mass DtBuC18C6 (g)	Volume
0.00036	4.4	25
0.0025	12.0	10
0.0090	43.6	10
0.065	313.7	10
0.12	563.9	10

Table 17. Sample masses and volumes for Sn speciation studies.

[DtBuC18C6]	Mass DtBuC18C6 (g)	Volume
0.00064	7.8	25
0.0057	27.4	10
0.017	82.9	10
0.067	322.4	10
0.13	651.7	10

Stock solutions of $^{212}Pb^{2+}$ were prepared by evaporating the generator eluted $^{212}Pb^{2+}$ solution and reconstituting the activity in 0.4 M HCl (the peak of the $^{212}Pb^{2+}$ extraction from batch results). A $^{113}Sn^{4+}$ stock solution was prepared in 4 M HCl (the peak of the $^{113}Sn^{4+}$ extraction from batch results). To a 1.5 mL centrifuge tube, 480 µL of 0.4 of 4 M HCl was added along with 500 µL of crown ether solution (each DtBuC18C6 concentration was performed in triplicate for both Sn^{4+} and Pb^{2+}). These were allowed to mix for one hour, on a rotary mixer, to ensure pre-conditioning of the organic phase. To each tube a 20 µL spike of the desired $^{212}Pb^{2+}$ or $^{113}Sn^{4+}$ activity was added, and they were allowed to mix for one hour on a rotary mixer. A 300 µL aliquot from each phase was taken and counted with a HPGe detector to determine the distribution ratios for Sn^{4+} and Pb^{2+} at each concentration of DtBuC18C6. Due to the extremely strong uptake of Hg by DtBuC18C6 no discernable speciation trend could be established by this method due to poor aqueous phase counting statistics even at low concentrations of crown ether.

6.1.3 Kinetics study

The HCl concentration where the maximum uptake occurs in the batch experiments (4 M HCl for $^{113}Sn^{4+}$, 1 M HCl for $^{212}Pb^{2+}$ and 0.4 M HCl for $^{197m}Hg^{2+}$) occurs in the batch experiments was the concentration of choice for each kinetics study. In the case of Hg a concentration with strong uptake was chosen, but not the strongest uptake due to the fact the extremely high k'

values of >5000 would have yielded poor counting statistics. The standards were made by placing 1 mL of HCl at the desired concentration (depending on if ^{212}Pb, ^{113}Sn or ^{197m}Hg) in a 1.5 mL centrifuge tube and adding 100 µL of a stock radionuclide solution. The standards were made in triplicate and counted with a HPGe detector for 120 seconds in the case of ^{212}Pb, 3600 seconds in the case of ^{113}Sn and 300 seconds in the case of ^{197m}Hg. The preconditioned samples were made by adding 1 mL of the desired concentration of HCl to a 1.5 mL centrifuge vial containing 10-20 mg Pb resin and placing on a vortex mixer for 1 hour. A 100 µl spike of either $^{212}Pb^{2+}$, $^{113}Sn^{4+}$ or $^{197m}Hg^{2+}$ in the above mentioned HCl concentration was added to the samples and each sample was mixed for a desired time interval before quickly filtering to isolate the solution from the resin. A 700 µL spike of each filtered solution was added to 400 µL of de-ionized water (to maintain original counting geometry) and the samples were counted with a HPGe detector for 240-300 seconds (^{212}Pb), 6300 seconds (^{113}Sn) or 300 seconds (^{197m}Hg).

6.1.4 Column study

General column study procedures are described in Chapter 3. Initial column studies were designed to separate only the group 14 homologs Pb and Sn rapidly. Aliquots of each tracer were combined and evaporated to dryness in a warm water bath with a forced air stream, then reconstituted in 1 mL of the appropriate HCl solution. The initial sample activity was determined by HPGe counting. For the sequential extraction experiments a ~2 mL/min (~4 mm Hg gauge reading) flow rate was maintained for vacuum flow. The resin cartridge was conditioned with 10 bed volumes (20 mL) of the appropriate HCl solution. Sequential extractions were performed with HCl concentrations based on the results from the batch experiments. The radionuclides were loaded on the column in 3 M HCl, where both are retained, and 0.4 M HCl was used to elute $^{113}Sn^{4+}$ and 8 M HCl to elute $^{212}Pb^{2+}$. Separate experiments were performed to reverse the elution order. Three rinse fractions at 3 M HCl were collected followed by 1 mL

elution fractions (x10) of the desired HCl concentration. Table 18 summarizes the Pb/Sn columns.

Table 18. Summary of vacuum flow column for Pb and Sn separation.

Fraction	Concentration of HCl (M)	Volume (mL) / Number of Fractions	Element Eluted
Load	3	1 (load solution)	All Retained
Rinse	3	1 / 3	All Retained
Pb Elute*	8	1 / 10	Pb
Sn Elute*	0.4	1 / 10	Sn

*Note: the second column had the Sn eluted before the Pb, to have reverse behavior.

Care was taken to stop the column flow just as liquid was about to reach the top-frit so the column never ran dry and each elution fraction was a consistent 1 mL. Fractions were counted by HPGe gamma spectroscopy.

Similar columns were run with the addition of Hg to the load solution to attempt a rapid separation of the homologs and pseudo-homologs of Fl with one chemical system. Initially a column was run with the same flow parameters as with the Pb/Sn separations and was loaded with all three radionuclides in 1 mL of 3 M HCl. After loading the column three rinse fractions of 3 M HCl were collected followed by 1 mL elution fractions (x8-16) of the desired HCl concentration. Table 19 summarizes the initial Pb, Sn and Hg column.

Table 19. Summary of vacuum flow column elution parameters for Pb, Sn and Hg separation.

Fraction	Concentration of HCl (M)	Volume (mL) / Number of Fractions	Element Eluted
Load	3	1 (load solution)	All Retained
Rinse	3	1 / 3	All Retained
Sn Elute	0.4	1 / 8	Sn
Pb Elute	8	1 / 9	Pb
Hg Elute	Conc.	1/ 16	Hg

Due to slow elution and adsorption kinetics of Hg, Hg was seen to bleed through the column and elute with a poor peak resolution (discussed below). Therefore, a second column was run in which the load solution was changed to 0.4 M HCl (closer to the peak extraction of Hg) and Sn was allowed to pass through the column without interaction. The column was then capped for 1 hour after the elution of Sn to allow for Hg to be fully retained, and was capped again for 1 hour after changing to concentrated HCl to assist with eluting the Hg in a tight elution peak. Table 20 summarizes the elution profile for this column.

Table 20. Summary of vacuum flow column elution parameters for second Pb, Sn and Hg separation.

Fraction	Concentration of HCl (M)	Volume (mL) / Number of Fractions	Element Eluted
Load	0.4	1 (load solution)	All but Sn retained
Sn	0.4	1 / 7	Sn
Pb Elute	8	1 / 9	Pb
Hg Elute	Conc.	1 / 12	Hg

6.2 Results and discussion

6.2.1 Batch study

The effects of HCl concentration on the uptake of Pb^{2+}, Sn^{4+} and Hg^{2+} by the Pb resin are shown in Figure 56.

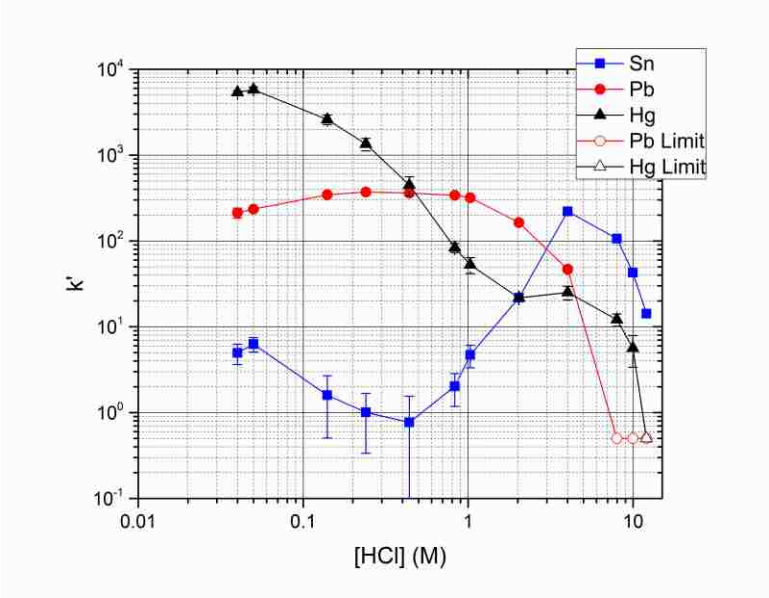

Figure 56. The batch uptake (k') of $^{212}Pb^{2+}$, $^{113}Sn^{4+}$ and $^{197m}Hg^{2+}$ as a function of hydrochloric acid concentration on Pb resin (50-100 µm) with a 3 hour (5 hour for Hg) equilibration time.

Lead shows strong affinity to the resin from 0.04 – 2 M HCl and then decreases significantly with increasing HCl concentration above 2 M, in good agreement with literature [201]. Tin shows slight uptake from 0.04 – 1 M HCl and then increases significantly to a peak extraction at around 4 M HCl. Currently there is no data available on the extraction of Sn^{4+} with DtBuC18C6 from hydrochloric acid media. It is expected that Sn^{4+} in [HCl] > 0.7 M exists as the $SnCl_6^{2-}$ anion [151,153,227]. Crown ethers are known to form positively charged hydronium ion complexes by coordinating with H_3O^+ where the hydronium ion fits perfectly into the ring [167,168]. Therefore, the increasing k' for Sn^{4+} above 1 M HCl suggests that two hydronium activated crown ethers form an association complex with the $SnCl_6^{2-}$ anion. The unexpected dip in Sn^{4+} extraction above 4 M HCl is most likely due to the bleeding of extractant material off the resin backbone. This was observed from evaporation of the high HCl concentration samples and noting organic residues. Despite forming similar complexes in HCl as Pb, Hg exhibits much stronger extraction over the same concentration ranges. As described in Ref. [226] and

discussed below (Section 6.2.2), Hg most likely extracts as $HgCl_2$·2DtBuC18C6. Therefore, the decrease in mercury extraction at higher HCl concentrations may be attributed to the formation of ionic $HgCl_3^-$ and $HgCl_4^{2-}$ [226].

6.2.2 Speciation study

Plotting the logarithm of the distribution ratios for $^{212}Pb^{2+}$ and $^{113}Sn^{4+}$ as a function of the logarithm of the concentration of DtBuC18C6 yields a line where the slope of a linear fit to the line is equivalent to the number of DtBuC18C6 molecules required to extract each metal atom. A general equilibrium equation for the extraction of a metal in a SX system is given by:

$$M^{n+}_{(aq)} + xL_{org)} \rightleftarrows ML_{x\,(org)} \qquad \text{(Eqn. 24)}$$

The equilibrium constant for this extraction, K is given by:

$$K = \frac{[ML_x]}{[M^{n+}][L]^x} \qquad \text{(Eqn. 25)}$$

Substituting in the distribution ration, Equation 7, and taking the logarithm of both sides gives:

$$\log D = x\log[L] + \log K \qquad \text{(Eqn. 26)}$$

From Equation 26, it can be seen that a plot of logD versus log[L] will give a linear relationship with the slope being equal to x, the number of ligands participating in the extraction.

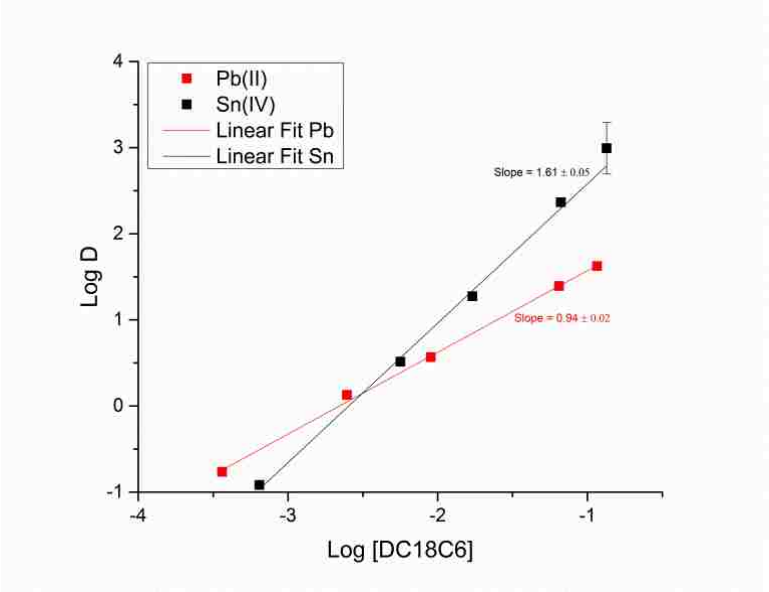

Figure 57. Distribution ratios for the extracted $^{212}Pb^{2+}$ and $^{113}Sn^{4+}$ as a function of DtBuC18C6 concentration in dichloromethane. The solid lines indicate the results of a linear regression fit to the Pb and Sn data, with slopes indicated.

From the linear regressions in Figure 57, the number of crown ligands coordinated to the Pb^{2+} metal ion is found to be 0.94 ± 0.02. This indicates that one DtBuC18C6 molecule is required to extract each Pb^{2+} ion into the organic phase, supporting the notion that Pb^{2+} extracts into the cavity of the crown ether. This yields an extraction mechanism of:

$$\mathrm{PbCl}_{2aq} + \mathrm{DtBuC18C6}_{\mathrm{org}} \rightleftarrows \mathrm{PbCl}_2 \cdot \mathrm{DtBuC18C6}_{\mathrm{org}}$$

Similarly, the number of crown ligands coordinated to the Sn^{4+} metal ion is found to be 1.61 ± 0.05. This suggests that two DtBuC18C6 crown ether ligands are needed to extract each Sn^{4+} ion. This supports the idea that the highly stable $SnCl_6^{2-}$ complex is being extracted by two positively charged DtBuC18C6·H_3O^+ complexes, described by the following mechanism:

$$\mathrm{SnCl}_{6\,\mathrm{aq}}^{2-} + 2\mathrm{DtBuC18C6}_{\mathrm{org}} + 2\mathrm{H_3O} \rightleftarrows \mathrm{SnCl}_6^{2-} \cdot [2(\mathrm{H_3O} \cdot \mathrm{DtBuC18C6})]_{\mathrm{org}}^{2+}$$

As a result the Sn^{4+} extraction does not depend on the cavity characteristics of the DtBuC18C6, but rather the rate of formation of the DtBuC18C6·H_3O^+ complex.

Data acquired by the same means with ^{197m}Hg yielded inconclusive results due to the short half-life of the radionuclide yielding low counting statistics, which were made worse by the very high distribution ratios for the extraction of Hg. Experiments found in literature conducted with the simpler dicyclohexano-18-crown-6 (DC18C6) as well as dibenzo-18-crown-6 (DB18C6) and the un-substituted 18-crown-6 (18C6) indicated that the following extraction mechanism is dominant for mercury [226]:

$$\mathrm{HgCl}_{2aq} + 2\mathrm{CE}_{\mathrm{org}} \rightleftarrows \mathrm{HgCl}_2 \cdot 2\mathrm{CE}_{\mathrm{org}}$$

Where CE=18C6, DC18C6 and DB18C6. This indicated that the planar $HgCl_2$ molecule is extracted between two crown ether molecules. While this study was conducted with Hg concentrations of 10^{-5} M instead of the carrier-free mercury of this study, it does indicate a more complex extraction than the traditional cavity based extraction exhibited by Pb. Decreases in the extractability between reported distribution ratios for 18C6 > DC18C6 > DB18C6 were attributed to the cavity sizes, which are 2.6 to 3.2 Å for 18C6 and DC18C6 [228] but increase to 4 Å for DB18C6 [229], as well as the decreasing basicity over that same sequence. The Hg^{2+} ion has an ionic radius of 1.1 Å which is much closer to the cavity diameter of 18C6 and DC18C6, and therefore can receive more stabilization from those cavities than the larger DB18C6 cavity [226]. The observed slight decrease in extraction with DC18C6 compared to 18C6 was attributed to increased steric hindrance lessening the effect of cavity stabilization [226].

6.2.3 Kinetics study

The data obtained from the batch studies indicates that Pb^{2+}, Sn^{4+} and Hg^{2+} can be separated using a pure HCl matrix with the Pb resin at an equilibration time of three to five hours. Due to the short-lived isotopes of Fl and the goal of an on-line chemical separation which will require flow rates on order of 1 mL min^{-1}, the kinetics of the extraction must be suitable on the second time-scale verses hour. The kinetics of Pb, Sn and Hg on the Pb resin at 1, 4, and 0.4

M HCl (maximum k' from batch studies for Pb and Sn, slightly lower extraction chosen for Hg due to large k'), respectively, was investigated, Figure 58.

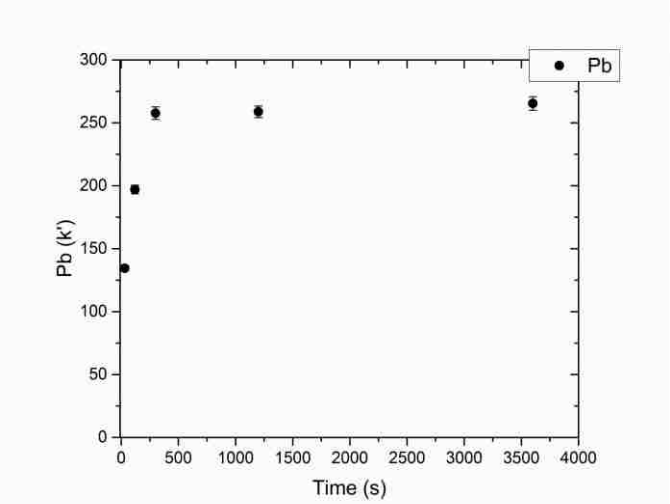

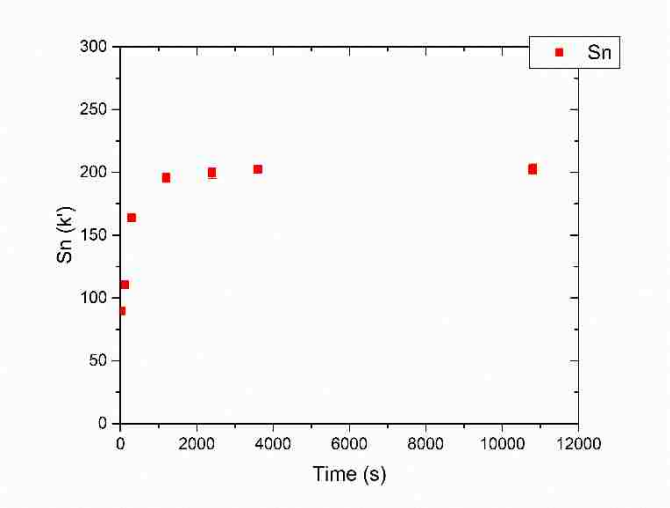

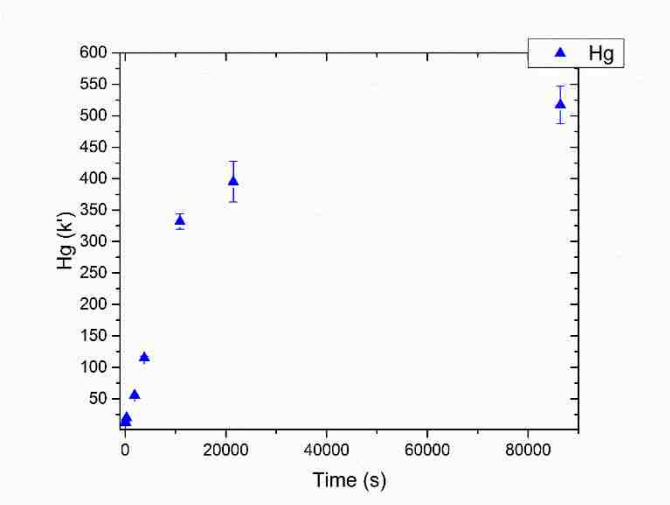

Figure 58. (Top) Kinetics of $^{212}Pb^{2+}$ in 1 M HCl media, (Middle) $^{113}Sn^{4+}$ in 4 M HCl media and (Bottom) $^{197m}Hg^{2+}$ in 0.4 M HCl media on Pb resin (50-100 µm), varying equilibration times.

The sorption of Pb^{2+} on the Pb resin is extremely fast with near immediate uptake and full equilibrium reached within five minutes. The sorption of Sn^{4+} on the Pb resin was considerably slower than that of Pb^{2+}, presumably from the need to extract a hydronium ion into the crown cavity before the extraction of the negatively charged $SnCl_6^{2-}$ complex, as well as the need for two properly oriented crownether molecules on the rigid resin backbone. However, full equilibrium was reached after approximately an hour. Sorption of Hg^{2+} was the slowest with full equilibrium not reached until beyond 8 hours and very little sorption observed until at least 1 hour had passed. Potential reasons for the slow equilibration of Hg^{2+} can be attributed to the extraction mechanism discussed in Section 5.2.2 above. Due to the more complex multiple ligand extraction and the fact that the crown ether cavity is still believed to stabilize the extracted mercury species [226], the overall rate of this extraction is very slow on the resin based system. This is potentially made even slower due to the requirement of two crown ethers in the correct orientation, which might be less favorable due to the rigid resin backbone.

It is possible that in a liquid-liquid extraction system, without the rigidity of the resin system, the Sn^{4+} and Hg^{2+} extractions may increase in speed. Similar Hg^{2+} extractions (though not carrier-free) by DC18C6 are reported to reach equilibrium in about 30 minutes [226]. However, it would be expected that the Sn^{4+} would still be faster than Hg due to the lack of involvement of the crown cavity in the extraction and would only be limited mainly by the kinetics of the H_3O^+ extraction.

6.2.4 Column study

The column experiments were used to determine if a sequential extraction of Pb^{2+} and Sn^{4+} could be achieved by varying only the HCl concentration. Based on the batch study results, a load solution of 3 M HCl was chosen due to the fact that both Pb^{2+} and Sn^{4+} are retained on the Pb resin at this concentration. Two separate columns were run, one with the goal of removing

Pb^{2+} before Sn^{4+} and the other with the reverse order. To remove Pb^{2+}, 8 M HCl was used while 0.4 M HCl was used to remove Sn^{4+} (Figure 59).

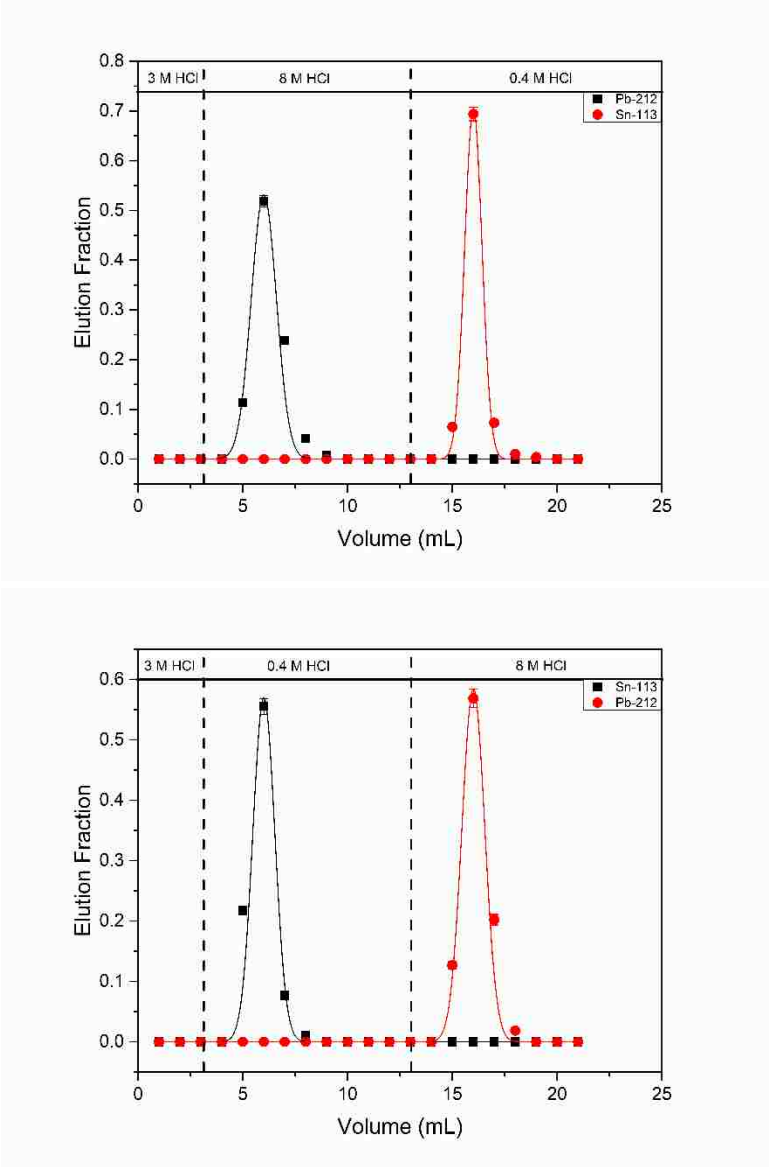

Figure 59. Column elution of 2 mL pre-packed Eichrom Pb resin cartridges at ~2 mL/min flow rate for the separation of Pb^{2+} from Sn^{4+} with (Top) Pb eluted first and (Bottom) Sn eluted first.

Both analytes behaved as expected with absolutely no breakthrough during column loading. Complete elution of Pb^{2+} was achieved with no Sn^{4+} breakthrough and vice versa, usually within

the first couple of free column volumes. These separation schemes are fast and yield an excellent separation between Pb^{2+} and Sn^{4+} regardless of their elution order.

Additional columns were done with Hg^{2+} added to the load solutions and attempts were made to rapidly separate Pb^{2+}, Sn^{4+} and Hg^{2+} by only varying the HCl concentrations. Based on the batch study results, a load solution of 3 M was chosen in hope that all three elements would be retained by the column, followed by elution of Sn^{4+} with 0.4 M HCl, then Pb^{2+} with 8 M HCl and finally Hg^{2+} with concentrated HCl, Figure 60.

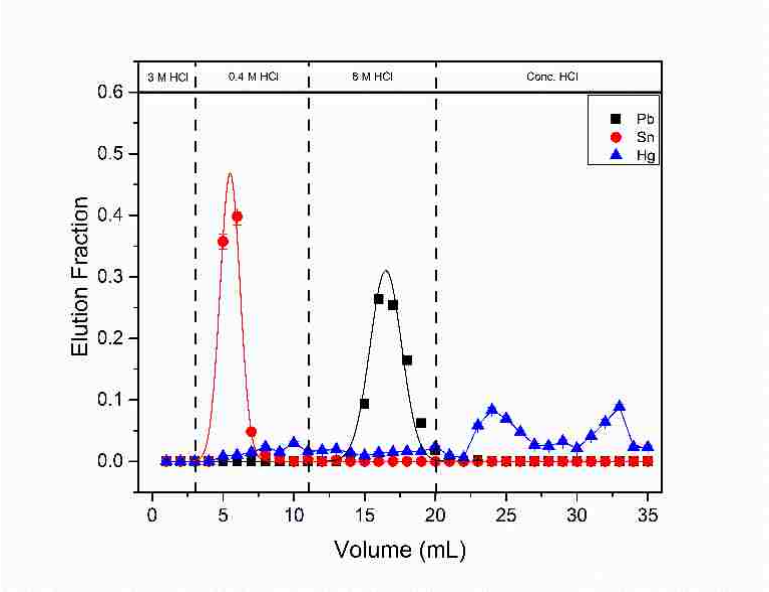

Figure 60. First column elution of 2 mL pre-packed Eichrom Pb resin cartridges at ~2 mL/min flow rate for the separation of Sn^{4+} from Pb^{2+} and Hg^{2+}.

The initial column elution presented in Figure 60 shows a small bleeding of Hg throughout the Sn and Pb fractions before it is eluted in the concentrated HCl fractions. The reason for the double elution peaks during the concentrated HCl fractions is due to the fact the column was capped for one hour between each peak, due to the fact after the initial peak it was realized the desorption kinetics of Hg were very slow. Results of this column indicated that 3 M HCl was too

high a concentration for the load solution due to the slow sorption kinetics of Hg, which led to the eventual bleeding of Hg off the column (see Section 6.2.3 for a discussion of the Hg kinetics tests). Once it was discovered that Hg had very slow equilibrium kinetics, a second column was run with a load solution concentration of 0.4 M HCl. Under these conditions Sn^{4+} is not retained by the column; however, the extraction of Hg^{2+} is closer to its maximum at this concentration and the hope was it would be retained at the ~2 mL/min flow rate, Figure 61.

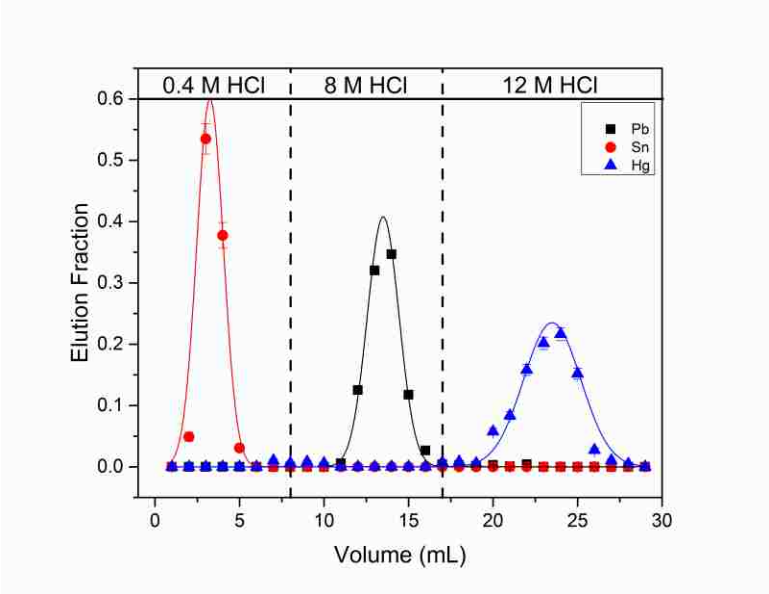

Figure 61. Second, improved, column elution of 2 mL pre-packed Eichrom Pb resin cartridges at ~2 mL/min flow rate for the separation of Sn^{4+} from Pb^{2+} and Hg^{2+}.

An additional change between the first and second column was that after loading the 1 mL 0.4 M HCl load solution and elution of Sn^{4+} with the 2 mL/min flow rate, the column was capped for one hour to ensure Hg^{2+} was retained. Then, with the 2 mL/min flow rate, Pb^{2+} was eluted with 8 M HCl. After addition of the first concentrated HCl fraction to the column, the column was again capped for one hour to assist with desorption of Hg^{2+}. After the hour had passed, elution of Hg^{2+} was finished with additional concentrated HCl fractions. As seen in Figure 61, the change of load

solution to 0.4 M HCl and the hour gaps between loading and eluting of Hg enable a clean separation of Pb^{2+} from Sn^{4+} and Hg^{2+}. The Hg^{2+} elution peak was still slightly broad but did elute as expected. In both cases, Figures 60 and 61, the Pb^{2+} and Sn^{4+} behaved as they did in the initial Sn and Pb separations depicted in Figure 59. While it was seen that Pb and Sn can be separated on the second time scale as required for a Fl experiment, the addition of the pseudo-homolog Hg made the separation not possible to perform on the second time scale. It would be possible, however, to determine whether Fl was more Pb or Sn like or neither; however, a definitive Hg-like conclusion as to its behavior would be nearly impossible with the current system due to the slow Hg kinetics of sorption and desorption. The use of thiacrown ethers (discussed in Chapter 7) shows promise for increasing the kinetics of the system for Hg.

6.3 Conclusions and Future Work

In this chapter, the extaction behavior of Pb^{2+}, Sn^{4+} and Hg^{2+} from HCl media was studied using Eichrom Pb resin, which contains the DtBuC18C6 extractant. In agreement with previously reported data, the batch results show Pb^{2+} extracts at low HCl concentrations, from 0.04 – 2 M. It was also observed that Sn^{4+} extracts above 1 M HCl. While Hg^{2+} shows large extraction at low HCl concentrations and negligible extraction at high HCl concentrations. The extracted Pb species is most likely the Pb^{2+} ion in the crown ether cavity with charge balanced by Cl^-. Due to the formation of $SnCl_6^{2-}$, Sn most likely extracts as an ion-associate complex between the negatively charged Sn chloro-complex and two hydronium crown ether complexes. Mercury most likely is extracted as $HgCl_2$ between two crown cavities.

The results also showed that the reaction kinetics were relatively slow on the scale of minutes to hours to achieve full equilibrium. However, the k' for both Pb^{2+} and Sn^{4+} was >50 within a few seconds, indicating that the separation can be performed on the second timescale, even though complete equilibrium is not reached. However, the Hg^{2+} kinetics were much slower

than that of Pb^{2+} and Sn^{4+}, and the three elements could not be separated on the second time scale.

Speciation studies examined Sn^{4+} that was extracted by DtBuC18C6. The slope from linear regressions of the K_d of Pb^{2+} and Sn^{4+} as a function of the concentration of DtBuC18C6 was found to be 0.94 ± 0.02 and 1.61 ± 0.05, respectively. This corresponds to the well-known notion that Pb^{2+} extracts directly into the crown ether cavity, and gives strength to the notion that two positively charged crown ether-hydronium ion complexes extract one $SnCl_6^{2-}$ species. While data was inconclusive due to poor counting statistics, the Hg^{2+} extraction is believed to be: $HgCl_2 \cdot 2$DtBuC18C6.

The column studies established separation schemes to isolate pure Pb^{2+} or Sn^{4+} fractions from the Pb resin through the modification of the HCl concentration. The increased number of theoretical plates in the column system compared to that of the batch system allows for much faster flow rates, such as the 2 mL/min used in this work, while retaining full extraction of both analytes. Thus, the column experiments confirmed the results from batch studies and provide evidence that the Pb resin is suitable for the selective extraction of both Pb^{2+} and Sn^{4+}. If an appropriate apparatus was developed and the extraction behavior of Fl was studied using this same crown ether, comparing to the behavior of Pb^{2+} and Sn^{4+}, the results would indicate whether Fl is more Pb^{2+} or Sn^{4+} like.

Additional column studies aimed at separating the homologs Pb^{2+} and Sn^{4+} as well as the pseudo-homolog Hg^{2+} on the second time scale from a pure HCl matrix were also performed. Results indicated that with large equilibration times between column loading and elution of Hg^{2+} clean elution fractions could be obtained. However, when the column was run with ~2 mL/min flow rates, Hg^{2+} bled through the column when the flow was not halted to allow for it to fully

adsorb and desorb. As a result, while it would be possible to discern if Fl was Pb or Sn like, the use of Eichrom's Pb resin would yield inconclusive data as to whether Fl is Hg like.

Before an on-line Fl experiment can be performed, further experiments are necessary to determine the maximum rate at which the extraction can be carried out while maintaining the same level of separation. Future work is also needed to develop a continuous automated chemistry apparatus capable of running columns and preparing samples on the time scales required for a Fl experiment. Assuming an automated system was capable of performing the chemical separations and sample preparation on the desired time scales, the chemical system presented in this work would be capable of determining whether Fl in the aqueous phase is more Pb^{2+} or Sn^{4+} like; however, due to the extremely slow kinetics Hg^{2+} like behavior would be difficult to discern with any level of confidence. An on-line experiment would first need to be performed and optimized with the short-lived Pb and Sn homologs produced in the same manner Fl would be, so direct comparisons between Fl and the homologs could be made. If Fl was seen in an on-line experiment optimized for Sn elution (high HCl concentrations) one would expect Fl to be forming more negatively charged complexes and be extracting based on ion exchange. Similarly, a system optimized for Pb elution (low HCl concentration) would indicate, if seen, that Fl extracts into the crown ether cavity most likely as a cation.

It is possible with more work that at very low HCl concentrations Hg^{2+} may be retained by the column at large flow rates. If this is the case an experiment with a load solution of 0.001 M HCl would retain both Pb^{2+} and Hg^{2+} while Sn^{4+} passes through. Under these conditions an observed Fl atom could be confirmed to be Sn^{4+} like. Due to the extremely high Hg^{2+} extraction at this low of a concentration, changing to 8 M HCl to elute Pb^{2+}, during which a Fl atom could be considered Pb^{2+} like might be possible while retaining Hg^{2+} like atoms on the column. Experiments were performed loading the column at 0.4 M HCl and waiting one hour before

changing to 8 M HCl to elute Pb^{2+}. Without this one hour wait it was seen that approximately 20-30% of the Hg^{2+} bled off the column. Now while the extraction is stronger at 0.001 M as seen in the Figure 6-2 batch study, it would still be expected that due to the slow kinetics at least some Hg^{2+} would bleed off the column in the Pb^{2+} fraction. Therefore, while these conditions would enable Sn^{4+} like character to be elucidated from Pb^{2+} and Hg^{2+} it would still be difficult to discern if there is any true Hg^{2+} like character in Fl.

CHAPTER 7: EICHROM'S PB RESIN WITH FL HOMOLOGS IN NITRIC ACID

Initial experiments were performed to test experimental procedures for Pb uptake on the Pb resin from HNO_3 and compare them against literature results. Following confirmation of procedures characterization of the Pb resin for extraction of Pb, Sn and Hg began from HCl, Chapter 6. In this chapter a look into the extraction behavior of the direct homologs of Fl, Pb and Sn, on Eichrom's Pb resin is explored from a HNO_3 matrix.

Batch experiments were conducted to determine the validity of initial experimental procedures by comparing the Pb extraction from HNO_3 to literature values. Subsequent batch experiments with Sn^{4+} in HNO_3 matrices were performed to assess the HNO_3 system as a potential for Fl chemistry and compare it to that of the HCl system discussed in Chapter 6. Kinetic studies for the sorption of Pb^{2+} on the Pb resin from HNO_3 are performed and a column separation of Pb^{2+} and Sn^{4+} is described. Comparisons to the HCl system from Chapter 6 are given, and a potential Fl experiment that begins from an HNO_3 system is outlined.

7.1 Experimental

7.1.1 Reagents and Materials

Similar to Chapter 6, the same Pb resin was used. All acids were prepared by volumetric dilution from trace-metal grade acids and de-ionized water. A total of 11 different HNO_3 concentrations were used for experiments, Table 21.

Table 21. Acid solutions for various HNO3 Pb resin studies.

Acid	Concentration (M)
HNO_3	0.001, 0.1, 0.2[#], 0.4, 0.8[#], 1.0, 1.4[*], 2.0, 4.0, 6.0, 8.0, 10.0, Conc.[*]

[*]Used only in Pb batch study.
[#]Used only in Sn batch study.

Tracer solutions of ^{212}Pb and ^{113}Sn were made by taking tracers prepared the same was as described in Chapter 6 and evaporating and reconstituting them in 2.0 M HNO_3 (evaporated two times with concentrated HNO_3 before adding 2.0 M to ensure conversion).

7.1.2 Batch Studies

General batch study procedures are outlined in Chapter 3. The Pb^{2+} batch study was performed in the same manner as the batch study in Chapter 6, with a few minor differences. To a 1.5 mL (15 mL for Pb experiment) centrifuge vial, 10-20 mg Pb resin was added along with 1 mL of HNO_3 from one of the concentrations in Table 21. The resin was allowed to mix for one hour on a vortex mixer to allow for preconditioning. A 100 µL spike containing either ^{212}Pb or ^{113}Sn was added to the solutions and placed on a vortex mixer for 3 hours to allow equilibration. During equilibration each sample was counted for 300 seconds by HPGe gamma spectroscopy. After equilibration the samples were filtered through a 0.45 µm PTFE filter into a separate 1.5 mL (15 mL for Pb experiment) centrifuge tube. In the Pb experiment this centrifuge tube was counted by HPGe gamma spectroscopy. In the Sn experiment a 700 µL spike was taken and added to a new 1.5 mL centrifuge tube along with 400 µL of de-ionized water to maintain counting geometry before being counted by HPGe gamma spectroscopy. In the Pb experiment the backend counts may have up to 10% solution loss due to the filter which adds a slightly larger error to the final results; however, due to the fact the extractions of Pb onto the Pb resin was very large the effect from solution loss was barely noticeable. This procedure was not modified until later when the analytes exhibited nearly zero uptake on the Pb resin and the solution loss resulted in much greater errors. The Pb resin capacity factor (k') was calculated as described in Chapter 3. Reported errors for the Pb experiment are from counting statistics as this was only performed once; for the Sn experiment, the errors are from the standard deviation of three replicates.

7.1.3 Kinetic Study

The kinetic study was performed similarly to the analogous procedure in Chapter 6. A 2 M HCl ^{212}Pb stock solution was evaporated to dryness with a few drops of concentrated HNO_3 and cycled to dryness twice with 1 M HNO_3 before being brought up in 3 mL 1 M HNO_3 to serve as the stock solution for the kinetic study. Three standards were made by adding 1 mL 1 M HNO_3 along with a 100 µL spike of the ^{212}Pb stock solution, and counted by HPGe gamma spectroscopy for 120 seconds, the average of these counts served as the front end value for each sample. Samples were prepared, in triplicate, by adding 1 mL 1 M HNO_3 and 10-20 mg Pb resin to a 1.5 mL centrifuge tube and mixing on a vortex mixer for 1 hour to allow for preconditioning of the resin. Following preconditioning a 100 µL spike of the ^{212}Pb stock solution was added to the samples and each was mixed for the desired time interval (30 seconds to 3 hours), before quickly filtering to isolate the solution from the resin. A 700 µL spike of each filtered solution was added to 400 µL of de-ionized water (to maintain counting geometry) and the samples were counted by HPGe gamma spectroscopy for 120 to 300 seconds.

7.1.4 Column Studies

General column study procedures are described in Chapter 3. An aliquot of ^{212}Pb and ^{113}Sn were brought to dryness in a 15 mL centrifuge tube 2 times with HNO_3 before being reconstituted in 1 mL 1 M HNO_3 (column load solution). This was counted by HPGe gamma spectroscopy for 300 seconds to determine initial activity. A 2 mL pre-packed vacuum flow Pb resin column was conditioned with 10 mL 1 M HNO_3 with a flow rate of ~2 ml/min. The 2 mL/min flow rate was maintained for all elution fractions. The stock solution was added on to the column and then collected as the load fraction. To elute ^{212}Pb and ^{113}Sn 1 mL elution fractions (x7-8) of the desired HNO_3 or HCl concentration were collected in separate 15 mL centrifuge tubes. Table 22 summarizes the HNO_3 Pb/Sn column.

Table 22. Summary of vacuum flow column for Pb and Sn separation in HNO3.

Fraction	Concentration of HCl* or HNO_3# (M)	Volume (mL) / Number of Fractions	Element Eluted
Load	1#	1 (load solution)	Pb retained
Sn Elute	1#	1 / 7	Sn finished eluting
Pb Elute*	8*	1 / 8	Pb elute

Care was taken to stop the column flow just as liquid was about to reach the top-frit so the column never ran dry and each elution fraction was a consistent 1 mL. Fractions were counted by HPGe gamma spectroscopy. Data analysis was performed as described in Chapter 3.

7.2 Results and Discussion

7.2.1 Batch Study

The effects of HNO_3 concentration on the uptake of Pb^{2+} and Sn^{4+} by the Pb resin are shown in Figure 62.

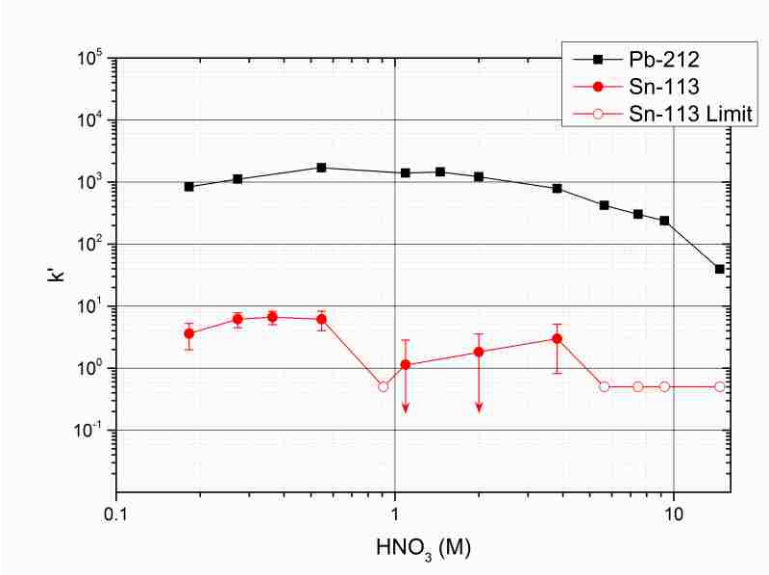

Figure 62. The batch uptake (k') of $^{212}Pb^{2+}$ and $^{113}Sn^{4+}$ as a function of nitric acid media on Pb resin (50-100 µm) with a 3 hour equilibration time.

Consistent with literature, Pb shows a very strong affinity for the resin for close to the entire range of concentrations tested and still has a k' of 39±10 at concentrated HNO_3 [201]. The uptake from HNO_3 is about an order of magnitude higher than with HCl, owing to increased stability of the extracted complex:

$$\mathrm{Pb(HNO_3)_{2aq} + DtBuC18C6 \rightleftarrows Pb(HNO_3)_2 \cdot DtBuC18C6}$$

In HNO_3 Sn^{4+} most likely forms the oxide SnO_2, which due to the size of Sn^{4+} cation has no ability to fit into the crown cavity and does not extract [135]. Due to the fact this is a neutral species the analogous ion-exchange complex with the crown ether that occurs in the HCl system cannot occur in the HNO_3 system.

7.2.2 Kinetic Study

Batch study data presented in Figure 62 indicates that Pb and Sn may be separated from an HNO_3 matrix. Due to the fact Sn does not extract kinetic studies were not performed on Sn^{4+}; however, kinetic studies were performed to see if Pb^{2+} has suitable kinetics for a future Fl experiment. The kinetics of Pb on the resin at 1 M HNO_3 (near peak extraction) was investigated, Figure 63.

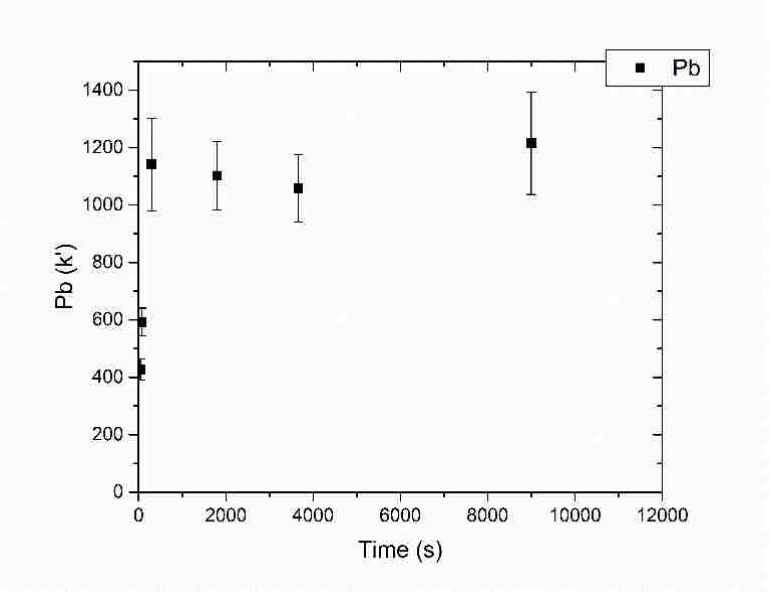

Figure 63. Kinetics of $^{212}Pb^{2+}$ in 1 M HNO3 media on Pb resin (50-100 µm), varying equilibration times.

The sorption of Pb^{2+} was extremely fast with k' values of > 400 achieved in 30 seconds or less. This result is far faster and stronger uptake than that observed for Pb^{2+} in HCl media (Figure 6-4). This indicates that the $Pb(NO_3)_2$ complex forms faster and extracts more rapidly than the analagous chloride species most likely due to higher stability with DtBuC18C6. Similar to the HCl system, full equilibrium is reached within five minutes. Large errors in the longer equilibration times are due to poor backend counting statistics due to the large k' values. Results indicate that it is possible to extract Pb with the Pb resin from HNO_3 on the second time scale, a property required for a Fl experiment.

7.2.3 Column Study

Column experiments were performed to determine if a sequential extraction of Pb^{2+} and Sn^{4+} was possible starting from an HNO_3 matrix. Due to the fact Sn does not extract on the Pb resin from any HNO_3 concentration, a load solution of 1 M HNO_3 was chosen to have strong

retention of Pb. The Sn was eluted by continuing to take 1 M HNO_3 fractions before switching to 8 M HCl to elute Pb (Figure 64).

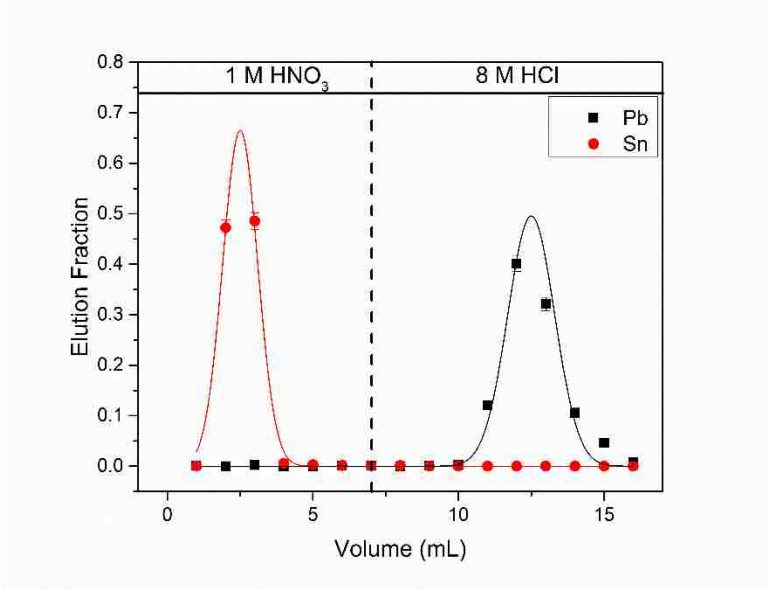

Figure 64. Column elution of 2 mL pre-packed Eichrom Pb resin cartridges at ~2 mL/min flow rate for the separation of Pb^{2+} from Sn^{4+} with an HNO3 starting matrix.

As expected, Sn^{4+} passed through the column without extraction in the 1 M HNO_3 load and elution fractions. Changing to 8 M HCl, the same concentration used to elute Pb^{2+} in Chapter 6, yielded complete elution of the Pb^{2+} on the column. Due to the fact that even at concentrated HNO_3 Pb has a significant k', elution of Pb from an HNO_3 matrix was not possible.

7.3 Conclusions and Future Work

This chapter explores the extraction behavior of the Fl direct homologs Pb and Sn from an HNO_3 matrix with the EIchrom Pb resin. Similar to literature, Pb^{2+} shows much stronger uptake over the entire range of HNO_3 concentrations than in the HCl system presented in Chapter 6. The extraction mechanism is similar with $Pb(NO_3)_2$ being extracted into the cavity, and the increased extractability is most likely due to stronger complex stability with the crown

ether. In HNO_3 Sn^{4+} more than likely exists as SnO_2, a neutral species, which due to the small ionic radius of Sn cannot be extracted by the crown ether. Given the fact the Sn extraction in HCl was most likely due to an ion-exchange type extraction with a cationic crown ether species, in HNO_3 the lack of anionic Sn species can be attributed to the lack of extraction. While it was not tested due to the lack of Hg radioisotopes, Hg should form similar complexes to that of Pb in HNO_3, and it can be expected that Hg would also extract on the Pb resin. Therefore, it might be possible to separate Pb, Sn and Hg with the Pb resin.

Kinetic study results indicate that the update kinetics for Pb^{2+} from an HNO_3 matrix on the Pb resin are much faster than from the HCl system of Chapter 6. While Hg was not tested, due to analogous complex formation it might be the case that Hg kinetics would also increase from the HNO_3 system. In the second time scale of a Fl experiment, the kinetic study indicates Pb would not be at full equilibrium; however, sufficient extraction (much higher than in HCl) would be achieved to reach an equilibrium-like state where behavior of Pb can be examined on the second time scale. It is possible to separate Pb and Sn on the second time scale from an HNO_3 matrix.

Column studies ran at ~2 mL/min flow rates on a vacuum box with 2 mL pre-packed Pb resin cartridges shows clean separations of Pb^{2+} and Sn^{4+}. Even with the fast flow rates, complete recovery of both Pb and Sn was attainable with no detectable cross-contamination between elution of each. Therefore, it would be possible from an HNO_3 matrix using the Pb resin to separate the direct homologs of Fl on time scales necessary for a Fl experiment.

Due to the possibility of Fl having Hg behavior, prior to any on-line experiment, future work must be performed to determine the uptake parameters and kinetics of Hg on the Pb resin from an HNO_3 matrix. From the results presented in this chapter, an experiment could be designed to determine whether Fl is similar to Pb^{2+}. A column experiment which was run on-line

with 1 M HNO_3 for a set duration then switched to 8 M HCl for a set duration would be able to determine if FL was Pb^{2+}/Hg^{2+} like or Sn^{4+} like. If a Fl atom was observed in the 1 M HNO_3 fractions it would be more similar to Sn^{4+} than Pb^{2+}. If a Fl atom was observed in the 8 M HCl fractions it would be more similar to either Pb^{2+} or Hg^{2+}, due to the fact that Hg^{2+} under the flow rates required for an on-line Fl experiment would elute off the Pb resin from 8 M HCl (Chapter 6). Another possibility is to use a liquid-liquid extraction system with DtBuC18C6 as the organic extractant with an initial 1 M HNO_3 stream and then back extraction of the organic phase with 8 M HCl, counting each aqueous phase. In this case Sn^{4+} like behavior would be observed in the 1 M HNO_3 aqueous phase and Pb^{2+} or Hg^{2+} behavior in the 8 M HCl aqueous phase. Both of these proposed experiments assume that an automated chemistry system can perform these separations and prepare dried α-spectroscopy samples for Fl detection at the time scales required.

CHAPTER 8: THIACROWNS WITH FL HOMOLOGS AND PSEUDO-HOMOLOGS

As discussed in Chapter 4, the non-commercially available thiacrown ether hexathia-18-crown-6 (HT18C6) was synthesized and characterized for use in extractions. Due to their increased affinity for softer metals it was believed that thiacrown ethers or some derivative of them may show stronger extractions and better kinetics for the Fl homologs and pseudo-homologs.

In this chapter, initial studies of the extraction behavior of the synthesized HT18C6 and the smaller commercially available tetrathia-12-crown-4 (TT12C4), Figure 65, are investigated.

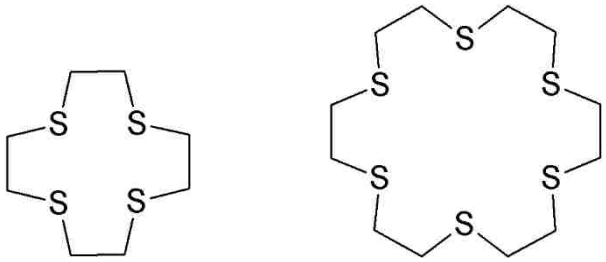

Figure 65. (Left) Tetrathia-12-crown-4, (Right) Hexathia-18-crown-6.

Liquid-liquid extraction studies with the thiacrowns in dichloromethane (DCM) are performed and compared. Insight into potential extraction systems and synthesis of thiacrowns which may show better extraction are discussed.

8.1 Discussion on solubility

The solubility of HT18C6 in DCM, nitrobenzene, dimethyl sulfide (DMS) and toluene was briefly tested. Table 23 summarizes the observations.

Table 23. Observed HT18C6 solubility.

Organic	Approximate Concentration (M)	Observation
Dichloromethane	0.0001-0.003	Dissolved at all concentrations after one hour began to precipitate out of solution in 0.003 M (possible suspension)
Nitrobenzene	0.0001-0.003	Dissolved only slightly at 0.0001 M undissolved higher
Dimethyl sulfide	0.0001-0.03	Dissolved and stayed dissolved at all concentrations tested
Toluene	0.0001	Did not dissolve

After observation of particulates in 0.003 M HT18C6 in DCM, concentrations of approximately 0.0001 M were chosen for all experiments. DMS was not used for experiments due to the potential for it to extract Hg on its own.

8.2 Reagents and Materials

The HT18C6 used was synthesized as described in Chapter 4, with no further purification. TT12C4 (≥ 90%, Sigma Aldrich) was purchased from Sigma Aldrich and used as received. DCM (99.9 %, un-stabilized, Fisher) was used without further purification. Acids were prepared by volumetric dilution from trace-metal grade acids and de-ionized water (18 MΩ·cm), in the concentrations presented in Table 15 above. Tracer solutions were identical to the tracers discussed in Chapter 6.1.1.

8.3 HT18C6

8.3.1 Solvent Extraction studies Experimental

General solvent extraction (SX) procedures are presented in Chapter 3.3. Two SX experiments were performed, the first being a preliminary experiment to measure the uptake of Hg by HT18C6, and the second was to explore the extraction behavior of Pb, Sn and Hg. For the

Hg extraction experiment a solution was prepared by dissolving 22 mg of HT18C6 in 25 mL of DCM in a volumetric flask, and sonicating the solution to ensure the HT18C6 dissolved. This yielded a solution that was ~0.003 M HT18C6. Using the acid concentrations from Table 15, 0.48 mL of acid was added to 0.5 mL of the HT18C6 stock solution in DCM. These solutions were mixed with a vortex mixer for 30 min to precondition the phases. A 20 µL spike of a stock solution containing ^{197m}Hg in 2.0 M HCl was added and the samples were allowed to mix on a vortex mixer for 1 hour. Following equilibration, 300 µL of each phase were added to clean 1.5 mL centrifuge tubes using a direct displacement pipet, and counted by HPGe gamma spectroscopy (300-1800 seconds to obtain suitable counting statistics) to determine distribution ratios as described in Chapter 3.3.2. This experiment was done in triplicate using the same HT18C6 stock solution.

To determine the extraction behavior of Pb, Sn and Hg a new HT18C6 stock solution was prepared by dissolving approximately 22 mg of HT18C6 in 25 mL of DCM in a volumetric flask by the same method mentioned above. This yielded a solution that was ~0.0001 M HT18C6. The phases were equilibrated by the same manner mentioned above and the experiment was performed in the same manner, with the exception that the 20 µL spike was from a stock solution containing ^{212}Pb, ^{113}Sn and ^{197m}Hg in 2.0 M HCl. This experiment was only performed one time and the errors were determined from the propagation of counting statistics rather than originating from standard deviation of replicates.

8.3.2 Solvent extraction studies results and discussion

Initial SX studies aimed to determine the Hg uptake by HT18C6 in DCM from an HCl matrix. Figure 66 shows the effect of HCl concentration on the uptake of Hg by HT18C6 in DCM.

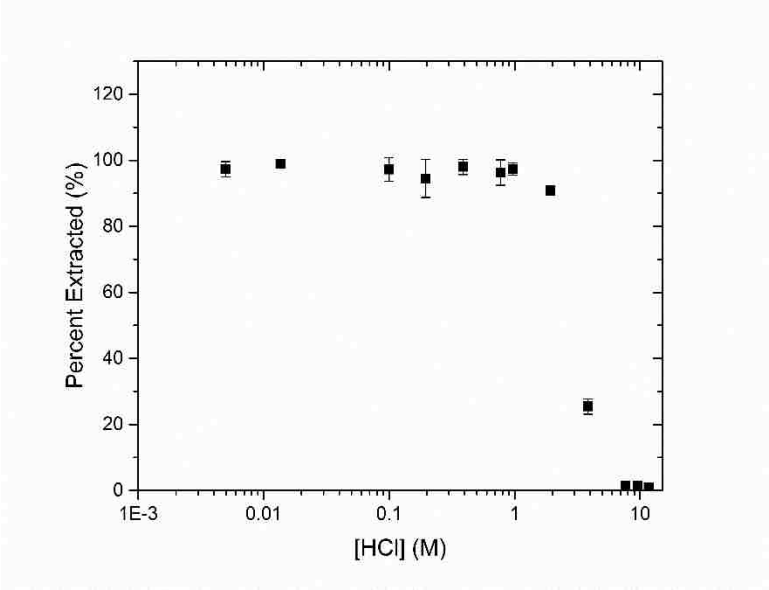

Figure 66. Uptake of ^{197m}Hg as a function of HCl concentration by ~0.003 M HT18C6 in DCM. Errors from standard deviation of three replicates.

Mercury shows very strong affinity with near 100 % extraction for concentrations up to and including 1 M HCl. As the concentration increases beyond 1 M HCl Hg extraction decreases untill it reaches zero by 8 M HCl. Due to the exodentate nature of the sulfurs in HT18C6 (see Chapter 1), it is possible for Hg to either be extracted off the side of the crown ring, or for the crown to conform around the Hg, or potentially a hybrid bridged structure between Hg and multiple HT18C6 rings. Due to the fact that energy must be expended to distort an exodentate thiacrown to bind a metal similarly to the traditional crown ether, the most likely complex is a bridged or sandwich complex [178,181-184]. Due to the fact that the solubility of HT18C6 was very low, it was impossible to do a speciation study by varying the crown concentration to attempt to elucidate the number of HT18C6 molecules involved in the extraction.

The above experiment was repeated with the addition of ^{212}Pb and ^{113}Sn to the radionuclide stock solution containing ^{197m}Hg, Figure 67.

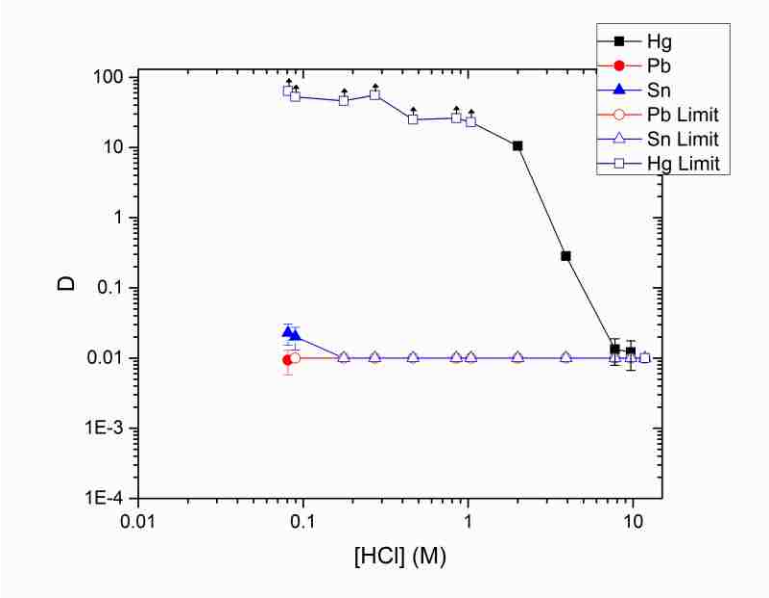

Figure 67. Uptake of ^{212}Pb, ^{113}Sn and ^{197m}Hg as a function of HCl concentration by ~0.0001 M HT18C6 in DCM. Errors from counting statistics.

As can be seen the same behavior was observed for Hg as in Figure 66; however, unexpectedly Pb showed no extraction over the entire concentration range tested. Limits were set by calculating distribution ratios based on background counts in the aqueous phase or organic phase (whichever was fundamentally zero) over the counting duration. Other thiacrown systems have been shown to extract Pb^{2+}, but in most cases a substituent on the thiacrown forced the sulfurs to be oriented endodentate to the ring like a traditional crown ether [230]. Therefore, the HT18C6 macrocycle may not be able to form a bridged or sandwich complex with Pb^{2+} and the energy required for conformation to an endodentate configuration is most likely too large to favor bonding of Pb^{2+} in the cavity. Unlike DtBuC18C6 discussed above, extraction of a cationic species to activate the crown ether is probably not possible with HT18C6 and thus the $SnCl_6^{2-}$ complex is not extracted.

8.4 TT12C4

8.4.1 Solvent Extraction studies experimental

The extraction behavior of Pb, Sn, and Hg on TT12C4 was determined in the same manner as for HT18C6 described in Section 8.3.1. The same radionuclide stock solution was used. The stock solution of TT12C4 was prepared by dissolving 24.8 mg of TT12C4 in 25 mL of DCM, giving a final TT12C45 concentration of ~0.0001 M, in a volumetric flask in the same manner as for HT18C6. The same experiment except using the TT12C4 stock in place of the HT18C6 one from Section 8.3.1 was performed. One replicate was performed and error was propagated from counting statistics.

8.4.2 Solvent Extraction Studies Results and Discussion

Figure 68 shows the extraction of ^{212}Pb, ^{113}Sn and ^{197m}Hg by TT12C4 in DCM as a function of HCl concentration.

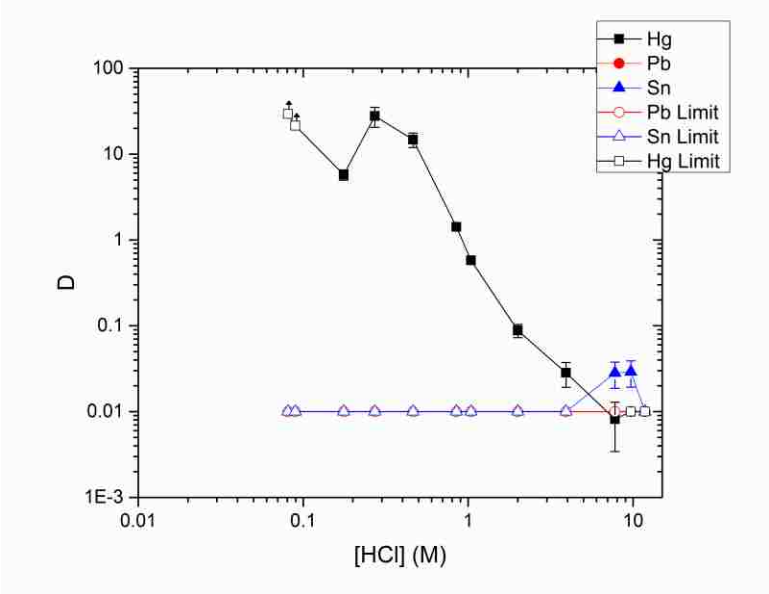

Figure 68. Uptake of ^{212}Pb, ^{113}Sn and ^{197m}Hg as a function of HCl concentration by ~0.0001 M TT12C4 in DCM. Errors from counting statistics.

As can be seen, similar behavior is exhibited by TT12C4 and HT18C6. The extraction behavior is overall less than that observed with HT18C6 for Hg, which, due to the fact the extraction is most likely not cavity based, could have to do with the fact that there are less sulfurs present in TT12C4. The fact that both TT12C4 (1.2-1.5 Å cavity) and HT18C6 (2.6-3.2 Å cavity) extract Hg but not Pb indicate that the extraction is not occurring within the cavity of the crown ether, but rather some bridged or sandwich complex. This can be assumed due to the large ionic radius of Hg^{2+} (1.1 Å) being too small to fit in the TT12C4 cavity even if it was to conform to an endodentate configuration [226].

8.5 Conclusions and Future Work

Due to the endodentate nature of the sulfurs in thiacrowns compared to the oxygens of normal crowns, the extraction mechanisms have the potential to be different, see Chapter 1. It is well established that soft nature of sulfur makes thiacrowns especially good at complexing heavy-metal ions such as Hg^{2+} and Pb^{2+} [230]. Due to the fact both HT18C6 and TT12C4 extracted Hg^{2+} with the TT12C4 extraction being less than the HT18C6, but still significant, it can be inferred that the extraction is not based on the cavity but rather some bridged or sandwich complexation of Hg (due to the significantly different cavity diameters between the thiacrowns) [178]. Since Pb^{2+} would be expected to extract by thiacrowns but did not in these cases, it also strengthens the idea that this extraction is not cavity based and that the thiacrowns tested could not form a configuration suitable for extraction of Pb^{2+}.

Due to solubility limitations, changing the thiacrown concentrations to test extraction of Hg^{2+} as a function of the thiacrown concentration was not performed. This experiment could help elucidate the extracted complex. It is most likely a sandwich complex or bridged complex which would require multiple thiacrown molecules per metal extracted.

Potential synthesis of HT18C6 derivatives with substituents that force the thiacrown into an endodentate configuration should show increased extraction of both Hg^{2+} and Pb^{2+}. This would enable similar complexation as with the analogous 18C6 complex except with the softer sulfurs which should increase the kinetics and extraction magnitude significantly.

Initial extraction tests indicated that the Hg was extracted within minutes. This is significantly faster than what was observed with DtBuC18C6. Future work could explore these kinetics more to determine the exact increase in extraction rate. However, due to the fact HT18C6 was unable to extract Pb, it was determined that the un-substituted thiacrown would not suite a Fl chemical experiment due to its inability to distinguish between Pb, Sn and Hg. Therefore, before further experiments are performed a HT18C6 molecule with substituents that force an endodentate configuration should be synthesized and characterized. This macrocycle should show extraction of at least Pb and Hg. As an aside, however, the HT18C6 macrocycle appears to be very specific for Hg compared to the other homologs and pseudo-homologs of Fl. Therefore, it may be possible to design an experiment where only Hg or non-Hg like character is determined by use of the specific HT18C6 extractant, due to the fact no affinity for Pb or Sn was observed.

CHAPTER 9: ELEMENT 115 HOMOLOGS

This chapter described the initial studies on the extraction behavior of element 115 homologs on the Eichrom Pb resin and HT18C6. As mentioned in Chapter 1, element 115 currently sits at the bottom of group 15 on the periodic table. The direct homologs of element 115 are, therefore, Bi and Sb.

In this chapter, batch experiments are performed with ^{207}Bi and ^{220m}Sb with the Eichrom Pb resin from both HCl and HNO_3 matrices. Insights into a potential extraction system using mixed HCl or HNO_3 with KI is also explored. The uptake from SX studies with HT18C6 in DCM from HCl is explored for both Bi and Sb. Potential future experiments are discussed as well as implications for an element 115 on-line experiment.

9.1 Reagents and Materials

As described in Chapter 6, the Pb resin (50-100 µm, 40 % w:w, Eichrom Industries, Inc.) was used for batch studies. Dichloromethane (99.9 %, un-stabilized, Fisher) was used without further purification. Acids were prepared by volumetric dilution from trace-metal grade acids and de-ionized water (18 MΩ·cm). A total of 11 different HCl and HNO_3 concentrations were used for experiments, Table 24.

Table 24. Acid solutions for various studies element 115 homolog studies.

Acid	Concentration (M)
HCl	0.001, 0.01[#], 0.1, 0.2, 0.4, 0.8, 1.0, 2.0, 4.0, 6.0*, 8.0, 10.0, Conc.[#]
HNO_3	0.001, 0.1, 0.2, 0.4, 0.8, 1.0, 2.0, 4.0, 6.0, 8.0, 10.0

[#]Only used on HT18C6 study.
*Only used on Pb resin study.

Potassium iodide used for experiments was a Baker Analyzed Reagent (≥99.8 %) and used without purification.

9.2 Experimental

9.2.1 Batch studies

General batch study procedures are described in Chapter 3. Uptake parameters for Bi^{3+} and Sb^{5+} on Pb resin were explored from both HNO_3 and HCl (only HNO_3 for Sb). The procedure was identical to that described in Chapter 6.1.1. To a 1.5 mL centrifuge tube, 10-20 mg Pb resin was added along with 1 mL of HCl or HNO_3 with the concentrations from Table 24. The samples were placed on a vortex mixer for 1 hour to allow preconditioning of the resin. Radionuclide stock solutions of ^{207}Bi and ^{220m}Sb were prepared in 2.0 M HCl or HNO_3 and 100 µL spikes were added to the wet resin in the appropriate acid matrix (Bi and Sb experiments were done separately). The solutions were equilibrated for 3 hours during which time each sample was counted by an HPGe gamma spectrometer for 300-900 seconds in order to attain sufficient counting statistics. Following equilibration the resin was filtered through a 0.45 µm PTFE filter to separate the resin from the solution. A 700 µL aliquot of each filtered solution was added to 400 µL de-ionized water in a new 1.5 mL centrifuge tube to maintain initial counting geometry. Each experiment was performed in triplicate and reported errors are based on the standard deviation of the three replicates. The Pb resin capacity factor (k') was calculated as described in Chapter 3. Reported values for HNO_3 and HCl concentrations were calculated from the combination of the 1 mL of initial acid and the 100 µL of the 2 M spike solution.

Based on literature data, which indicated that Sb^{3+} can be separated from Bi^{3+} with 18-crown-6 in DCM from iodide media [231], batch experiments were preformed to test the validity of this extraction with the Pb resin and modified matrices. A KI solution was prepared by dissolving 24.92 g KI in 50 mL of de-ionized water in a volumetric flask resulting in a solution of

3.0 M KI. To a 1.5 mL centrifuge tube 1 mL of HNO_3 of HCl (0.001, 0.4, 1.0, 2.0, 6.0, 8.0 or 10.0 M) was added to 10-20 mg Pb resin along with 30 µL of the KI solution to yield 0.08 M KI. The samples were allowed to pre-condition by mixing with a vortex mixer for 1 hour. A 100 µL spike of the ^{207}Bi stock solution described above was added to the wet resin in 2.0 M HNO_3 or HCl (depending on sample matrix). The samples were allowed to equilibrate by mixing on a vortex mixer for 3 hours, while being counted for 300 seconds via HPGe gamma spectroscopy. The resin was removed by filtering with a 0.45 µm PTFE filter, and a 700 µL spike was added to 430 µL of de-ionized water in a new 1.5 mL centrifuge tube to maintain counting geometry and counted for 1 hour each via HPGe gamma spectroscopy. The Pb resin capacity factor (k') was calculated as described in Chapter 3, with limits on high k' values set based on background counts observed in the channel from 1 hour counts. Errors were determined by propagation of counting statistics as each experiment was only performed once.

9.2.2 HT18C6 SX studies

General SX procedures are described in Chapter 3. HT18C6 stock solution was prepared by dissolving 20.4 mg HT18C6 in a 25 mL volumetric flask with DCM, giving a final solution concentration of approximately 0.0023 M. To a 1.5 mL centrifuge tube, 480 µL HT18C6 stock solution along with 500 µL HCl in the concentrations from Table 24 were added. These solutions were allowed to mix for 30 min on a vortex mixer to allow for preconditioning of the phases. A 20 µL spike of 2.0 M HCl containing ^{207}Bi and ^{124}Sb (prior to addition the stock solution was evaporated to dryness with 10 µL H_2O_2 to ensure the Sb was in the Sb^{5+} state, before being brought up in 2.0 M HCl) was added and the samples allowed to mix for 3 hours on a vortex mixer to allow equilibration. After equilibration 300 µL of both the organic and aqueous phase were added to new 1.5 mL centrifuge tubes with a direct displacement pipette and each phase was counted by HPGe gamma spectrometry for 300-3600 seconds to obtain suitable statistics.

Distribution ratios were calculated as described in Chapter 3, with errors determined from counting statistics since only one replicate was performed.

9.3 Results and Discussion

9.3.1 Eichrom Pb Resin

Initial batch results performed in triplicate with Bi^{3+} from both HNO_3 and HCl are shown in Figure 69.

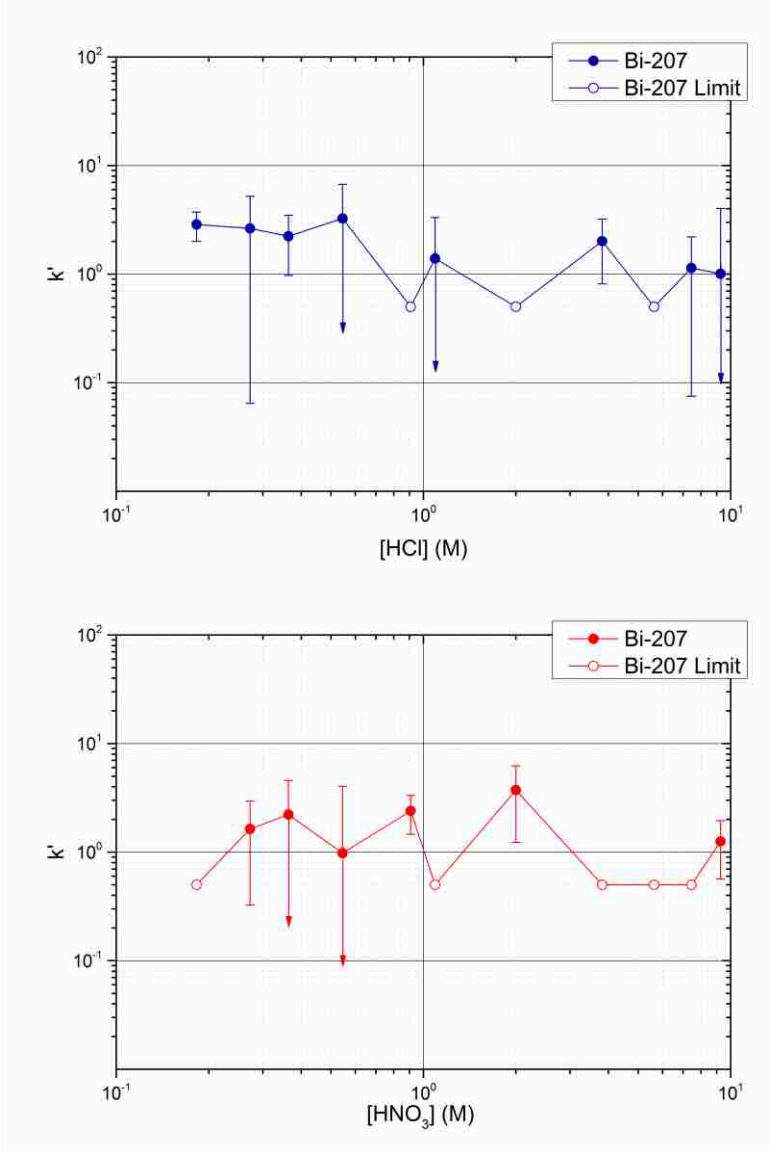

Figure 69. The batch uptake (k') of ^{207}Bi as a function of hydrochloric acid (Top) and nitric acid (Bottom) on Pb resin (50-100µm) with a 3 hour equilibration time.

As seen in Figure 69, Bi shows no uptake on the Pb resin in either acid system. Despite the fact that in HCl it can form $BiCl_5^{2-}$, which one might expect to analogously extract as an ion-associated complex with a H_3O^+ cationic crown complex, no extraction is shown [232]. This can be attributed to unfavorable charge distribution compared to that of $SnCl_6^{2-}$ possibly due to the size increase. In HNO_3 Bi tends to form a large number of both cationic and anionic complexes or neutral complexes, which do not interact with the crown ether [154,155]. In nitric acid Bi most

likely exists as $Bi(NO_3)_3$, which, since the analogous $Pb(NO_3)_2$ complex does extract, may be hindered due to steric factors from interaction with the crown core [154].

Batch studies were not performed on Sb from HCl due to the fact it was desired to ensure its oxidation state was Sb^{5+}. Figure 70 shows batch results performed in triplicate with Sb^{5+} from HNO_3.

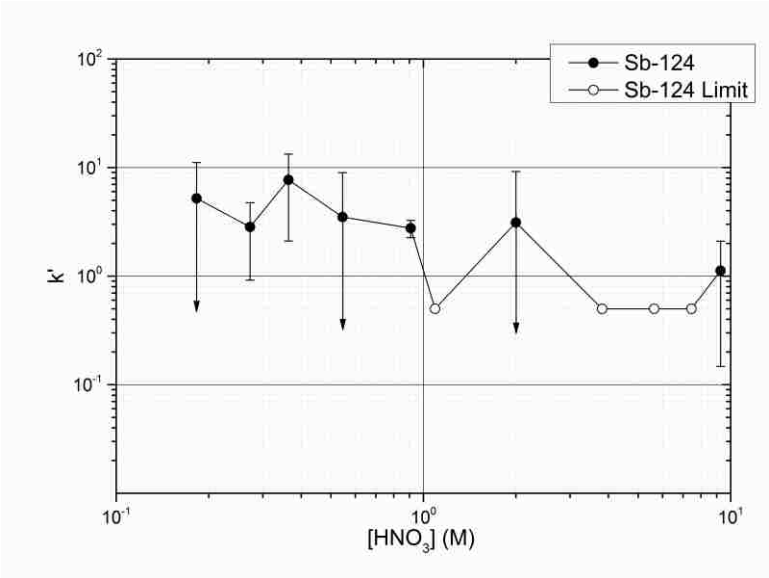

Figure 70. The batch uptake (k') of ^{120m}Sb as a function of nitric acid on Pb resin (50-100µm) with a 3 hour equilibration time.

As can be seen in Figure 70, Sb shows no uptake on the Pb resin. As mentioned in Chapter 1, antimony tends to form oxides in HNO_3, even cationic oxides [157], which may be responsible for its lack of extraction on the Pb resin considering this differs greatly from extracted Pb and Sn species. While it is known that Sb can form SbX_6^- (where X= F, Cl, Br) these are unfavorable and easily hydrolyzed [157,220]. Therefore, an analogous extraction from HCl to Sn^{4+} is unlikely.

It is well known that the most favorable anionic halide formation by both Bi^{3+} and Sb^{3+} are the BiI_4^- and SbI_4^- complexes [231]. Literature experiments indicated it is possible to extract Bi^{3+} and Sb^{3+} from H_2SO_4 matrices into DCM containing 18C6 [231]. The mechanism for this

extraction is first the extraction of K^+ into the crown cavity and then extraction of the BiI_4^- and SbI_4^- complex by ion association. Initial experiments to assess the validity of this type of extraction with the Pb resin from a HNO_3 or HCl matrix mixed with KI were assessed. Batch results for Bi^{3+} extraction from an HNO_3 and HCl/KI matrix are shown in Figure 71.

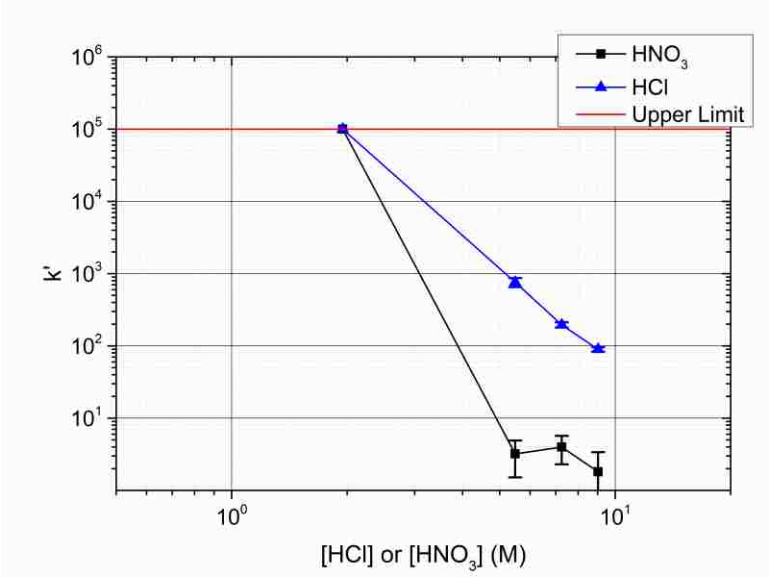

Figure 71. The batch uptake (k') of ^{207}Bi as a function of hydrochloric and nitric acid media with 0.08 M KI on Pb resin (50-100 µm) with a 3 hour equilibration time.

As can be seen from Figure 71, extremely strong uptake of Bi^{3+} is seen in both HNO_3 and HCl in the presence of 0.08 M KI until an acid concentration of 2 M at which time in both acid matrices the extraction drops. The k' limit was set based on the number of background counts (essentially zero) in the one hour long backend counts. The believed extraction mechanism is:

$$\mathrm{BiI}_{4\mathrm{aq}}^{-} + \mathrm{DtBuC18C6}_{\mathrm{org}} \rightleftarrows \ \mathrm{BiI}_4^- \cdot [\mathrm{X} \cdot \mathrm{DtBuC18C6}]_{\mathrm{org}}^+$$

Where X= H_3O^+ or K^+. This drop in extraction could be attributed to potential for competing complex formation with the iodide due to the large concentration increases and potentially due to the removal of K^+ from the crown cavity; however, at higher acid concentrations the crown ether cavity will be populated by H_3O^+ which should enable the ion-exchange extraction to still

happen. The formation of non-anionic species in HNO_3 should be higher with the prevalence of oxide species compared to that of the halide based HCl solution, hence the faster decrease in k' with increase in HNO_3. This experiment was not performed with Sb, but based on literature and the Bi experiment Sb should extract from this system [231]. While this extraction system allows the direct homolog of element 115, Bi, to extract, it is not practical for an on-line element 115 experiment. Due to the fact a weighable quantity of KI is present in the system, a significant amount of mass would be present without additional purification when preparing α-spectrometry samples, which would affect direct measurement of the element 115 α-decay chains. A pure HI system may enable extraction, with the mechanism:

$$\mathrm{XI}_{4\mathrm{aq}}^{-} + \mathrm{DtBuC18C6}_{\mathrm{org}} \rightleftarrows \ \mathrm{XiI}_{4}^{-} \cdot [\mathrm{H_3O} \cdot \mathrm{DtBuC18C6}]_{\mathrm{org}}^{+}$$

Where X= Bi or Sb. However, the resin is subject to degradation by the pure HI system, so long term experiments with this system would prove difficult.

9.3.2 HT18C6

Sulfide complexes of Bi and Sb are known to exist [220, 232]. Therefore, testing the extraction of Bi and Sb by the synthesized HT18C6 extractant out of DCM was performed, Figure 72.

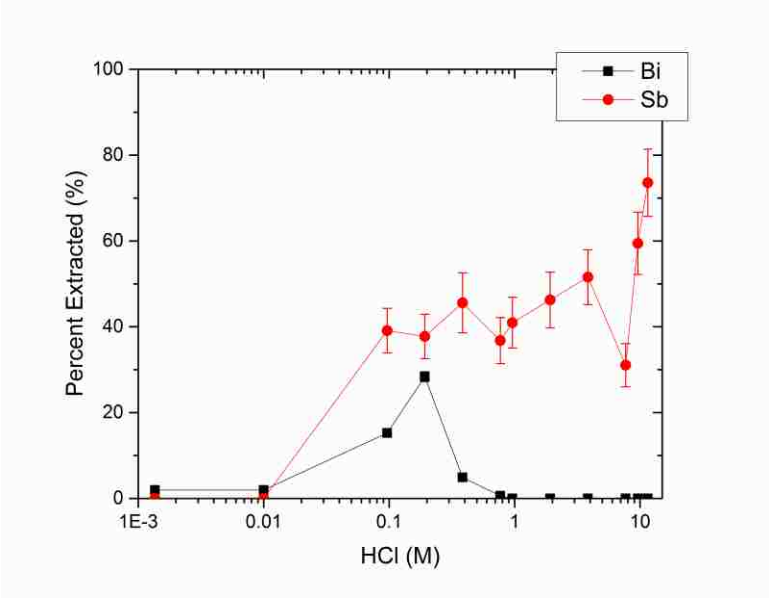

Figure 72. Extraction behavior of ^{207}Bi and ^{124}Sb by ~0.003 M HT18C6 in DCM, with 3 hour equilibration time. Errors from counting statistics.

As can be seen from Figure 72, a slight extraction of Bi is seen around 0.2 M HCl and a 40-80% extraction of Sb is seen for all concentrations ≥0.1 M HCl. Due to the fact Bi most likely exists as a chloro-species a sandwich or bridged sulfur Bi complex is most likely partially formed, yielding the slight extraction around 0.1 M HCl. Antimony is known to make sulfide and complex sulfide complexes. In acidic halide solution Sb has a higher affinity for making hydrolyzed or oxide complexes instead of halide complexes (though halide complexes have been observed) [157]. Therefore, the extraction system is most likely a bridged or sandwich complex with an antimony complex ion interacting with the HT18C6 ring sulfurs. Due to the lack of ^{124}Sb this experiment was only performed once, and very little insight to the extracted complex can be garnered from the results. However, it is noted that Bi and Sb do have some interaction with the thiacrown ether, yielding a possibility of a much stronger extraction, after the mechanism is determined, by tuning a thiacrown to match the desired properties.

9.4 Conclusions and Future Work

This chapter explored potential systems for an element 115 chemistry experiment through the analysis of extraction behavior of Bi^{3+}, Sb^{3+} and Sb^{5+} with the Pb resin and HT18C6. From simple acid systems, such as pure HNO_3 or HCl systems, essentially no extraction is shown for Bi^{3+} and Sb^{5+} on the Eichrom Pb resin. This is most likely due to the fact that the charge densities of the potential $BiCl_5^{2-}$ complex different greatly from the analogous $SnCl_6^{2-}$ complex which is extracted and the tri-nitrate complex in nitric acid being more stericly hindered from interaction with the crown cavity than the di-nitrate Pb complex. In the case of Sb^{5+} its existence as hydrolyzed species or oxides of varying charge in nitric acid could explain its lack of interaction with the crown ether.

A more promising extraction is based off the fact Bi^{3+} and Sb^{3+} readily form iodide complexes of the form BiI_4^- and SbI_4^-. It was shown that from both HNO_3 and HCl mixed with 0.08 M KI it was possible to extract Bi^{3+} over a wide range of acid concentrations. Presumably as an anionic iodide complex associating with a K^+ activated crown ether or H_3O^+ activated crown ether core. Similar extractions in literature used H_2SO_4 as the acid and only very dilute to favor the iodide complex formation, competing complex formation as HNO_3 and HCl concentrations increased can be attributed to the drop in extraction. A possible fix for this would be to perform the extraction from pure HI so only the iodide complex would be formed and use H_3O^+·DtBuC18C6 as the extraction media based on ion exchange with anionic Bi or Sb. While, due to the lack of Sb isotopes, this was not performed with Sb, this iodide extraction should be possible with Sb^{3+}. The KI based system is not suitable for an element 115 experiment due to the need to remove KI prior to α-spec sample evaporation, since this would add a mass that would make identification of characteristic α-particles of element 115 and its daughters difficult. The time it would take to remove the Ki would be too long due to the short half-life of element 115.

However, the HI system, if extraction proved to be sufficient, would be a potential modification that would yield little excess mass upon evaporation for preparation of α-spectroscopy samples.

Unexpectedly, Bi^{3+} and Sb^{5+} showed an affinity for extraction by HT18C6 out of HCl media. This extraction mechanism is unknown, and at best reached 80 % for Sb^{5+} at higher HCl concentrations, with a maximum for Bi^{3+} of 20 % at 0.2 M HCl. Most likely the extracted complex is some form of bridged or sandwich sulfide complex with Bi and Sb, due to the exodentate nature of the un-substituted HT18C6. While in this state, it is not a suitable system for an element 115 experiment, due to the observed extraction of both Bi and Sb future work could elucidate the extracted species and seek to synthesize a thiacrown ether with properties better suited to this extraction. This could yield an element 115 chemical system based on thiacrown ethers.

At this time the work presented in this chapter is preliminary. Results indicate that with more work a potential Pb resin based system for element 115 may be possible from HI media. They also indicate the potential for novel thiacrown ethers to be synthesized that could show great affinity for the element 115 homologs, Bi and Sb, and yield a potential system.

CHAPTER 10: OTHER MACROCYCLES

Prior to determining to use only crown ethers and thiacrown ethers brief studies were performed using other macrocyclic extractants. Two of these extractants are 2,2,2-cyrptand and p-tert-butylcalix[6]arene, Figure 73 and 74.

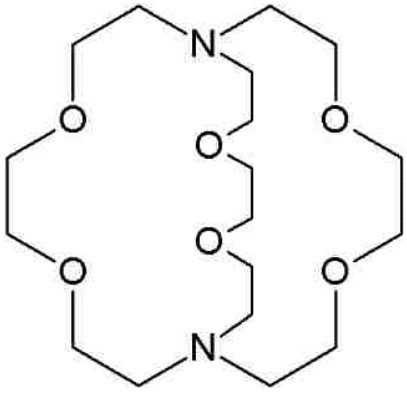

Figure 73. Molecular structure of 2,2,2-cryptand.

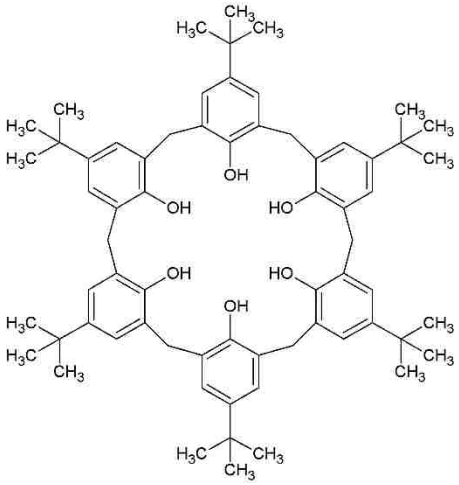

Figure 74. Molecular structure of p-tert-butylcalix[6]arene.

Like with crown ethers cryptands and calixarenes extract metals by complexation in their cavities [164]. Cryptands show far stronger binding constants and specificity compared to that of

traditional crown ethers due to the pocketed nature of the molecule. Whereas calixarenes have even less ability to change their cavity to suit a changing host [164].

In this chapter initial studies are presented using the 2,2,2-cryptand and p-tert-butylcalix[6]arene to determine their extraction capabilities for the Fl homolog Pb. SX studies are presented for the extraction of ^{212}Pb by 2,2,2-cryptand and p-tert-butylcalix[6]arene in DCM from an HCl matrix.

10.1 Experimental

10.1.1 Reagents and Materials.

Both 2,2,2-cryptand (Aldrich, ≥ 98 %) and p-tert-butylcalix[6]arene (Aldrich, ≥ 90 %) were used without further purification as received from Sigma Aldrich. Dichloromethane (99.9 %, un-stabilized, Fisher) was used without further purification. Acids were prepared by volumetric dilution as in Chapter 6, with the same concentrations from Table 15 (except 0.01 M was not used for the calixarene study). Solutions of 2,2,-cryptand and p-tert-butylcalix[6]arene for SX studies were prepared in 25 mL and 50 mL volumetric flasks respectively as shown in Table 25.

Table 25. Organic phase solutions of 2,2,2-cryptand and p-tert-butylcalix[6]arene.

Extractant	Mass used (g)	Concentration (M)
2,2,2-cryptand	0.2354	0.013
p-tert-butylcalix[6]arene	0.0496	0.0010

10.1.2 SX Studies

General SX procedures are presented in Chapter 3. For the 2,2,2-cryptand study, 480 µL of the appropriate acid concentration was added to 500 µL of the 2,2,2 cryptand stock solution in a 1.5 mL centrifuge tube. The phases were allowed to precondition for 1 hour by mixing on a

vortex mixer. A 20µL spike of ^{212}Pb in 2.0 M HCl was added to each sample and the samples were allowed to equilibrate by mixing on a vortex mixer for one hour. Following equilibration, each sample was centrifuged for 30 seconds at 6000 rpm before 300 µL of each phase were removed with a direct displacement pipet and placed in new 1.5 mL centrifuge tubes. Each separated phase was counted for 90 to 450 seconds by HPGe gamma spectroscopy. Distribution ratios were calculated as described in Chapter 3. Final reported acid concentrations were calculated by the corrected acid concentration after addition of the 20 µL spike.

For the p-tert-butylcalix[6]arene study the same procedure as used for the 2,2,2-cryptand study was performed with the following changes: 400 µL of aqueous phase was allowed to precondition with 500 µL of the p-tert-butylcalix[6]arene stock solution; a 100 µL spike of ^{212}Pb in 0.5 M HCl was added to each solution; 200 µL of each phase was taken with a direct displacement pipet; and each sample was counted by HPGe gamma spectroscopy for 120 to 300 seconds. Distribution ratios were calculated as described in Chapter 3. Final reported acid concentrations were calculated by the corrected acid concentration after addition of the 100 µL spike.

10.2 Results and Discussion

10.2.1 SX studies

Figure 75 shows the extraction of ^{212}Pb by 2,2,2-cryptand in DCM as a function of HCl concentration.

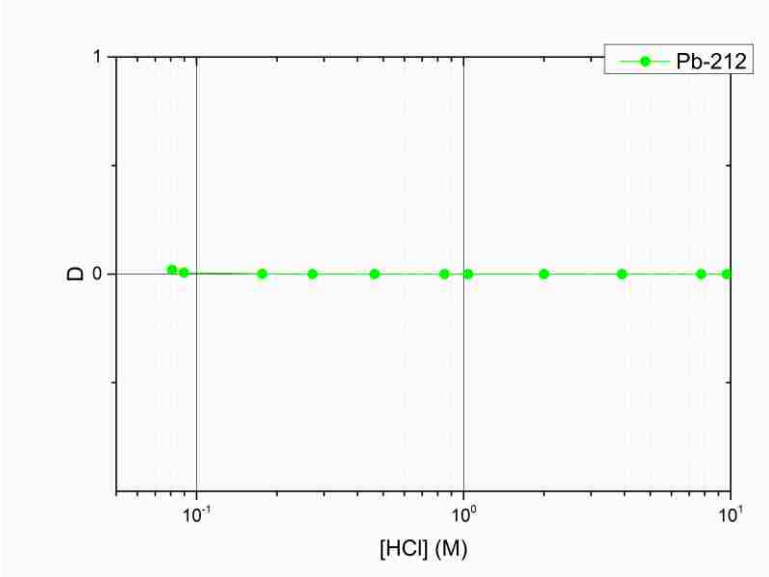

Figure 75. Extraction behavior of ^{212}Pb as a function of HCl concentration with 0.013 M 2,2,2-cryptand in DCM.

As can be seen in Figure 75, no extraction of Pb is seen on 2,2,2-cryptand from a pure HCl matrix. This can be attributed to the fact that the specificity of the cryptand and the fact that counterbalancing the Pb^{2+} ion is restricted due to the pocketed nature of the cryptand when compared with the traditional crown ether. Literature extractions of Pb^{2+} by cryptands use substituted cryptands and an ion exchange method, whereby first extracting a cation into the cavity of the cryptand and then extracting an anionic Pb species [233]. From the pure HCl system performed in this study, an ion-exchange based extraction is not possible, due to the lack of a cationic species to be extracted by the cryptand first.

The extraction of ^{212}Pb by p-tert-butylcalix[6]arene in DCM as a function of HCl concentration is shown in Figure 76.

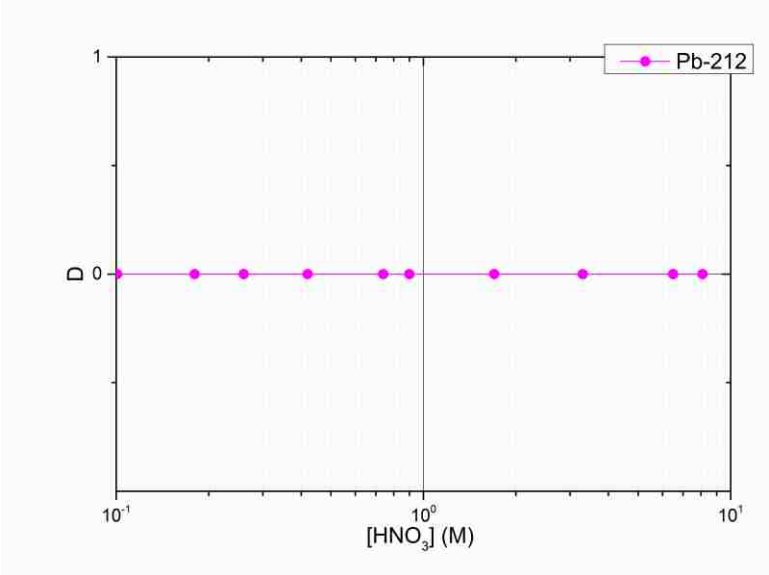

Figure 76. Extraction behavior of ^{212}Pb as a function of HCl concentration with 0.001 M p-tert-butylcalix[6]arene.

As seen in Figure 76, no extraction of Pb is observed over the range of HCl concentrations studied. The only extractions of Pb^{2+} shown in literature with a calixarene was with a highly substituted with a novel proton-ionizable group calix[4]arene that showed high selectivity for Pb^{2+} from HNO_3 [234]. Due to the similarities in compound formation between HCl and HNO_3 for Pb, the cavity size of calix[6]arene may be too large to be selective for the Pb^{2+} ion considering the smaller calix[4]arene was used for successful extractions from a pure acid system. The lack of proper substituents which increased selectivity of the calix[4]arene may also be attributed to the lack of extraction. A substituted calix[4]arene showed high selectivity for Hg^{2+}, which has a similar ionic radius to Pb^{2+}, as well, indicating the calix[6]arene cavity may simply be too large [235].

10.3 Conclusions and Future Work

Solvent extraction studies presented in chapter served as a comparison for the different 6 membered macrocylce rings. Results showed that un-substituted 2,2,2-cryptand and the slightly substituted p-tert-butylcalix[6]arene do not extract Pb^{2+} from an HCl matrix. This result

led to the direction of work being focused towards the DtBuC18C6 extractant on Eichrom's Pb resin and the HT18C6 extractant. Due to the difficulty calixarenes have with changing their cavity size compared to crownethers, the calix[6]arene used may simply have been too large to extract Pb^{2+} given the fact literature extractions of Pb^{2+} with calixarenes involved the use of a highly substituted calix[4]arene [234]. Due to the increased selectivity of the cryptands compared to traditional crownethers and the restriction the pocketed cavity places on cation binding, simple acid systems may not be capable of extracting Pb^{2+} using cryptands. This is supported by literature uses of cryptands to extract lead based on ion-exchange type systems [233].

Fututre work with calixarenes and cryptands, while may prove promising, would require difficult novel synthesis of substituted molecules which are not commercially available. Due to the types of extractions found in literature, more work should focus on synthesis of thiacrowns which should show extreme affinity for the soft metals.

CHAPTER 11: CONCLUSIONS

The primary focus of this dissertation was to examine the possibility of using macrocyclic extractants to develop a chemical system that could give insight into the chemical behavior of Fl and element 115. Specifically, the question: is their location on the periodic table consistent with only their proton number or truly consistent with their chemistry? Predictions for Fl have indicated that it may behave like the other members of Group 14, or it could be far less reactive and even as unreactive as a noble gas. Therefore, calling into question its placement in Group 14 of the periodic table because of potentially vastly deviating chemical properties, due to strong relativistic effects, from the group homologs Pb and Sn. Element 115 has far fewer predictions, but those that do exist point to vastly different properties from the other elements in Group 15. The predicted most stable oxidation state of element 115 is 115^{+}, due to relativistic effects, an oxidation state not exhibited by the other members of the chemical group except under special circumstances.

Macrocycles have shown promise in other areas of chemistry for complexation with metal cations, specifically crown ethers. Therefore, research was devoted to exploring the possibility of using crown ethers to separate the homologs and pseudo-homologs of Fl and element 115 in such a way that the system could be applied to an on-line study of the two transactinides. Other macrocycles were explored and insight toward the use of thiacrown ethers (sulfur analogs of crown ethers) as potentially more selective and faster extractants for the softer metals, such as Pb, Hg and Bi, which are the homologs of Fl and element 115.

This chapter will summarize the conclusions presented in the above chapters. A discussion of the future work needed to be able to perform an on-line chemistry experiment with Fl or element 115 is presented.

11.1 Conclusions Production of Carrier-Free Radionuclides

The LNNL CAMS facility was used to produce carrier-free radionuclides via proton irradiations of high purity stable metal foils. For the purpose of this work, the following nuclear reactions were used: $^{124}Sn(p,n)^{124}Sb$, $^{197}Au(p,n)^{197}Hg$, and $^{113}In(p,n)^{113}Sn$, with proton energies in the 10-15 MeV range. Rapid separation schemes were developed for isolating the produced radionuclides from bulk target material without the use of carrier, to yield high purity carrier-free radionuclides for transactinide homolog chemistry experiments. The target chamber used for irradiations can be used to irradiate any stack of foils to produce other carrier-free radionuclides for different purposes. A radioisotope generator to elute carrier-free ^{212}Pb and ^{212}Bi was developed from a cation-exchange column loaded with LLNL legacy ^{232}U. The generator was shown to be capable of eluting usable carrier free Bi and Pb for a period (still on-going) of 2 years.

11.2 Conclusions Fl Homolog Chemistry

The Eichrom Pb extraction chromatography resin, based on the DtBuC18C6 extractant, was chosen as the initial starting point for developing a Fl chemical system. The resin was developed with the idea of being used to remove Pb from environmental systems, since the DtBuC18C6 extracted was known to have affinity for Pb^{2+}. Prior to this work the 18C6 crown ether had not been used to extract Sn and had not been used previously to extract ultra-trace carrier-free Pb and Hg radionuclides.

Batch study results showed the possibility of separating Pb, Sn and Hg from each other using the Pb resin by only changing the concentration of HCl. However, kinetic results presented showed that while Pb reached equilibrium in approximately 5 minutes, Sn and Hg did not reach equilibrium until approximately 1 hour and > 8 hours respectively. Sn, unlike Hg, attained

significant k' values in a matter of seconds, 89.8 ± 1.3, similar to Pb, 134.5 ± 2.0. Hg showed no appreciable extraction increase until at least 30 minutes equilibration time had passed.

Initial column studies were performed with vacuum flow pre-packed Pb resin cartridges that demonstrated the ability to separate Pb and Sn after first retaining them on the resin bed using flow rates of 2 mL/min. Analogous studies with the addition of Hg to the load solution proved ineffective with Hg bleeding through the initial few column fractions at 3 M HCl due to low uptake and slow adsorption kinetics. However, loading the column in 0.4 M HCl, a condition where Sn shows no affinity to the resin, proved it was possible to retain Pb and Hg while eluting Sn. However, in order to ensure Hg would be retained throughout the 8 M HCl elution of Pb, where its k' values dip to 12.1 ± 2.0 (from batch results), the column was capped for 1 hour. The column was also capped for 1 hour after successful elution of Pb due to the first column showing that, once retained, Hg desorption kinetics were also slow.

These HCl studies with the Eichrom Pb resin demonstrated the possibility of rapidly separating the direct homologs of Fl, Pb and Sn, on the time scales required for an on-line Fl experiment ($t_{1/2}$ ^{289}Fl ~2.6 seconds). However, the addition of the potential pseudo-homolog Hg complicated the system, and made a clean separation require hours instead of seconds due to both sorption and desorption kinetics of the Hg. In Chapter 6 an on-line Fl experiment is proposed, in which a column is ran at 0.001 M HCl where Sn^{4+} passes through the column and due to the extremely high k' values for Hg > 6000 and the fast kinetics and high retention of Pb at these concentrations, both Pb and Hg would be retained. From this, an experiment could be performed with changing the concentrations to create a Pb, Sn and Hg fraction. Where under the 0.001 M HCl load solution, the observed 20-30 % Hg bleed in the Pb elution noticed without a wait period with a 0.04 M HCl load solution might be avoidable, and thus three quick fractions could be obtained. Due to the short ^{289}Fl half-life of 2.6 seconds, collecting three fractions and

drying samples down to prepare α-spectrometry sources for identification of Fl and its decay daughters, would be impossible on those time scales with current automation technologies. Therefore, running an experiment in which a single concentration is ran and sample collected and prepared for α-spectroscopy for a set duration of time, then switching to a different condition is the best hope for attaining these speeds. With this in mind, using the Eichrom Pb resin and an HCl matrix would be capable of differentiating between both Sn^{4+} (since loading in 0.001-0.04 M HCl shows no bleed of Pb or Hg) and Pb^{2+} or Hg^{2+} character. However, differentiating between Pb or Hg character would be impossible due to insufficient separation, at the time scales required, between those two elements.

Nitric acid studies performed without Hg demonstrated a quick separation was possible between Pb and Sn. With Pb having significantly quicker kinetics in the HNO_3 system when compared with the HCl system. Due to similar Hg complex formation to Pb in HNO_3, it may be extractable and potentially with faster kinetics than in the HCl system. However, this system was abandoned due to the fact the Pb kinetics were not a large enough gain, and therefore, it was assumed the Hg kinetics would still be insufficient to unambiguously determine differences between Pb and Hg like character on the second time scale.

Due to the fact that the extraction chromatography resin contains the DtBuC18C6 extractant physisorbed to a backbone, the long term use of the resin may become difficult. At high acid concentrations the extractant was observed to bleed off the resin backbone. Decreases in k' values were also observed in kinetics studies which equilibrated the resin for longer than 18 hours. Therefore, for long term use on an on-line Fl experiment if a DtBuC18C6 extractant is desired a chemically bonded resin or polymerized crown ether system should be prepared. This system should have analogous extraction capability to the extraction chromatography resin.

Thiacrown ethers are well known to be capable of extracting, with high kinetics and specificity, softer metals. Work has been done that showed their affinity toward Hg^{2+}, however, little work into Pb extraction and Sn extraction with thiacrowns had been done. The extractant HT18C6 was synthesized and its affinity for Pb, Hg, and Sn was explored and compared to that of both the DtBuC18C6 extractant and a purchased TT12C4 extractant. While the extractant showed extremely high affinity for Hg^{2+} from an HCl system it showed no affinity for both Pb^{2+} and Sn^{4+}. Due to the exodentate nature of the sulfurs in thiacrown ethers they usually form sandwich or bridged complexes with metal cations. This is readily possible with Hg, and that is why it extracts easily from both the HT18C6 and the much smaller TT12C4. In order for Pb to extract either different complexes must be formed that can interact with these thiacrowns (i.e. a different matrix) or the thiacrown must be forced into an endodentate conformation which mimics that of a traditional crown ether and by analogy should readily extract the softer metal Pb much stronger than the traditional crown ether. Due to the fact an endodentate conformation requires an input of energy which is not present from a room temperature system, new thiacrowns must be synthesized with substituents which force the ring sulfurs to take an endodentate charge conformation. This can be achieved by synthesizing a complex such as dibenzo-hexathia-18-crown-6, Figure 77:

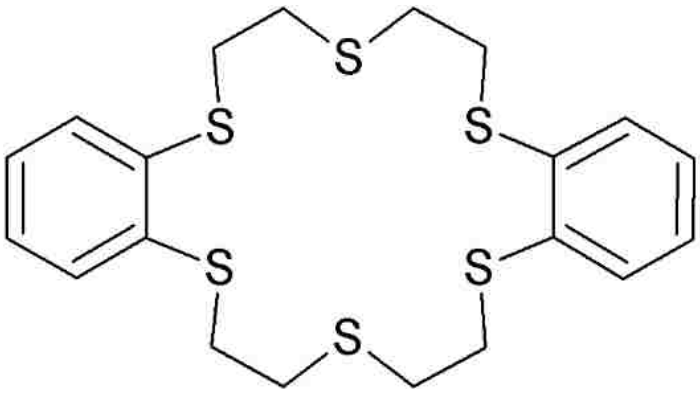

Figure 77. Structure of dibenzo-hexathia-18-crown-6.

Due to the possibility an endodentate thiacrown should show high affinity toward Pb^{2+} and continued affinity toward Hg^{2+}, and the fact the Hg kinetics observed from HT186 were much faster than with DtBuC18C6, a system based on an endodentate thiacrown may have the required kinetics for an Fl chemical system.

11.3 Conclusions Element 115 chemistry

Compared to the Fl homolog studies, element 115 homolog studies were more exploratory and preparatory. Initial studies using both HCl and HNO_3 matrices and the Eichrom Pb resin showed that both Bi and Sb were not extracted with the DtBuC18C6 extractant. Modifying a literature procedure which used iodide media in H_2SO_4 to extract Bi and Sb with 18C6, it was demonstrated that Bi could be extracted by the Pb resin from a mixed HCl/HNO_3/Ki matrix. Due to the unavailability of Sb isotopes, the experiment was only performed with Bi. However, it can be assumed, that a similar extraction based off the anionic BiI_4^- and SbI_4^- complex formation extracted by a potassium activated cationic crown ether complex could happen. Due to the usage of KI to form the iodide species, an unnecessary amount of mass is added to the system that would make preparation of α-spectroscopy samples for the unambiguous detection of element 115 in an on-line experiment difficult. This system might

work using a pure HI system with an H_3O^+ activated crown ether cavity forming the basis for the ion-exchange extraction. However, the HI system seriously degrades the extraction chromatography resin. Therefore, a polymerized crown system, or a crown ether resin with chemically bonded crown ether instead of the physisorbed crown ethers in the extraction chromatography system may be required.

Unexpectedly, HT18C6 showed slight affinity for both Bi and Sb from an HCl matrix. The extraction mechanism is believed to be a bridged or sandwich thiacrown complex with a Bi chloride complex and a Sb oxide or hydrolysis product interacting with the ring sulfurs, since sulfide complexes of both Bi and Sb are known. However, due to the lack of radioisotopes, this experiment was only performed once and very little insight as to the extraction mechanism could be garnered. It can be stated that the extraction was at best a 20-80% extraction so modification of the thiacrown to better suit the extraction mechanism, once it is determined, could yield an even better extraction of Bi and Sb.

11.4 Outlook to the Future

Experiments presented within this dissertation outline characterizations of the Fl and element 115 homologs and pseudo-homologs. Results showed the possibility of designing a chemical system based on macrocyclic extractants for probing the chemical properties of Fl, and a path forward to determining a system for element 115 was outlined. The biggest issue with the use of traditional crown ethers for an on-line Fl experiment was determined to be kinetics. The Hg kinetics were very slow when compared with that of Pb and Sn, and while it was shown that an experiment could be designed that would demonstrate whether or not Fl was Sn^{4+} like or either Pb^{2+} or Hg^{2+} like, differentiating between Pb^{2+} or Hg^{2+} like character would be nearly impossible due to the slow Hg kinetics.

Thiacrown ethers showed promise for separating Pb, Sn, and Hg; however, it was determine that a new thiacrown which had charge densities mimicking that of a traditional crown ether would be needed in order to show extraction of Pb, and thus be able to separate the three homologs of Fl.

The biggest hurdle to performing an on-line study of Fl or element 115 is the speed at which these systems must be ran. From production of the transactinide to the preparation of α-spectroscopy sources must be completed faster than the half-lives of Fl and element 115 (much shorter than that of Fl). Under current technology for chemical automation, the evaporation step to prepare an α-spectroscopy source would be longer than the half-life of the transactinide. Even though automated SX systems such as SISAK which use LSC detection can perform the chemical separations on the speed required for a Fl experiment, the LSC detection medium is insufficient for unambiguous determination of Fl production which requires multiple α-decay correlations and a SF event. Future work must develop an automated system capable of not only running the chemistry at the rates necessary for an online Fl or element 115 system but also capable of preparing α-spectroscopy samples within that same time frame. One possibility is to examine the use of microfluidics which would use very small liquid volumes and thus have far quicker and easier preparation for detection of the transactinide.

The work presented shows the promise of macrocyclic extractants for an on-line Fl or element 115 experiment. The future development of thiacrowns which are perfectly tuned for the extraction of the homologs and pseudo-homologs of these transactinides should show the required kinetics and selectivity needed for a Fl and element 115 on-line experiment. The results presented show potential Fl and element 115 chemical systems from the liquid phase, future work which focuses on the issue of automation speed and builds on these results with further

tuned macrocycles (to fix potential kinetic issues) will yield systems that can be applied to an on-line experiment in the future.

APPENDIX

Table 26. Raw data for Figure 44.

Volume (mL)	Day 1 Sn	Day 1 Corrected Sn	Day 2 Sn
0	0	0	0
4	0.348 ± 0.006	0.381 ± 0.007	0
8	0.369 ± 0.007	0.442 ± 0.008	0
12	0.061 ± 0.002	0.0075 ± 0.0008	0
16	0.045 ± 0.002	0	0
20	0.040 ± 0.002	0	0
24	0.051 ± 0.002	0.011 ± 0.001	0
28	0.051 ± 0.002	0.017 ± 0.001	0
32	0.221 ± 0.005	0	0.749 ± 0.012
36	0.0065 ± 0.0008	0	0.037 ± 0.002
40	0	0	0.0011 ± 0.0003

Table 27. Raw data for Figure 46.

Concentration (M)	k’ Au	k’ Hg
0.04	13961.6 ± 1546.4	2998.1 ± 601.7
0.14	19319.7 ± 1990.8	1398.0 ± 94.6
0.43	12728.5 ± 1348.5	397.2 ± 21.3
102	18527.8 ± 1887.4	242.8 ± 11.0
3.96	1983.2 ± 138.6	28.9 ± 2.9
9.84	76.1 ± 10.2	0.5
11.80	29.4 ± 6.7	0.5
15.63	6.6 ± 5.7	0.5

Table 28. Raw data for Figure 48.

Volume (mL)	Sb Elution Fraction	Sn Elution fraction
0	0	0
1	0	0.13 ± 0.01
2	0	0.84 ± 0.06
3	0	0.09 ± 0.01
4	0	0.04 ± 0.002
5	0	0
6	0	0
7	0	0
8	0	0
9	0	0
10	0	0
11	0	0
12	0	0
13	0	0
14	0	0
15	0.33 ± 0.03	0
16	0.29 ± 0.03	0
17	0.06 ± 0.01	0
18	0.04 ± 0.01	0
19	0	0
20	0	0
21	0	0
22	0	0
23	0	0

Table 29. Raw data for figure 49.

Volume (mL)	Day 1 Sn	Day 2 Sn
4	0	0
8	0	0
12	0	0
16	0	0
20	0.211 ± 0.009	0
24	0.385 ± 0.012	0
28	0.160 ± 0.008	0
32	0.024 ± 0.003	0
36	0	0
40	0.010 ± 0.002	0
44	0	0
48	0	0
52	0	0
56	0	0
60	0.042 ± 0.004	0.032 ± 0.003
64	0.604 ± 0.017	0.580 ± 0.017
68	0.515 ± 0.015	0.457 ± 0.014
72	0.165 ± 0.008	0.180 ± 0.008
76	0.118 ± 0.006	0.109 ± 0.006
80	0.011 ± 0.002	0.011 ± 0.002
84	0	0.0046 ± 0.001
88	0	0.0015 ± 0.0007
92	0	0

Table 30. Raw data for Figure 50.

Volume (mL)	Day 1 Sb Elution Fraction	Day 2 Sb Elution Fraction	Day 3 Sb Elution Fraction
6	0	0	0
10	0	0	0
14	0	0	0
18	0	0	0
22	0.087 ± 0.004	0	0
26	0.389 ± 0.008	0	0
30	0.089 ± 0.004	0	0
34	0.0217 ± 0.002	0	0
38	0	0.149 ± 0.005	0
42	0	0.029 ± 0.002	0
46	0	0.008 ± 0.001	0
50	0	0.003 ± 0.001	0
54	0	0	0.061 ± 0.003
58	0	0	0.015 ± 0.002
60	0	0	0

Table 31. Raw Data Figure 53.

Volume (mL)	^{212}Pb Percent Elution	^{228}Th Percent Elution
1	0.014 ± 0.001	0.006 ± 0.001
2	2.78 ± 0.01	0.017 ± 0.001
3	23.27 ± 0.05	0.055 ± 0.002
4	23.77 ± 0.05	0.103 ± 0.003
5	10.51 ± 0.03	0.169 ± 0.004
6	2.43 ± 0.02	0.222 ± 0.004
7	0.50 ± 0.006	0.243 ± 0.005
8	0.25 ± 0.005	0.296 ± 0.005
9	0.17 ± 0.004	0.291 ± 0.005
10	0.18 ± 0.004	0.332 ± 0006

Table 32. Raw data for Figure 56.

Concentration of HCl (M)	k' Sn	k' Pb	k' Hg
0.04	4.95 ± 1.32	213.12 ± 28.95	5366.86 ± 223.87
0.05	6.28 ± 1.20	235.00 ±2.08	5776.49 ± 448.04
0.14	1.59 ± 1.09	344.54 ± 21.86	2596.91 ± 327.94
0.24	1.01 ± 0.67	371.22 ± 29.23	1344.63 ± 222.8
0.44	0.77 ± 0.78	361.50 ± 12.08	447.10 ± 112.71
0.83	2.02 ± 0.84	339.72 ± 17.39	83.43 ± 9.92
1.03	4.71 ± 1.38	319.13 ± 8.63	52.76 ± 11.11
2.03	21.80 ± 1.58	163.76 ± 3.26	21.68 ± 0.96
4.01	220.79 ± 10.60	46.66 ± 3.75	25.08 ± 4.50
7.97	106. 65 ± 4.91	1	12.13 ± 1.97
9.96	42.72 ± 2.11	1	5.64 ± 2.27
12	14.22 ± 1.31	1	1

Table. 33. Raw data for Figure 57.

Element	Log[DtbuC18C6]	Log D
Sn	-3.19	-0.92 ± 0.04
	-2.25	0.51 ± 0.05
	-1.77	1.27 ± 0.03
	-1.17	2.36 ± 0.03
	-0.87	2.99 ± 0.29
Pb	-3.44	-0.77 ± 0.03
	-2.61	0.13 ± 0.04
	-2.05	0.57 ± 0.04
	-1.19	1.39 ± 0.05
	-0.94	1.63 ± 0.03

Table 34. Raw data for 58 (Top).

Time	k' Pb
30	134.47 ± 2.06
120	197.01 ± 3.44
300	257.70 ± 4.99
1200	258.78 ± 4.61
3600	265.44 ± 5.37

Table 35. Raw data for 58 (Middle).

Time	k' Sn
30	89.72 ± 1.28
120	110.65 ± 1.83
300	163.90 ± 2.70
1200	195.91 ± 3.77
2400	195.52 ± 4.22
3600	202.36 ± 2.34
10800	202.60 ± 4.08
86400	191.62 ± 3.68

Table 36. Raw data for 58 (Bottom).

Time	k' Hg
39	11.74 ± 0.28
67	13.13 ± 0.65
300	19.6 ± 0.8
1890	55.50 ± 1.23
3803	114.87 ± 3.00
10900	331.61 ± 12.09
21480	394.98 ± 32.28
86400	517.29 ± 29.96

Table 37. Raw Data for 59 (Top).

Volume (mL)	Elution Fraction Pb	Elution Fraction Sn
1	0	0
2	0	0
3	0	0
4	0	0
5	0.113 ± 0.005	0
6	0.518 ± 0.011	0
7	0.238 ± 0.005	0
8	0.041 ± 0.003	0
9	0.007 ± 0.001	0
10	0	0
11	0	0
12	0	0
13	0	0
14	0	0
15	0	0.064 ± 0.004
16	0	0.694 ± 0.014
17	0	0.073 ± 0.004
18	0	0.010 ± 0.001
19	0	0.004 ± 0.0002
20	0	0
21	0	0

Table 38. Raw Data for 59 (Bottom).

Volume (mL)	Elution Fraction Sn	Elution Fraction Pb
1	0	0
2	0	0
3	0	0
4	0	0
5	0.217 ± 0.007	0
6	0.555 ± 0.013	0
7	0.077 ± 0.004	0
8	0.010 ± 0.0004	0
9	0	0
10	0	0
11	0	0
12	0	0
13	0	0
14	0	0
15	0	0.127 ± 0.006
16	0	0.569 ± 0.014
17	0	0.202 ± 0.008
18	0	0.018 ± 0.002
19	0	0
20	0	0
21	0	0

Table 39. Raw Data for Figure 60.

Volume (mL)	Elution Fraction Pb	Elution Fraction Sn	Elution Fraction Hg
1	0	0	0
2	0	0	0
3	0	0	0
4	0	0.357 ± 0.013	0
5	0	0.398 ± 0.014	0.008 ± 0.002
6	0	0.048 ± 0.004	0.010 ± 0.002
7	0	0.011 ± 0.002	0.015 ± 0.002
8	0	0.005 ± 0.001	0.023 ± 0.003
9	0	0	0.015 ± 0.002
10	0	0.003 ± 0.001	0.030 ± 0.003
11	0	0	0.016 ± 0.002
12	0	0.001 ± 0.001	0.017 ± 0.002
13	0	0	0.019 ± 0.002
14	0.008 ± 0.001	0	0.014 ± 0.002
15	0.093 ± 0.003	0	0.009 ± 0.002
16	0.264 ± 0.006	0	0.014 ± 0.002
17	0.254 ± 0.006	0	0.015 ± 0.002
18	0.164 ± 0.004	0	0.016 ± 0.002
19	0.062 ± 0.003	0	0.016 ± 0.002
20	0.017 ± 0.001	0	0.023 ± 0.002
21	0.004 ± 0.001	0	0.009 ± 0.002
22	0.001 ± 0.0003	0	0.006 ± 0.001
23	0.002 ± 0.0005	0	0.058 ± 0.003
24	0	0	0.083 ± 0.005
25	0	0	0.069 ± 0.004
26	0	0	0.047 ± 0.004
27	0	0	0.027 ± 0.003
28	0	0	0.025 ± 0.003
29	0	0	0.032 ± 0.003
30	0	0	0.021 ± 0.002
31	0	0	0.041 ± 0.003
32	0	0	0.064 ± 0.004
33	0	0	0.088 ± 0.005
34	0	0	0.023 ± 0.003
35	0	0	0.023 ± 0.002

Table 40. Raw Data for Figure 61.

Volume (mL)	Elution Fraction Pb	Elution Fraction Sn	Elution Fraction Hg
1	0	0	0
2	0	0.049 ± 0.008	0
3	0	0.535 ± 0.025	0
4	0	0.378 ± 0.021	0
5	0	0.031 ± 0.006	0
6	0	0	0
7	0	0	0.010 ± 0.002
8	0	0	0.006 ± 0.002
9	0	0	0.008 ± 0.002
10	0	0	0.006 ± 0.002
11	0.006 ± 0.0005	0	0
12	0.125 ± 0.002	0	0
13	0.320 ± 0.004	0	0
14	0.347 ± 0.004	0	0
15	0.118 ± 0.002	0	0
16	0.027 ± 0.001	0	0
17	0.0042 ± 0.0004	0	0.007 ± 0.002
18	0.0026 ± 0.0003	0	0.008 ± 0.002
19	0.0016 + 0/0003	0	0.006 ± 0.002
20	0.0030 ± 0.004	0	0.058 ± 0.005
21	0.0006 ± 0.0002	0	0.083 ± 0.006
22	0.0042 ± 0.0005	0	0.158 ± 0.009
23	0	0	0.202 ± 0.010
24	0	0	0.216 ± 0.011
25	0	0	0.152 ± 0.009
26	0	0	0.027 ± 0.004
27	0	0	0.010 ± 0.002
28	0	0	0.005 ± 0.002
29	0	0	0

Table 41. Raw data for figure 62.

Concentration of HNO_3 (M)	k' ^{212}Pb	k' ^{113}Sn
0.18	835.91 ± 23.2	3.62 ± 1.64
0.27	1119.6 ± 40.6	6.14 ± 1.65
0.36	--	6.64 ± 1.61
0.55	1702.0 ± 63.4	6.15 ± 2.13
0.91	--	Limit
1.1	1398.7 ± 58.0	1.14 ± 1.71
1.5	1451.9 ± 52.5	--
2.0	1216.4 ± 44.2	1.83 ± 1.73
3.8	786.7 ± 23.7	2.98 ± 2.16
5.6	421.2 ± 13.9	Limit
7.5	302.7 ± 7.85	Limit
9.3	237.8 ± 6.3	Limit
14.6	39.4 ± 0.6	Limit

Table 42. Raw Data for figure 63.

Time (s)	k' Pb
39	427 ± 36
72	592 ± 49
300	1142 ± 161
1800	1102 ± 119
3660	1058 ± 117
9000	1215 ± 178

Table 43. Raw Data for figure 64.

Volume (mL)	Elution Fraction Pb	Elution Fraction Sn
1	0	0.0009 ± 0.0007
2	0	0.472 ± 0.016
3	0	0.486 ± 0.016
4	0	0.006 ± 0.002
5	0	0.003 ± 0.001
6	0	0.0014 ± 0.0008
7	0	0
8	0	0
9	0.001 ± 0.001	0
10	0.003 ± 0.001	0
11	0.120 ± 0.008	0
12	0.401 ± 0.015	0
13	0.320 ± 0.014	0
14	0.106 ± 0.008	0
15	0.046 ± 0.005	0
16	0.008 ± 0.002	0

Table 44. Raw data for Figure 66.

Concentration of HCl (M)	Percent Extraction (%)
0.005	97.33 ± 2.28
0.01	98.95 ± 0.47
0.1	97.22 ± 3.51
0.2	94.49 ± 5.76
0.4	98.00 ± 2.32
0.8	96.30 ± 3.86
1	97.37 ± 1.88
1.9	90.91 ± 1.47
3.8	25.44 ± 2.32
7.7	1.35 ± 0.69
9.6	1.42 ± 0.31
11.5	1.02 ± 0.57

Table 45. Raw Data for figure 67.

Concentration of HCl (M)	D Pb	D Hg	D Sn
0.08	0.009 ± 0.004	> 63.59	0.022 ± 0.007
0.09	Limit	> 52.66	0.020 ± 0.007
0.2	Limit	> 46.13	Limit
0.3	Limit	> 55.76	Limit
0.5	Limit	> 24.92	Limit
0.9	Limit	> 26.18	Limit
1.0	Limit	> 22.99	Limit
2.0	Limit	10.52 ± 1.10	Limit
3.9	Limit	0.284 ± 0.033	Limit
7.8	Limit	0.013 ± 0.005	Limit
9.7	Limit	0.012 ± 0.006	Limit
11.8	Limit	Limit	Limit

Table 46. Raw data for figure 68.

Concentration of HCl (M)	D Pb	D Hg	D Sn
0.08	Limit	>29.36	Limit
0.09	Limit	>21.45	Limit
0.2	Limit	5.76 ± 0.79	Limit
0.3	Limit	27.82 ± 7.32	Limit
0.5	Limit	14.74 ± 2.83	Limit
0.9	Limit	1.42 ± 0.15	Limit
1.0	Limit	0.58 ± 0.06	Limit
2.0	Limit	0.09 ± 0.01	Limit
3.9	Limit	0.028 ± 0.009	Limit
7.8	Limit	0.008 ± 0.004	0.03 ± 0.01
9.7	Limit	Limit	0.03 ± 0.01
11.8	Limit	Limit	Limit

Table 47. Raw data for figure 69 (Top).

Concentration HCl (M)	k' Bi
0.18	2.87 ± 0.86
0.27	2.64 ± 2.57
0.36	2.23 ± 1.26
0.54	3.26 ± 3.46
0.91	Limit
1.1	1.39 ± 1.93
2.0	Limit
3.8	2.01 ± 1.20
5.6	Limit
7.5	1.14 ± 1.07
9.3	1.91 ± 3.01

Table 48. Raw data for figure 69 (Bottom).

Concentration HCl (M)	k' Bi
0.18	Limit
0.27	1.64 ± 1.31
0.36	2.22 ± 2.34
0.54	0.98 ± 3.07
0.91	2.40 ± 0.93
1.1	Limit
2.0	3.73 ± 2.50
3.8	Limit
5.6	Limit
7.5	Limit
9.3	1.26 ± 0.69

Table 49. Raw data for figure 70.

Concentration HNO_3 (M)	k' Bi
0.18	Limit
0.27	1.64 ± 1.31
0.36	2.22 ± 2.34
0.54	0.98 ± 3.07
0.91	2.40 ± 0.93
1.1	Limit
2.0	3.73 ± 2.50
3.8	Limit
5.6	Limit
7.5	Limit
9.3	1.26 ± 0.69

Table 50. Raw data for figure 71.

HCl (M)	k' Bi
0.18	Limit
0.53	Limit
1.06	Limit
1.95	Limit
5.49	758.22 ± 109.43
7.26	195.15 ± 16.44
9.02	89.38 ± 6.03

HNO_3 (M)	k' Bi
0.18	Limit
0.53	Limit
1.06	Limit
1.95	Limit
5.49	3.21 ± 1.69
7.26	3.99 ± 1.70
9.02	1.81 ± 1.56

Table 51. Raw data for figure 72.

Concentration of HCl (M)	Percent Extracted Bi (%)	Percent Extracted Sb (%)
0.001	1.95 ± 0.32	0
0.01	1.95 ± 0.23	0
0.1	15.25 ± 0.84	39.11 ± 5.19
0.2	28.36 ± 1.22	37.76 ± 5.15
0.4	4.91 ± 0.47	45.59 ± 6.99
0.8	0.63 ± 0.16	36.78 ± 5.38
1.0	0	40.96 ± 5.99
1.9	0	46.25 ± 6.50
3.8	0	51.56 ± 6.37
7.7	0	31.06 ± 5.03
9.6	0	59.44 ± 7.26
11.5	0	73.56 ± 7.83

Table 52. Raw data for figure 75.

Concentration of HCl (M)	D Pb
0.08	0.020 ± 0.002
0.09	0.007 ± 0.001
0.18	0.001 ± 0.0005
0.27	0
0.46	0
0.85	0
1.0	0
2.0	0
3.9	0
7.8	0
9.7	0
11.8	0

Table 53. Raw data for figure 76.

Concentration of HCl (M)	D Pb
0.10	0
0.18	0
0.26	0
0.42	0
0.74	0
0.9	0
1.7	0
3.3	0
6.5	0
8.1	0

REFERENCES

[1] Y. T. Oganessian, A. V. Yeremin, G. G. Gulbekian, S. I. Bogomolov, V. I. Chepigin, B. N. Gikal, V. A. Gorshkov, M. G. Itkis, A. P. Kabachenko, V. B. Kutner, A. Y. Lavrentev, O. N. Malyshev, A. G. Popeko, J. Roháč, R. N. Sagaidak, S. Hofmann, G. Münzenberg, M. Veselsky, S. Saro, N. Iwasa and K. Morita, "Search for new isotopes of element 112 by irradiation of 238-U with 48-Ca," *Eur. Phys. J. A,* vol. 5, pp. 63-68, 1999.

[2] G. T. Seaborg, The Transuranium Elements, New Haven, CT: New Haven Yale University Press, 1958.

[3] D. C. Hoffman, F. O. Lawrence, J. L. Mewherter and F. M. Rourke, "Detection of plutonium-244 in nature," *Nature,* vol. 234, pp. 132-134, 1971.

[4] G. T. Seaborg and W. D. Loveland, The Elements Beyond Uranium, The University of Michigan: John Wiley & Sons, INc., 1990.

[5] E. Fermi, E. Amaldi, O. D'Agostino, F. Rasetti and E. Segré, "Artificial radioactivity produced by neutron bombardment," *Proc. R. Soc. Lond. A,* vol. 146, no. 857, pp. 483-500, 1934.

[6] E. McMillan and P. H. Abelson, "Radioactive element 93," *Phys. Rev.,* vol. 57, no. 12, pp. 1185-1186, 1940.

[7] G. T. Seaborg, E. M. McMillan, J. W. Kennedy and A. C. Wahl, "Radioactive element 94 from deuterons on uranium," *Phys. Rev.,* vol. 69, no. 7-8, pp. 366-367, 1946.

[8] G. T. Seaborg, "The chemical and radioactive properties of the heavy elements," *Chem. Eng. News,* vol. 23, no. 23, pp. 2190-2193, 1945.

[9] S. G. Thompson, A. Ghiorso and G. T. Seaborg, "Element 97," *Phys. Rev.,* vol. 77, no. 6, pp. 838-839, 1950.

[10] S. G. Thomson, K. Street, A. Ghiorso and G. T. Seaborg, "The new element californium (atomic number 98)," *Phys. Rev.,* vol. 80, no. 5, pp. 790-796, 1950.

[11] A. Ghiorso, S. G. Thompson, G. H. Higgins, G. T. Seaborg, M. H. Studier, P. R. Fields, H. Diamond, J. F. Mech, G. L. Pyle, J. R. Hulzenga, A. Hirsch, W. M. Manning, C. I. Browne, H. L. Smith and R. W. Spence, "New elements einsteinium and fermium, atomic numbers 99 and 100," *Phys. Rev.,* vol. 99, no. 3, pp. 1048-1049, 1955.

[12] A. Ghiorso, B. G. Harvey, G. R. Choppin, S. G. Thompson and G. T. Seaborg, "The new element mendelevium, atomic number 101," *Phys. Rev.,* vol. 98, no. 5, pp. 1518-1519, 1955.

[13] A. Ghiorso, T. Sikkeland, A. E. Larsh and R. M. Latimer, "New element, lawrencium, atomic number 103," *Phys. Rev. Lett.,* vol. 6, no. 9, pp. 473-475, 1961.

[14] A. Ghiorso, T. Sikkeland, j. R. Walton and G. T. Seaborg, "Element No. 102," *Phys. Rev. Lett.,* vol. 1, no. 1, pp. 18-21, 1958.

[15] M. Schädel, The Chemistry of Superheavy Elements, Boston: Kluwer Academic Publishers, 2003.

[16] IUPAC, "Discovery of the transfermium elements," *Pure & Appl. Chem.,* vol. 65, no. 8, pp. 1815-1824, 1993.

[17] G. N. Flerov, Y. T. Oganesyan, T. V. Lobanov, V. J. Kuznetsov, V. A. Druin, V. P. Perelygin, K. A. Gavrilov, S. P. Tret'yakova and V. M. Plotko, "Synthesis and physical identification of the isotope with mass number 260 of element 104," *Sov. Atom. Energy,* vol. 17, no. 4, pp. 310-312, 1964.

[18] A. Ghiorso, M. Nurmia, J. Harris, K. Eskola and P. Eskola, "Positive identification of two alpha-particle-emitting isotopes of element 104," *Phys. Rev. Lett.,* vol. 22, no. 24, pp. 1317-1320, 1969.

[19] G. N. Flerov, Y. T. Oganesyan, Y. V. Lobanov, Y. A. Lazarev, S. P. Tret'yakova, I. V. Kolesov and V. M. Plotko, "The synthesis of element 105," *Sov. Atom. Energy,* vol. 29, no. 4, pp. 967-975, 1970.

[20] A. Ghiorso, M. Nurmia, K. Eskola, J. Harris and P. Eskola, "New element hahnium, atomic number 105," *Phys. Rev. Lett.,* vol. 24, no. 26, pp. 1498-1503, 1970.

[21] A. Ghiorso, J. M. Nitschke, J. R. Alonso, M. Nurmia, G. T. Seaborg, E. K. Hulet and R. W. Lougheed, "Element 106," *Phys. Rev. Lett.,* vol. 33, no. 25, pp. 1490-1493, 1974.

[22] G. Münzenberg, S. Hofmann, F. P. Heßberger, W. Reisdorf, K. H. Schmidt, J. H. R. Schneider, P. Armbrusler, C. C. Sahm and B. Thuma, "Identification of element 107 by alpha correlation chains," *Z. Phys. A,* vol. 300, no. 1, pp. 107-108, 1981.

[23] G. Münzenberg, P. Armbruster, H. Folger, F. P. Heßberger, S. Hofmann, J. Keller, K. Poppensieker, W. Reisdorf, K. -H. Schmidt, H. -J. Schöt, M. E. Leino and R. Hingmann, "The identification of element 108," *Z. Phys. A,* vol. 317, no. 2, pp. 235-236, 1984.

[24] G. Münzenberg, P. Armbruster, F. P. Herßberger, S. Hofmann, K. Poppensieker, W. Reisdorf, J. H. R. Schneider, W. F. W. Schneider, K. -H. Schmidt, C. -C. Sahm and D. Vermeulen, "Observation of one correlated alpha-decay in the reaction 58-Fe on 209-Bi -> 267-109," *Z. Phys. A,* vol. 309, no. 1, pp. 89-90, 1982.

[25] S. Hofmann, V. Ninov, F. P. Herßberger, P. Armbruster, H. Folger, G. Münzenberg, H. J. Schött, A. G. Popeko, A. V. Yeremin, A. N. Andreyev, S. Saro, R. Janik and M. Leino, "Production and decay of 269-110," *Z. Phys. A,* vol. 350, no. 4, pp. 277-280, 1995.

[26] S. Hofmann, V. Ninov, F. P. Herßberger, P. Armbruster, H. Folger, G. Münzenberg, H. J. Schött, A. G. popeko, A. V. Yeremin, A. N. Andreyev, S. Saro, R. Janik and M. Leino, "The new element 111," *Z. Phys. A,* vol. 350, no. 4, pp. 281-282, 1995.

[27] S. Hofmann, V. Ninov, F. P. Herßberger, P. Armbruster, H. Folger, G. Münzenberg, H. J. Schött, A. G. Popeko, A. V. Yeremin, S. Saro, R. Janik and M. Leino, "The new element 112," *Z. Phys. A,* vol. 354, no. 3, pp. 229-230, 1996.

[28] Y. T. Oganessian, V. K. Utyonkov, Y. V. Lobanov, F. S. Abdullin, A. N. Polyakov, I. V. Shirokovsky, Y. S. Tsyganov, G. G. Gulbekian, S. L. Bogomolov, B. N. Gikal, A. N. Mezentsev, S. Iliev, V. G. Subbotin, A. M. Sukhov, G. V. Buklanov, K. Subotic, M. G. Itkis, K. J. Moody, J. F. Wild, N. J. Stoyer, M. A. Stoyer and R. W. Lougheed, "Synthesis of superheavy nuclei in the 48-Ca + 244-Pu reaction," *Phys. Rev. Lett.,* vol. 83, no. 16, pp. 3154-3157, 1999.

[29] Y. T. Oganessian, V. K. Utyonkov, Y. V. Lobanov, F. S. Abdullin, A. N. Polyakov, I. V. Shirokovsky, Y. S. Tsyganov, G. G. Gulbekian, S. L. Bogomolov, B. N. Gikal, A. N. Mezentsev, S. Iliev, V. G. Subbotin, A. M. Sukhov, O. V. Ivanov, V. Buklanov, K. Subotic, M. G. Itkis, K. J. Moody, J. F. Wild, N. J. Stoyer, M. A. Stoyer, R. W. Lougheed, C. A. Laue, Y. A. Karelin and A. N. Tatarinov, "Observation of the decay of 292-116," *Phys. Rev. C,* vol. 63, no. 1, p. 011301, 2000.

[30] Y. T. Oganessian, V. K. Utyonkoy, Y. V. Lobanov, F. S. Abdullin, A. N. Polyakov, I. V. Shirokovsky, Y. S. Tsyganov, G. G. Gulbekian, S. L. Bogomolov, A. N. Mezentsev, S. Iliev, V. G. Subbotin, A. M. Sukhov, A. A. Voinov, G. V. Buklanov, K. Subotic, V. I. Zagrebaev, M. G. Itkis, J. B. Patin, K. J. Moody, j. F. Wild, M. A. Stoyer, N. J. Stoyer, D. A. Shaughnessy, J. M. Kenneally and R. W. Lougheed, "Experiments on the synthesis of element 115 in the reaction 243-Am(48-Ca, xn) 291-x-115," *Phys. Rev. C,* vol. 69, no. 2, p. 021601, 2004.

[31] K. Morita, K. Morimoto, D. Kaji, T. Akiyama, S. Goto, H. Haba, E. Ideguchi, R. Kanungo, K. Katori, H. Koura, H. Kudo, T. Ohnishi, A. Ozawa, T. Suda, K. Sueki, H. Xu, T. Yamaguchi, A. Yoneda, A. Yoshida and Y. Zhao, "Experiment on the synthesis of element 113 in the reaction 209-Bi(70-Zn,n)278-113," *J. Phys. Soc. Jpn.,* vol. 73, no. 10, pp. 2593-2596, 2004.

[32] Y. T. Oganessian, F. S. Abdullin, P. D. Bailey, D. E. Beneker, M. E. Bennett, S. N. Dmitriev, J. G. Ezold, J. H. Hamilton, R. A. Henderson, M. G. Itkis, Y. V. Lobanov, A. N. Mezentsev, K. J. Moody, S. L. Nelson, A. N. Polyakov, C. E. Porter, A. V. Ramayya, F. D. Riley, J. B. Roberto, M. A. Ryabinin, K. P. Rykaczewski, R. N. Sagaidak, D. A. Shaughnessy, I. V. Shirokovsky, M. A. Stoyer, V. G. Subbotin, R. Sudowe, A. M. Sukhov, Y. S. Tsyganov, V. K. Utyonkov, A. A. Voinov, G. K. Vostokin and P. A. Wilk, "Synthesis of a new element with atomic number Z=117," *Phys. Rev. Lett.,* vol. 104, no. 14, p. 142502, 2010.

[33] Y. T. Oganessian, V. K. Utyonikov, Y. V. Lobanov, F. S. Abdullin, A. N. Polyakov, R. N. Sagaidak, I. V. Shirokovsky, Y. S. Tsyganov, A. A. Voinov, G. G. Gulbekian, S. L. Bogomolov, B. N. Gikal, A. N. Mezentsev, S. Iliev, V. G. Subbotin, A. M. Sukhov, K. Subotic, V. I. Zagrebaev, G. K. Vostokin, M. G. Itkis, K. J. Moody, J. B. Patin, D. A. Shaughnessy, M. A. Stoyer, N. J. Stoyer, P. A. Wilk, J. M. Kenneally, J. H. Landrum, J. F. Wild and R. W. Lougheed, "Synthesis of the isotopes of elements 118 and 116 in the 249-Cf and 245-Cm+48-Ca fusion reactions," *Phys. Rev. C,* vol. 74, no. 4, p. 044602, 2006.

[34] Y. T. Oganessian, V. K. Utyonkov, S. N. Dmitriev, Y. V. Lobanov, M. G. Itkis, A. N. Polyakov, Y. S. Tsyganov, A. N. Mezentsev, A. V. Yeremin, A. A. Voinov, E. A. Sokol, G. G. Gulbekian, S. L. Bogomolov, S. Iliev, V. G. Subbotin, A. M. Sukhov, G. V. Buklanov, S. V. Shishkin, V. I. Chepygin, G. K. Vostokin, N. V. Aksenov, M. Hussonnois, K. Subotic, V. I. Zagrebaev, K. J. Moody, J. B. Patin, J. F. Wild, M. A. Stoyer, N. J. Stoyer, D. A. Shaughnessy, J. M. Kenneally, P. A. Wilk, R. W. Lougheed, H. W. Gäggeler, D. Shumann, H. Bruchertseifer and R. Eichler, "Synthesis of elements 115 and 113 in the reaction 243-Am+48-Ca," *Phys. Rev. C,* vol. 72, no. 3, p. 034611, 2005.

[35] W. D. Myers and W. J. Swiatecki, "Nuclear masses and deformations," *Nucl. Phys.,* vol. 81, no. 2, pp. 1-58, 1966.

[36] H. Meldner, "Predictions of new magic regions and masses for superheavy nuclei from calculations with realistic shell model single particle hamiltonians," *Ark. Fys.,* vol. 36, pp. 593-598, 1967.

[37] M. Schädel, "Chemistry of superheavy elements," *Angew. Chem. Int. Ed.,* vol. 45 , no. 3, pp. 368-401, 2006.

[38] S. G. Nilsson, C. F. Tsang, A. Sobiczewski, Z. Szymański, S. Wycech, C. Gustafson, I. -L. Lamm, P. Möller and B. Nilsson, "On the nuclear structure and stability of heavy and superheavy elements," *Nucl. Phys. A,* vol. 131, no. 1, pp. 1-66, 1969.

[39] Y. T. Oganessian, V. K. Utyonkov, Y. V. Lobanov, F. S. Abdullin, A. N. Polyakov, I. V. Shirokovsky, Y. S. Tsyganov, G. G. Gulbekian, S. L. Bogomolov, B. N. Gikal, A. N. Mezentsev, S. Iliev, V. G. Subbotin, A. M. Sukhov, A. A. Voinov, G. V. Buklanov, K. Subotic,

V. I. Zagrebaev, M. G. Itkis, J. B. Patin, K. J. Moody, J. F. Wild, M. A. Stoyer, N. J. Stoyer, D. A. Shaughnessy, J. M. Kenneally and R. W. Lougheed, "Measurements of cross sections for the fusion-evaporation reactions 244-Pu(48-Ca,xn)292-x-114 and 245-Cm(48-Ca,xn)293-x-115," *Phys. Rev. C,* vol. 69, no. 5, p. 054607, 2004.

[40] S. Cwiok, W. Nazarewicz and P. H. Heenen, "Structure of odd-N superheavy elements," *Phys. Rev. Lett.,* vol. 83, no. 6, pp. 1108-1111, 1999.

[41] P. Moller and J. R. Nix, "Stability of heavy and superheavy elements," *J. Phys. G: Nucl. part. Phys.,* vol. 20, no. 11, p. 1681, 1994.

[42] S. Cwoik, J. Dobaczewski, P. -H. Heenen, P. Magierski and W. Nazarewicz, "Shell structure of the superheavy elements," *Nucl. Phys. A,* vol. 611, no. 2-3, pp. 211-246, 1996.

[43] R. K. Gupta, S. K. Patra and W. Greiner, "Structure of 294,302-120 nuclei using the relativistic meanfield method," *Mod. Phys. Lett. A,* vol. 12, no. 23, pp. 1727-1736, 1997.

[44] K. Rutz, M. Bender, T. Bürvenich, T. Schilling, P. -G. Reinhard, J. A. Maruhn and W. Greiner, "Superheavy nuclei in self-consistent nuclear calculations," *Phys. Rev. C,* vol. 56, no. 1, pp. 238-243, 1997.

[45] A. T. Kruppa, M. Bender, W. Nazarewicz, P. -G. Reinhard, T. Vertse and S. Cwiok, "Shell corrections of superheavy nuclei in self-consistent calculations," *Phys. Rev. C,* vol. 61, no. 3, p. 034313, 2000.

[46] Z. Patyk, J. Skaiski, A. Sobiczewski and S. Cwiok, "Potential energy and spontaneous-fission half-lives for heavy and superheavy nuclei," *Nucl. Phys. A,* vol. 502, pp. 591-600, 1989.

[47] Z. Patyk and A. Sobiczewski, "Main deformed shells of heavy nuclei studied in a multidimensional deformation space," *Phys. Lett. B,* vol. 256, no. 3-4, pp. 307-310, 1991.

[48] Y. A. Lazarev, Y. V. Lobanov, Y. T. Oganessian, V. K. Utyonkov, F. S. Abdullin, G. V. Buklanov, B. N. Gikal, S. Iliev, A. N. Mezentsev, A. N. Polyakov, I. M. Sedykh, I. V. Shirokovsky, V. G. Subbotin, A. M. Sukhov, Y. S. Tsyganov, E. Zhuchko, R. W. Lougheed, K. J. Moody, J. F. Wild, E. K. Hulet and J. H. McQuaid, "Discovery of enhanced nuclear stability near the deformed shells N=162 and Z=108," *Phys. Rev. Lett.,* vol. 73, no. 5, pp. 624-627, 1994.

[49] A. Türler, R. Dressler, B. Eichler, H. W. Gäggeler, D. T. Jost, M. Schädel, W. Brüchle, K. E. Gregorich, N. Trautmann and S. Taut, "Decay Properties of 265-Sg(Z=06) and 266-Sg(Z=106)," *Phys. Rev. C,* vol. 57, no. 4, pp. 1648-1655, 1998.

[50] P. A. Wilk, K. E. Gregorich, A. Türler, C. A. Laue, R. Eichler, V. Ninov, J. L. Adams, U. W. Kirbach, M. R. Lane, D. M. Lee, J. B. Patin, D. A. Shaughnessy, D. A. Strellis, H. Nitsche and D. C. Hoffman, "Evidence for new isotopes of element 107: 266-Bh and 267-Bh," *Phys. Rev. Lett.,* vol. 85, no. 13, pp. 2697-2700, 2000.

[51] S. Hofmann and G. Münzenberg, "The discovery of the heaviest elements," *Rev. Mod. Phys.,* vol. 72, no. 3, pp. 733-767, 2000.

[52] S. Hofmann, "New elements - approaching Z = 114," *Rep. Prog. Phys.,* vol. 61, p. 639, 1998.

[53] K. Bächmann and P. Hoffmann, "Chemische probleme bei der darstellung überschwerer elemente durch kernreaktionen," *Radiochim. Acta,* vol. 15, no. 4, pp. 153-163, 1971.

[54] R. Bass, "Fusion of heavy nuclei in a classical model," *Nucl. Phys. A,* vol. A231, pp. 45-63, 1974.

[55] S. Hofmann, "Synthesis and properties of superheavy elements," *J. Nucl. Radiochem. Sci.,* vol. 4, no. 1, pp. R1-R13, 2003.

[56] Y. T. Oganessian, V. K. Utyonkov, Y. V. Lobanov, F. S. Abdullin, A. N. Polyakov, I. V. Shirokovsky, Y. S. Tsyganov, G. G. Gulbekian, S. L. Bogomolov, B. N. Gikal, A. N. Mezentsev, S. Iliev, V. G. Subbotin, A. M. Sukhov, G. V. Buklanov, K. Subotic, M. G. Itkis, K. J. Moody, J. F. Wild, N. J. Stoyer, M. A. Stoyer and R. W. Lougheed, "Synthesis of superheavy nuclei in the 48-Ca+244-Pu reaction," *Phys. Rev. C,* vol. 62, no. 4, p. 041604, 2000.

[57] L. Stavsetra, K. E. Gregorich, J. Dvorak, P. A. Ellison, I. Dragojevic, M. A. Garcia and H. Nitsche, "Independent verification of element 114 production in the 48-Ca + 242-Pu reaction," *Phys. Rev. C,* vol. 103, no. 13, p. 132502, 2009.

[58] P. A. Ellison, K. E. Gregorich, J. S. Berryman, D. L. Bleuel, R. M. Clark, I. Dragojevic, J. Dvorak, P. Fallon, C. Fineman-Sotomayor, J. M. Gates, O. R. Gothe, i. Y. Lee, W. D. Loveland, J. P. McLaughlin, S. Paschalis, M. Petri, J. Qian, L. Stavestra, M. Wiedeking and H. Nitsche, "New superheavy element isotopes: 242-Pu(48-Ca,5n)285-114," *Phys. Rev. lett.,* vol. 105, no. 18, p. 182701, 2010.

[59] Y. T. Oganessian, V. K. Utyonkov, Y. V. Lobanov, F. S. Abdullin, A. N. Polyakov, I. V. Shirokovsky, Y. S. Tsyganov, G. G. Gulbekian, S. L. Bogomolov, B. N. Gikal, A. N. Mezentsev, S. Iliev, V. G. Subbotin, A. M. Sukhov, A. A. Voinov, G. V. Buklanov, K. Subotic, V. I. Zagrabaev, M. G. Itkis, J. B. Patin , K. J. Moody, J. F. Wild, M. A. Stoyer, N. J. Stoyer, D. A. Shaughnessy, J. M. Kenneally, P. A. Wilk, R. W. Lougheed, R. I. Il'kaev and S. P. Vesnovskii, "Measurements of cross sections and decay properties of the isotopes of

elements 112, 114 and 116 produced in the fusion reactions 235,238-U, 242-Pu, and 248-Cm+48-Ca," *Phys. Rev. C,* vol. 70, no. 6, p. 064609, 2004.

[60] P. Pyykko and J. P. Desclaux, "Relativity and the periodic system of the elements," *Acc. Chem. Res.,* vol. 12, no. 8, pp. 276-281, 1979.

[61] O. L. Keller, "Chemistry of the heavy actinides and light transactinides," *Radiochim. Acta,* vol. 37, no. 4, pp. 169-180, 1984.

[62] V. Pershina, "Part 2. Applications, Theoretical and Computational Chemistry, vol. 14," in *Relativistic Electronic Structure Theory*, Amsterdam, Elsevier, 2004, pp. 1-80.

[63] K. S. Pitzer, "Relativistic effects on chemical properties," *Acc. Chem. Res.,* vol. 12, no. 8, pp. 271-276, 1979.

[64] P. A. Christiansen, W. C. Ermler and K. S. Pitzer, "Relativistic effects in chemical systems," *Ann. Rev. Phys. Chem.,* vol. 36, pp. 407-432, 1985.

[65] R. Guillaumont, J. P. Adloff and A. Peneloux, "Kinetic and thermodynamic aspects of tracer-scale and single atom chemistry," *Radiochim. Acta,* vol. 46, no. 4, pp. 169-176, 1989.

[66] R. Guillaumont, J. P. Adloff, A. Peneloux and P. Delamoye, "Sub-tracer scale behavior of radionuclides. Applications to actinide chemistry," *Radiochim. Acta,* vol. 54, no. 1, pp. 1-16, 1991.

[67] J. V. Kratz, "Critical evaluation of the chemical properties of the transactinide elements," *Pure and App. Chem.,* vol. 75, no. 1, pp. 103-138, 2003.

[68] R. J. Borg and G. J. Dienes, "On the validity of single atom chemistry," *J. Inorg. Nucl. Chem.,* vol. 43, no. 6, pp. 1129-1133, 1981.

[69] A. Ghiorso, S. Yashita, M. E. Leino, L. Frank, J. Kalnins, P. Armbruster, J. -P. Dufour and P. K. Lemmertz, "SASSY, a gas-filled magnetic separator for the study of fusion reaction products," *Nucl. Instr. Meth. A,* vol. 269, no. 1, pp. 191-201, 1988.

[70] K. Subotic, Y. T. Oganessian, V. K. Utyonkov, Y. V. Lubanov, F. S. Abdullin, A. N. Polyakov, Y. S. Tsyganov and O. V. Ivanov, "Evaporation residue collection efficiencies and position spectra of the Dubna gas-filled recoil separator," *Nucl. Instr. Meth. A,* vol. 481, no. 1-3, pp. 71-80, 2002.

[71] H. Persson, G. Skarnemark, M. Skålberg, J. Alstad, J. O. Liljenzin, G. Bauer, F. Harberberger, N. Kaffrell, J. Rogowski and N. Trautmann, "SISAK 3 - an improved system

for rapid radiochemical separations by solvent extraction," *Radiochim. Acta,* vol. 48, no. 3-4, pp. 177-180, 1989.

[72] M. Schädel, W. Brüëhle, E. Jäger, E. Schimpf, J. V. Kratz, U. W. Scherer and H. P. Zimmermann, "ARCA II - A new apparatus for fast, repetitive HPLC separations," *Radiochim. Acta,* vol. 48, no. 3-4, pp. 171-176, 1989.

[73] M. Schädel, W. Brüchle and B. Haefner, "Fast radiochemical separations with an automated rapid chemistry apparatus," *Nucl. Instrum. Meth. Phys. Res. A,* vol. 264, no. 2-3, pp. 308-318, 1988.

[74] I. Zvara, Y. T. Chuburkov, R. Tsaletka, T. S. Zvarova, M. R. Shalaevskii and B. V. Shilov, "Chemical properties of element 104," *Sov. Atom. Energy,* vol. 21, no. 2, pp. 83-84, 1966.

[75] I. Zvara, Y. T. Chuburkov, V. Z. Belov, G. V. Buklanov, B. B. Zakhvataev, T. S. Zvarova, O. D. Maslov, R. Caletka and M. R. Shalaevsky, "Experiments on the chemistry of element 104 - kuchatovium. V. Adsorption of kurchatovium chloride from the gas stream on surfaces of glass and potassium chloride," *J. Inorg. Nucl. Chem.,* vol. 32, no. 6, pp. 1885-1894, 1970.

[76] I. Zvara, V. Z. Belov, L. P. Chelnokov, V. P. Domanov, M. Hussonois, Y. S. Korotkin, V. A. Schegolev and M. R. Shalayevsky, "Chemical separation of kurchatovium," *Inorg. Nucl. Chem. Lett.,* vol. 7, no. 11, pp. 1109-1116, 1971.

[77] B. L. Zhuikov, Y. T. Chuburkov, S. N. Tlmokhln, K. U. Jin and I. Zvara, "Is element 104 (kurchatovium) a p-element? I. Chromatography of atoms with hydrogen as a carrier gas," *Radiochim. Acta,* vol. 46, no. 3, pp. 113-116, 1989.

[78] A. Türler, H. W. Gäggaler, K. E. Gregorich, H. Barth, W. Brüëhle, K. R. Czerwinski, M. K. Gober, N. J. Hannink, R. A. Henderson, D. C. Hoffman, D. T. Jost, C. D. Kacher, B. Kadkhodayan, J. Kovacs, J. V. Kratz, S. A. Kreek, D. M. Lee, J. D. Leyba, M. J. Nurmia, M. Schäel, U. W. Scherer, Schimpf, D. Vermeulen, A. Weber, H. P. Zimmermann and I. Zvara, "Gas Phase chromatography of halides of elements 104 and 105," *J. Radioanal. Nucl. Chem. (Articles),* vol. 160, no. 2, pp. 327-339, 1992.

[79] A. Türler, G. V. Buklanov, B. Eichler, H. W. Gäggeler, M. Grantz, S. Hüener, D. T. Jost, V. Y. Lebedev, D. Piguet, S. N. Timokhin, A. B. Yakushev and I. Zvara, "Evidence for relativistic effects in the chemistry of element 104," *J. Alloys Comp.,* Vols. 271-273, no. 12, pp. 287-291, 1998.

[80] B. Kadkhodayan, A. Türler, K. E. Gregorich, P. A. Baisden, K. R. Czerwinski, B. Eichler, H. W. Gäggeler, T. M. Hamilton, D. T. Jost, C. D. Kacher, A. Kovacs, S. A. Kreek, M. R. Lane, M. F. Mohär, M. P. Neu, N. J. Stoyer, E. R. Sylwester, D. M. Lee, M. J. Nurmia, G. T. Seaborg and

D. C. Hoffman, "On-line gas chromatographic studies of chlorides of rutherfordium and homologs Zr and Hf," *Radiochim. Acta,* vol. 72, no. 4, pp. 169-178, 1996.

[81] E. R. Sylwester, K. E. Gregorich, D. M. Lee, B. Kadkhodayan, A. Türler, J. L. Adams, C. D. Kacher, M. R. Lane, C. Laue and C. A. McGrath, "On-line gas chromatographic studies of Rf, Zr, and Hf bromides," *Radiochim. Acta,* vol. 88, no. 12, p. 837, 2000.

[82] R. Silva, J. Harris, M. Nurmia, K. Eskola and A. Ghiorso, "Chemical separation of rutherfordium," *Inorg. Nucl. Chem. Lett.,* vol. 6, no. 12, pp. 871-877, 1970.

[83] E. K. Hulet, R. W. Lougheed, J. F. Wild, J. H. Landrum, J. M. Nitschke and A. Ghiorso, "Chloride complexation of element 104," *J. Inorg. Nucl. Chem.,* vol. 42, no. 1, pp. 78-82, 1980.

[84] K. R. Czerwinski, K. E. Gregorich, N. J. Hannink, C. D. Kacher, B. A. Kadkhodayan, S. A. Kreek, D. M. Lee, M. J. Nurmia, A. Türler, G. T. Seaborg and D. C. Hoffman, "Solution chemistry of element 104: Part I. Liquid-liquid extractions with trisooctylamine," *Radiochim. Acta,* vol. 64, no. 1, pp. 23-28, 1994.

[85] K. R. Czerwinski, K. E. Gregorich, N. J. Hannink, C. D. Kacher, B. A. Kadkhodayan, S. A. Kreek, D. M. Lee, M. J. Nurmia, A. Türler, G. T. Seaborg and D. C. Hoffman, "Solution chemistry of element 104: Part II. Liquid-liquid extractions with tributylphosphate," *Radiochim. Acta,* vol. 64, no. 1, pp. 29-36, 1994.

[86] C. D. Kacher, K. E. Gregorich, D. M. Lee, Y. Watanabe, B. Kadkhodayan, B. Wierczinski, M. R. Lane, E. R. Sylwester, D. A. Keeney, M. Hendricks, N. J. Stoyer, J. Yang, M. Hsu and D. C. Hoffman, "Chemical studies of rutherfordium (element 104): Part II. Solvent extraction studies into tributylphosphate from Hbr solutions," *Radiochim. Acta,* vol. 75, no. 3, pp. 127-134, 1996.

[87] C. D. Kacher, K. E. Gregorich, D. M. Lee, Y. Watanabe, B. Kadkhodayan, B. Wierczinski, M. R. Lane, E. R. Sylwester, D. A. Keeney, M. Hendricks and D. C. Hoffman, "Chemical studies of rutherfordium (element 104): Part III. Solvent extraction studies into triisooctylamine from HF solutions.," *Radiochim. Acta,* vol. 75, no. 3, pp. 135-140, 1996.

[88] D. Schumann, H. Nitsche, S. Taut, D. T. Jost, H. W. Gäggeler, A. B. Yakushev, G. V. Buklanov, V. P. Domanov, D. T. Lien, B. Kubica, R. Misiak and Z. Szegiowski, "Sorption behavior of rutherfordium and thorium from HCl/Hf containing aqueous solution," *J. Alloys Comp.,* Vols. 271-273, no. 12, pp. 307-311, 1998.

[89] E. Strub, J. V. Kratz, A. Kronenberg, A. Nähler, P. Thörle, S. Zauner, W. Brüchle, E. Jäger, M. Schädel, B. Schausten, E. Schimpf, L. Zongwei, U. Kirbach, D. Schumann, D. Jost, A. Türler, M. Asai, Y. Nagame, M. Sakama, K. Tsukada, H. W. Gäggeler and J. P. Glatz,

"Fluoride complexation of rutherfordium (Rf, element 104)," *Radiochim Acta,* vol. 88, pp. 265-271, 2000.

[90] H. Haba, K. Tsukada, M. Asai, I. Nishinaka, M. Sakama, S. Goto, M. Hirata, S. Ichikawa, Y. Nagame and T. Kaneko, "Startup of transactinide chemistry in JAERI," *Radiochim. Acta,* vol. 89, no. 11, pp. 733-736, 2001.

[91] J. P. Omtvedt, j. Alstad, H. Breivik, J. E. Dyve, K. Eberhardt, C. M. FoldenIII, T. Ginter, K. E. Gregorich, E. A. Hult, M. Johansson, U. W. Kirbach, D. M. Lee, M. Mendel, A. Nähler, V. Ninov, L. A. Omtvedt, J. B. Patin, G. Skarnemark, L. Stavestra, R. Sudowe, N. Wiehl, B. Wierczinski, P. A. Wilk, P. M. Zielinski, J. V. Kratz, N. Trautmann, H. Nitsche and D. C. Hoffman, "SISAK liquid-liquid extractions experiments with preseparated 257-Rf," *J. Nucl. Radiochem. Sci.,* vol. 3, no. 1, pp. 121-124, 2002.

[92] I. Zvara, V. Z. Belov, V. P. Domanov and M. R. Shalaevskii, "Chemical isolation of nilsbohrium as ekatantalum in the form of anhydrous bromide. II. Experiments with a spontaneously fissioning isotope of nilsbohrium.," *Sov. Radiochem.,* vol. 18, pp. 328-334, 1976.

[93] H. W. Gäggeler, D. T. Jost, J. Kovacs, U. W. Scherer, A. Weber, D. Vermeulen, A. Türler, K. E. Gregorich, R. A. Henderson, K. R. Czerwinski, B. Kadkhodayan, D. M. Lee, M. Nurmia, D. C. Hoffman, J. V. Kratz, M. K. Gober, H. P. Zimmermann, M. Schädel, W. Brüchle, E. Schimpf and I. Zvara, "Gas phase chromatography experiments with bromides of tantalum and element 105," *Radiochim. Acta,* vol. 57, no. 2-3, pp. 93-100, 1992.

[94] A. Türler, B. Eichler, D. T. Jost, D. Piguet, H. W. Gäggeler, K. E. Gregorich, B. Kadkhodayan, S. A. Kreek, D. M. Lee, M. Mohar, E. Sylwester, D. C. Hoffman and S. Hübener, "On-line gas phase chromatography with chlorides of niobium and hahnium (element 105)," *Radiochim. Acta,* vol. 73, no. 2, pp. 55-66, 1996.

[95] S. N. Timokhin, A. B. Yakushev, X. Honggui, V. P. Perelygin and I. Zvara, "Chemical identification of element 106 by thermochromatography," *J. Radioanal. Nucl. Chem. Lett.,* vol. 212, no. 1, pp. 31-34, 1996.

[96] A. B. Yakushev, S. N. Timokhin, M. V. Vedeneev, X. Honggui and I. Zvara, "Comparative study of oxochlorides of molybdenum, tungsten and element 106," *J. Radioanal. Nucl. Chem.,* vol. 205, no. 1, pp. 63-67, 1996.

[97] M. Schädel, W. Brüchle, R. Dressler, B. Eichler, H. W. Gäggeler, R. Günther, K. E. Gregorich, D. C. Hoffman, S. Hübener, D. T. Jost, j. V. Kratz, W. Paulus, D. Schumann, S. Timokhin, N. Trautmann, A. Türler, G. Wirth and A. Yakushev, "Chemical properties of element 106 (seaborgium)," *Nature,* vol. 388, pp. 55-57, 1997.

[98] M. Schädel, "First aqueous chemistry with seaborgium (element 106)," *J. Alloys Comp.,* Vols. 271-273, pp. 312-315, 1998.

[99] H. W. Gäggeler, "Chemistry gains a new element: Z=106," *J. Alloys. Comp.,* Vols. 271-273, pp. 277-282, 1998.

[100] I. Zvara, A. B. Yakushev, S. N. Timokhin, X. Honggui, V. P. Perelygin and Y. T. Chuburkov, "Chemical identification of element 106 (thermochromatography of oxochlorides)," *Radiochim. Acta,* vol. 81, no. 4, pp. 179-188, 1998.

[101] S. Hübener, S. Taut, A. Vahle, R. Dressler, B. Eichler, H. W. Gäggeler, D. T. Jost, D. Piguet, A. Türler, W. Brüchle, E. Jäger, M. Schädel, E. Schimpf, U. Kirbach, N. Trautmann and A. B. Yakushev, "Physico-chemical characterization of seaborgium as oxide hydroxide," *Radiochim. Acta,* vol. 89, pp. 737-741, 2001.

[102] K. E. Gregorich, R. A. Henderson, D. M. Lee, M. J. Nurmia, R. M. Chasteler, H. L. Hall, D. A. Bennett, C. M. Gannett, R. B. Chadwick, J. D. Leyba, D. C. Hoffman and G. Herrmann, "Aqueous chemistry of element 105.," *Radiochim. Acta,* vol. 43, no. 4, pp. 223-232, 1988.

[103] J. V. Kratz, H. P. Zimmermann, U. W. Scherer, M. Schädel, W. Brüchle, K. E. Gregorich, C. M. Gannett, H. L. Hall, R. A. Henderson, D. M. Lee, J. D. Leyba, M. J. Nurmia, D. C. Hoffman, H. Gäggeler, D. Jost, U. Baltensperger, Ya Nai-Qi Paul Scherrer, A. Türler and C. lienert, "Chemical properties of element 105 in aqueous solution: Halide complex formation and anion exchange into triisooctyl amine," *Radiochim. Acta,* vol. 48, no. 3-4, pp. 121-134, 1989.

[104] W. Paulus, J. V. Kratz, E. Strub, W. Brüchle, V. Pershina, B. Schausten, J. L. Adams, K. E. Gregorich, D. C. Hoffman, M. R. Lane, C. Laue, D. M. Lee, C. A. McGrath, D. K. Shaughnessy, D. A. Strellis and E. R. Sylwester, "Chemical properties of element 105 in aqueous solution: Extraction of the fluoride-, chloride-, and bromide complexes of the group-5 elements into an aliphatic amine," *Radiochim. Acta,* vol. 84, no. 2, pp. 69-78, 1999.

[105] D. Trubert, C. Le Naour, F. M. Guzman, M. Hussonnois, L. Brillard, J. F. Le Du, O. Constantinescu, J. Gasparro, V. Barci, B. Weiss and G. Ardisson, "Chemical isolation of dubnium (element 105) in fluoride media," *Radiochim Acta,* vol. 90, no. 3, pp. 127-132, 2002.

[106] M. Schädel, W. Brüchle, E. Jäger, B. Schausten, G. Wirth, W. Paulus, R. Günther, K. Eberhardt, J. V. Kratz, A. Seibert, E. Strub, P. Thörle, N. Trautmann, A. Waldek, S. Zauner, D. Schumann, U. Kirbach, B. Kubica, R. Misiak, H. Niewodniczanski, Y. Nagame and K. E.

Gregorich, "Aqueous chemistry of seaborgium (Z=106)," *Radiochim. Acta,* vol. 83, no. 3, pp. 163-166, 1998.

[107] A. Türler, W. Brüchle, R. Dressler, B. Eichler, R. Eichler, H. W. Gäggeler, M. Gärtner, J. -P. Glatz, K. E. Gregorich, S. Hübener, D. T. Jost, V. Y. Lebedev, V. Pershina, M. Schädel, S. Taut, S. N. Timokhin, N. Trautmann, A. Vahle and A. B. Yakushev, "First measurement of a thermochemical property of a seaborgium compound," *Angew. Chem. Int. Ed.,* vol. 38, no. 15, pp. 2212-2213, 1999.

[108] M. Schädel, W. Brüchle, B. Schausten, E. Schimpf, E. Jäger, G. Wirth, R. Günther, J. V. Kratz, W. Paulus, A. Seibert, P. Thörle, N. Trautmann, S. Zauner, D. Schumann, M. Andrassy, R. Misiak, K. E. Gregorich, D. C. Hoffman, D. M. Lee, E. R. Sylwester, Y. Nagame and Y. Oura, "First aqueous chemistry with seaborgium (element 106)," *Radiochim. Acta,* vol. 77, no. 3, pp. 149-160, 1997.

[109] A. Türler, "Gas Phase chemistry experiments with transactinide elements," *Radiochim. Acta,* vol. 72, no. 1, pp. 7-18, 1996.

[110] R. Eichler, W. Brüchle, R. Dressler, C. E. Düllmann, B. Eichler, H. W. Gäggeler, K. E. Gregorich, D. C. Hoffman, S. Hübener, D. T. Jost, U. W. Kirbach, C. A. Laue, V. M. Lavanchy, H. Nitsche, J. B. Patin, D. Piguet, M. Schädel, D. A. Shaughnessy, D. A. Strellis, S. Taut, L. Tobler, Y. S. Tsyganov, A. Türler, A. Vahle, P. A. Wilk and A. B. Yakushev, "Chemical characterization of bohrium (element 107)," *Nature,* vol. 407, pp. 63-65, 2000.

[111] C. E. Düllmann, W. Brüchle, R. Dressler, K. Eberhardt, B. Eichler, R. Eichler, H. W. Gäggeler, T. N. Ginter, F. Glaus, K. E. Gregorich, D. C. Hoffman, E. Jäger, D. T. Jost, U. W. Kirbach, D. M. Lee, H. Nitsche, J. B. Patin, V. Pershina, D. Piguet, Z. Qin, M. Schädel, B. Schausten, E. Schimpf, H. -J. Schött, S. Soverna, R. Sudowe, P. Thörle, S. N. Timokhin, N. Trautmann, A. Türler, A. Vahle, G. Wirth, A. B. Yakushev and P. M. Zielinski, "Chemical investigation of hassium (element 108)," *Nature,* vol. 418, pp. 859-862, 2002.

[112] R. Eichler, N. V. Aksenov, A. V. Belozerov, G. A. Bozhikov, V. I. Chepigin, R. Dmitriev, R. Dressler, H. W. Gäggeler, V. A. Gorshkov, F. Haenssler, M. G. Itkis, A. Laube, V. Y. Levedev, O. N. Malyshev, Y. T. Oganessian, O. V. Petrushkin, D. Piguet, P. Rasmussen, S. V. Shishkin, A. V. Shutov, A. I. Svirikhin, E. E. Tereshatov, G. K. Vostokin, M. Wegrzecki and A. V. Yeremin, "Chemical characterization of element 112," *Nature,* vol. 447, pp. 72-75, 2007.

[113] A. B. Yakushev, G. V. Buklanov, M. L. Chelnokov, V. I. Chepigin, S. N. Dmitriev, V. A. Gorshkov, S. Hübener , V. Y. Lebedev, O. N. Malyshev and Y. T. Oganessian, "First attempt to chemically identify element 112," *Radiochim. Acta,* vol. 89, no. 11, p. 743, 2001.

[114] A. B. Yakushev, G. V. Buklanov, M. L. Chelnokov, V. I. Chepigin, S. N. Dmitriev, V. A. Gorhkov, S. Hübener, V. Y. Lebedev, O. N. Malyshev, Y. T. Oganessian, A. G. Popeko, E. A.

Sokol, S. N. Timokhin, A. Türler, V. M. Vasko, A. V. Yeremin and I. Zvara, "On the way to chemically identify element 112," in *Contribution to the Workshop on Recoil Separator for Superheavy Element Chemistry, GSI*, Darmstadt, Germany, 2002.

[115] S. N. Dmitriev, N. V. Aksenov, Y. V. Albin, G. A. Bozhikov, M. L. Chelnokov, V. I. CHepygin, R. Eichler, A. V. Isaev, D. E. Katrasev, V. Y. Lebedev, O. N. Malyshev, O. V. Petrushkin, L. S. Porobanuk, M. A. Ryabinin, A. V. Sabel'nikov, E. A. Sokol, A. V. Svirikhin, G. Y. Starodub, I. Usoltsev, G. K. Vostokin and A. V. Yeremin, "Pioneering experiments on the chemical properties of element 113," *Mend. Comm.,* vol. 24, no. 5, pp. 253-256, 2014.

[116] R. Eichler, N. V. Aksenov, Y. V. Albin, A. V. Belozerov, G. A. Bozhikov, V. I. Chepigin, S. N. Dmitriev, R. Dressler, H. W. Gäggeler, V. A. Gorshikov, R. A. Henderson, A. M. Johnsen, J. M. Kenneally, V. Y. Lebedev, O. N. Malyshev, K. J. Moody, Y. T. Oganessian, O. V. Petrushkin, D. Piguet, A. G. Popeko, P. Rasmussen, A. Serov, D. A. Shaughnessy, S. V. Shishkin, A. V. Shutov, M. A. Stoyer, N. J. Stoyer, A. I. Svirikhin, E. E. Tereshatov, G. K. Vostokin, M. Wegrzecki, P. A. Wilk, D. Wittwer and A. V. Yeremin, "Indication for a volatile element 114," *Radiochim. Acta,* vol. 98, no. 3, pp. 133-139, 2010.

[117] A. Yakushev, J. M. Gates, A. Türler , M. Schädel, C. E. Düllmann, K. Eberhardt, H. G. Essel, J. Even, U. Forsberg, A. Gorshkov, R. Graeger, K. E. Gregorich, W. Hartmann, R. -D. Herzberg, F. P. Heßberger, D. Hild, A. Hübner, E. Jäger, J. Khuyagbaatar , B. Kindler, J. V. Kratz, J. Krier, N. Kurz, B. Lommel, L. J. Niewisch, H. Nitsche, J. P. Omtvedt, E. Parr, Z. Qin, D. Rudolph, J. Runke, B. Schausten, E. Schimpf, A. Semchenkov, J. Steiner, P. Thörle-Pospiech, J. Uusitalo, M. Wegrzecki and N. Wiehl, "Superheavy element flerovium (element 114) is a volatile metal," *Inorg. Chem.,* vol. 53, no. 3, pp. 1624-1629, 2014.

[118] V. Pershina, "Electronic Structures and Chemistry of the Heaviest Elements," in *Relativistic Methods for Chemists*, Netherlands, Springer, 2010, pp. 451-520.

[119] O. L. Keller, J. L. Burnett, T. A. Carlson and C. W. Nestor, "Predicted properties of the super heavy elements. I. Elements 113 and 114, Eka-Thallium and Eka-Lead," *J. Phys. Chem.,* vol. 74, no. 5, pp. 1127-1134, 1970.

[120] E. Eliav, U. Kaldor, Y. Ishikawa and P. Pyykkö, "Element 118: the first rare gas with an electron affinity," *Phys. Rev. Lett.,* vol. 77, no. 27, pp. 5350-5352, 1996.

[121] D. C. Hoffmann, D. M. Lee and V. Pershina, "Transactinide elements and future elements," in *The Chemistry of the Actinide and Transactinide Elements, 3rd ed.*, Dordrecht, Springer, 2006, pp. 1652-1752.

[122] K. S. Pitzer, "Are elements 112, 114, and 118 relatively inert gases?," *J. Chem. Phys.,* vol. 63, no. 2, pp. 1032-1033, 1975.

[123] B. Eichler, "Das Fluchtigkeitsverhalten von Transactiniden im Bereich um Z=114," *Kernenergie,* vol. 19, no. 10, pp. 307-311, 1976.

[124] W. Liu, C. van Wüllen, Y. K. Han, Y. J. Choi and Y. S. Lee, "Spectroscopic constants of Pb and Eka-lead compounds: comparison of different approaches," in *Advances in Quantum Chemistry*, vol. 39, London, Elsevier, Inc., 2001, pp. 325-355.

[125] V. Pershina, J. Anton and B. Fricke, "Intermetallic compounds of the heaviest elements and their homologs: The electronic structure and bonding of MM', where M=Ge, Sn, Pb, and element 114, and M'=Ni, Pd, Pt, Cu, Ag, Au, Sn, Pb, and element 114," *J. Chem. Phys,* vol. 127, no. 13, p. 134310, 2007.

[126] C. Wullen, "Chapter 10 Relativistic density functional calculations on small molecules," in *Theoretical and Computational Chemistry Vol. 14*, Elsavier B. V, , 2004, pp. 598-655.

[127] C. S. Nash and a. et, "Atomic and Molecular Properties of Elements 112, 114 and 118," *J. Phys. Chem. A,* vol. 109, no. 15, pp. 3493-3500, 2005.

[128] K. S. Pitzer and K. Balasubramanian, "Properties of ten electronic states of diatomic lead from relativistic quantum calculations," *J. Phys. Chem.,* vol. 86, no. 16, pp. 3068-3070, 1982.

[129] M. C. Heaven, T. A. Miller and V. E. Bondybey, "Laser spectroscopy of lead molecules produced by laser vaporization," *J. Phys. Chem.,* vol. 87, no. 12, pp. 2072-2075, 1983.

[130] V. Pershina, "Relativistic electronic structure studies on the heaviest elements," *Radiochim. Acta,* vol. 99, no. 7-8, pp. 459-476, 2011.

[131] V. Pershina, J. Anton and T. Jacob, "Theoretical predictions of adsorption behavior of elements 112 and 114 and their homologs Hg and Pb," *J. Chem. Phys.,* vol. 131, no. 8, p. 084713, 2009.

[132] A. Zaitsevskii, C. van Wüllen, E. A. Rykova and A. V. Titov, "Two-component relativistic density functional theory modeling of the adsorption of element 114 (eka-lead) on gold," *Phys. Chem. Chem. Phys.,* vol. 12, no. 16, pp. 4152-4156, 2010.

[133] O. L. Keller, C. W. Nestor and B. Fricke, "Predicted properties of the superheavy elements. III. Element 115, Eka-bismuth," *J. Phys. Chem.,* vol. 78, no. 19, pp. 1945-1949, 1974.

[134] W. Liu, C. van Wüllen, F. Wang and L. Li, "Spectroscopic constants of MH and M2 (M=Tl, E113, Bi, E115): direct comparisons of four- and two-component approaches in the

framework of relativistic density functional theory," *J. Chem. Phys.,* vol. 116, no. 9, pp. 3626-3634, 2002.

[135] N. N. Greenwood and A. Earnshaw, Chemistry of the Elements, New York: Pergamon press, 1984.

[136] J. R. Devoe, "Radiochemistry of cadmium," Committee on Nuclear Science, Univ. of Michigan, 1960.

[137] H. M. Neuman, "Antimony (V) species in hydrochloric acid solution," *J. Amer. Chem. Soc.,* vol. 76, no. 10, pp. 2611-2615, 1954.

[138] A. G. Gaikwad and S. M. Khopkar, "Cation exchange separation of thallium (I) from other elements in mixed solvents," *Anal. Lett.,* vol. 19, no. 1-2, pp. 113-121, 1986.

[139] D. N. Sunderman and C. W. Townley, "Radiochemistry of Indium," Batelle Memorial Inst., Columbus, OH, 1960.

[140] K. A. Kraus, F. Nelson and G. W. Smith, "Anion-exchange studies. IX. Adsorbability of a number of metals in hydrochloric acid solutions," *J. Phys. Chem.,* vol. 58, no. 1, pp. 11-17, 1954.

[141] D. Jentzech and I. Frotscher, "Anwendung von ionenaustauschern in der analytisechen chemie. II. Mitteilung. Adsorptionsverhalten von elementen an einem anionenaustauscher in salzsaurer lösung," *Z. Anal. Chem.,* vol. 144, pp. 17-25, 1955.

[142] L. G. Hepler, J. W. Kury and Z. Z. Hugus, Jr., "The complexing of indium(III) by fluoride ions in aqueous solution: free energies, heats and entropies," *J. Phys. Chem.,* vol. 58, no. 1, pp. 26-28, 1954.

[143] S. Lacroix, "E'tude de quelques complexes et compose speu solubles des ions Al(III), Ga(III), In(III)," *Ann. Chim.,* vol. 4, pp. 5-83, 1949.

[144] L. R. Morss, N. Edelstein, J. Fuger and J. J. Katz, The Chemistry of the Actinides and Transactinide Elements Vol. 3, Netherlands: Springer, 2006.

[145] E. G. Rochow and E. W. Abel, The Chemistry of Germanium, Tin, and Lead, Oxford: Pergamon Press, 1973.

[146] T. M. Seward, "The formation of lead(II) chloride complexes to 300C: A spectrophotometric study," *Geochim. Chosmochim. Acta,* vol. 48, no. 1, pp. 121-134, 1984.

[147] L. I. Guseva and G. S. Tikhomirova, "A 211-Pb generator as a methodical approach to studying the chemistry of element 114 in solutions," *Radiochem.,* vol. 44, no. 2, pp. 167-170, 2002.

[148] L. I. Guseva, "A study of the ion-exchange behavior of Pb in dilute HBr solutions," *Radiochem.,* vol. 49, no. 1, pp. 84-88, 2007.

[149] E. K. Hyde, "Radiochemistry of Thorium," Lawrence Radiation Laboratory, Berkeley, 1959.

[150] L. I. Guseva, G. S. Tikhomirova and N. N. Dogadkin, "An 227-Ac=211-Pb generator for test experiments of solution chemistry of element 114," *J. Radioanal. Nucl. Chem.,* vol. 260, no. 1, pp. 167-172, 2004.

[151] W. E. Nervik, "The Radiochemistry of Tin," Lawrence Radiation Laboratory, Livermore, 1960.

[152] H. Remy, "Chapter 12," in *Treatise on Inorganic Chemistry*, Houston, Elsevier Publishing Co., 1956.

[153] J. S. Johnson and K. A. Kraus, "Hydrolytic behavior of metal ions. IX. Ultracentrifugation of Sn (IV) in acidic chloride and perchlorate solutions," *J. Phys. Chem.,* vol. 63, no. 3, pp. 440-441, 1959.

[154] M. A. Hooper and D. W. James, "Vibrational spectra of some group Vb halides-II," *J. Inorg. Nucl. Chem.,* vol. 35, no. 7, pp. 2335-2342, 1973.

[155] I. Hataye, H. Suganuma, H. Ikegami and T. Kuchiki, "Solvent extraction study on the hydrolysis of tracer cocnentrations of bismuth(III) in perchlorate and nitrate solutions," *Chem. Soc. Jap.,* vol. 55, no. 5, pp. 1475-1479, 1982.

[156] L. I. Guseva, "A study of the ion-exchange behavior of Bi as a homolog of element 115 in dilute hydrochloric acid solutions," *Radiochem.,* vol. 52, no. 3, pp. 270-275, 2010.

[157] N. C. Norman, Chemistry of Arsenic, Antimony and Bismuth, London: Blackie Academic & Professional, 1998.

[158] S. Ahrland and J. -O. Bovin, "The complex formation of antimony(III) in perchloric acid and nitric acid solutions," *Acta Chem. Scand. A,* vol. 28, no. 10, pp. 1089-1100, 1974.

[159] International Union of Pure and Applied Chemistry, Compendium of Chemical Terminology, Gold Book, IUPAC, 2014.

[160] C. J. Pderson, "Macrocyclic polyethers for complexing metals," *Aldrichim. Acta,* vol. 4, no. 1, 1971.

[161] J. -M. Lehn, M. R. Truter, W. Simon, W. E. Morf, P. C. Meier, R. M. Izatt, D. J. Eatough and J. J. Christensen, Alkali Metal Complexes with Organic Ligands, Verlag: Springer, 1973.

[162] D. C. Gutsche, Calixarenes: An Introduction, London: Royal Chemical Society, 2008.

[163] "The Nobel Prize in Chemistry 1987," Nobel Media, 1987. [Online]. Available: http://www.nobelprize.org/nobel_prizes/chemistry/laureates/1987/. [Accessed 20 November 2014].

[164] S. M. Khopkar, Analytical Chemistry of Macrocyclic and Supramolecular Compounds, 2nd ed., New Delhi: Narosa Publishing House Pvt. Ltd., 2008.

[165] C. J. Pederson and H. K. Frensdorff, "Macrocyclic polyethers and their complexes," *Angew Chem. In. Ed.,* vol. 11, no. 1, pp. 16-25, 1972.

[166] K. Z. Hossain, C. T. Camagong and T. Honjo, "Extraction of iridium (IV) from hydrochloric acid media with crown ether in chloroform, and its determination by ICP-AES," *J. Anal. Chem.,* vol. 369, no. 6, pp. 543-545, 2001.

[167] R. M. Izatt, B. L. Haymore and J. j. Christensen, "A stable OH3+–cyclic polyether complex characterised by infrared spectroscopy," *J. Chem. Soc. Chem. Comm.,* no. 23, pp. 1308-1309, 1972.

[168] P. C. Junk, "Structural aspects of oxonium ion/crown ether complexes," *Rev. Anal. Chem.,* vol. 21, no. 1-2, pp. 93-124, 2001.

[169] G. F. Smith and D. W. Margerum, "Diminution of the macrocyclic effect for nickel(II) complexes of thioethers in nonaqueous solvents," *J. Chem. Soc., Chem. Commun.,* no. 19, pp. 807-808, 1975.

[170] J. R. Meadow and E. E. Reid, "Ring compounds and polymers from polymethylene dihalides and dimercaptans," *J. Am. Chem. Soc.,* vol. 56, no. 10, pp. 2177-2180, 1934.

[171] W. Rosen and D. H. Busch, "Nickel(II) complexes of cyclic tetradentate thioethers," *J. Am. Chem. Soc.,* vol. 91, no. 17, pp. 4694-4697, 1969.

[172] E. Sekido, K. Saito, Y. Naganuma and H. Kumazaki, "Liquid-liquid extraction of some class b metal ions with thiacrown ether 1,4,8,11-tetrathiacyclotetradecane," *Anal. Sci.,* vol. 1, no. 4, pp. 363-368, 1985.

[173] T. F. Baumann, J. G. Reynolds and G. A. Fox, "Polymer pendant crown thioethers: synthesis, characterization and Hg(II) extraction studies of polymer-supported thiacrowns ([14]aneS4 and [17]aneS5)," *React. Funct. Polym.,* vol. 44, no. 2, pp. 111-120, 2000.

[174] A. J. Nelson, J. G. Reynolds, T. F. Baumann and G. A. Fox, "X-ray photoemission investigation of binding sites in polymer-bound thiacrowns used for environmental remediation of Hg in aqueous solutions," *Appl. Surf. Sci.,* vol. 167, no. 3-4, pp. 205-215, 2000.

[175] T. F. Baumann, J. G. Reynolds and G. A. Fox, "Polymer pendant crown thioethers: synthesis and Hg(II) extraction studies of a novel thiacrown polymer," *Chem. Commun.,* no. 16, pp. 1637-1638, 1998.

[176] O. Heitzsch, K. Gloe, H. Stephan and E. Weber, "Liquid-liquid extraction of Ag(I), HG(II), Au(III) and Pd(II) by some oligothia macrocyclic ligands incorporating aromatic and heteroaromatic subunits," *Solvent Extr. Ion Exch,* vol. 12, no. 3, pp. 475-496, 1994.

[177] H. A. Jenkins, S. J. Loeb and A. M. i. Riera, "Tetranuclear Ag(I) complexes with an octagonal Ag4S4 core: building large structures from small macrocycles," *Inorg. Chim. Acta,* vol. 246, no. 1-2, pp. 207-215, 1996.

[178] T. J. Robilotto, "Synthesis and characterization of (phosphine)- and (N-heterocyclic carbene)gold(I) halides, azides, alkynyls, triazoles, and dendrimers and the synthesis and characterization of gold(I) thiacrown macrocycles," Department of Chemistry, Case Western Reserve University, Cleveland, OH, 2011.

[179] R. E. DeSimone and M. D. Glick, "Structures of the macrocyclic polythiaether 1,4,8,11-tetrathiacyclotetradecane and implications for transition-metal chemistry," *J. Am. Chem. Soc.,* vol. 98, no. 3, pp. 762-767, 1976.

[180] W. N. Setzer, Y. Tang, G. J. Grant and D. G. VanDerveer, "Synthesis and complexation studies of mesocyclic and macrocyclic polythioethers. 9. Crystal and molecular structure of (1.4.7,10,13-pentathiacyclopentadecane)cadmium(II) perchlorate hydrate: a secen-coordinate cadmium," *Inorg. Chem.,* vol. 31, no. 6, pp. 1116-1118, 1992.

[181] E. R. Dockal, L. L. Diaddario, M. D. Glick and D. B. Rorabacher, "Structure of 1,4,8,11-tetrathiacyclotetradecanecopper(I) perchlorate: comparative geometries of analogous copper(I) and copper(II) complexes," *J. Am. Chem. Soc.,* vol. 99, no. 13, pp. 4530-4532, 1977.

[182] L. L. Diaddario, E. R. Dockal, M. D. Glick, L. A. Ochrymowycz and D. B. Rorabacher, "Structural changes accompanying electron transfer in copper(II)/copper(I) complexes

involving related open-chain cyclic tetrathia ether ligands," *Inorg. Chem.,* vol. 24, no. 3, pp. 356-363, 1985.

[183] P. J. Blower, J. A. Clarkson, S. C. Rawle, J. R. Hartman, R. E. Wolf, R. Yagbasan, S. G. Bott and S. R. Cooper, "Crown thioether chemistry. The silver(I) complexes of trithia-9-crown-3, trithia-12-crown-3, and hexathia-18-crown-6," *Inorg. Chem.,* vol. 28, no. 21, pp. 4040-4046, 1989.

[184] A. J. Blake , R. O. Gould, G. Reid and M. Schröder , "[Ag2([15]aneS5)2]2+: a binuclear silver(I) complex incorporating asymmetrically bridging thioether donors. ([15]aneS5= 1,4,7,10,13-pentathiacyclopentadecane)," *J. Chem. Soc. Chem. Comm.,* no. 14, pp. 974-976, 1990.

[185] F. G. Helfferich, Ion Exchange, New York: McGraw-Hill, 1962.

[186] DOWEX, "Fine Mesh Spherical Ion Exchange Resins Form No. 117-01509-904," Dow Chemical Co., Midland MI, 2011.

[187] R. Shabana, "Effect of resin cross-linking and temperature on anion exchange separation of gallium and indium," *J. Radioanal Nucl. Chem.,* vol. 41, no. 1-2, pp. 53-64, 1977.

[188] W. Rieman and H. F. Walton, Ion Exchange in Analytical Chemistry (Volume 38 of the International Series of Monographs in Analytical Chemistry), Oxford: Pergamon Press, 1970.

[189] J. S. Fritz and D. T. Gjerde, Ion Chromatography, Weinheim Germany: Wiley-VCH, 2009.

[190] J. Rydberg, M. Cox, C. Musikas and G. R. Choppin, Solvent Extraction Principles and Practice, 2nd ed., New York, NY: Marcel Dekker, Inc., 2004.

[191] T. Braun and G. Ghersini, Extraction Chromatography, vol. 2, New York: Elsevier Publishing Company Inc., 1975.

[192] E. P. Horwitz, "Extraction Chromatography of actinides and selected fission products: principles and achievement of selectivity," Eichrom Technologies, 2013. [Online]. Available: http://www.eichrom.com/products/extraction.aspx. [Accessed 02 12 2014].

[193] E. P. Horwitz and a. et, "A novel strontium-selective extraction chromatographic resin," *Sol. Extr. Ion Exc.,* vol. 10, no. 2, 1992.

[194] E. P. Horwitz and a. et, "Extraction chromatography verses solvent extraction: how similar are they?," *Separ. Sci. Tech.,* vol. 41, pp. 2163-2182, 2006.

[195] E. P. Horwitz and C. A. A. Bloomquist, "The preparation, performance and factors affecting band spreading of high efficiency extraction chromatographic columns for actinide separations," *J. Inorg. Nucl. Chem,* vol. 34, no. 12, pp. 3851-3871, 1972.

[196] E. P. Horwitz and C. A. A. Bloomquist, "High speed-high efficiency separation of the transplutonium elements by extraction chromatography," *J. Inorg. Nucl. Chem.,* vol. 35, no. 1, pp. 271-284, 1973.

[197] E. K. Elmaghraby, S. A. Said and F. I. Asfour, "Investigation of the proton induced reactions on tin at low energies," *Appl. Radiat. Isot.,* vol. 67, no. 1, pp. 147-151, 2009.

[198] G. Chodil, R. C. Jopson, H. Mark, C. D. Swift, R. G. Thomas and M. K. Yates, "(p,n) and (p,2n) cross sections on nine elements between 7.0 and 15.0 MeV," *Nucl. Phys. A,* vol. 93, no. 3, pp. 648-672, 1967.

[199] M. M. Musthafa, M. K. Sharma, B. P. Singh and R. Prasad, "Measurement and analysis of cross sections for (P,N) reaction in V-51 and In-113," *Appl. Radiat. Isot.,* vol. 62, no. 3, pp. 419-428, 2005.

[200] The DOW Chemical Company, Dowex: ION Exchange, Chicago: The Lakeside Press, 1958.

[201] E. P. Horwitx, M. L. Dietz, S. Rhoads, C. Felinto, N. H. Gale and J. Houghton, "A lead-selective extraction chromatographic resin and its application to the isolation of lead from geological samples," *Anal. Chim. Acta,* vol. 292, no. 3, pp. 263-273, 1994.

[202] E. P. Horwitz, D. R. McAlister, A. H. Bond and R. E. Barrans, "Novel extraction chromatographic resins based on tetraalkyldiglycolamides: characterization and potential applications," *Solvent Extr. Ion Exc.,* vol. 26, no. 3, pp. 319-344, 2005.

[203] E. P. Horwitz, R. Chiarizia, M. L. Dietz and H. Diamond, "Separation and preconcentration of actinides from acidic media by extraction chromatography," *Anal. Chim. Acta,* vol. 281, no. 2, pp. 361-372, 1993.

[204] J. D. Despotopulos, J. M. Gostic, M. E. Bennett, N. Gharibyan, R. A. Henderson, K. J. Moody, R. Sudowe and D. A. Shaughnessy, "Characterization of group 5 dubnium homologs on diglycolomide extraction chromatography resins from nitric and hydrofluoric acid matrices," *J. Radioanal. Nucl. Chem.,* vol. 303, no. 1, pp. 485-494, 2015.

[205] A. H. Thakkar, "A rapid sequential separation of actinides using Eichrom's extraction chromatographic material," *J. Radioanal. Nucl. Chem,* vol. 252, no. 2, pp. 215-218, 2002.

[206] E. P. Horwitz, C. A. A. Bloomquist, L. J. Sauro and D. J. Henderson, "The liquid-liquid extraction of certain tripositive transplutonium ions from salted nitrate solutions with a

tertiary and quaternary amine," *J. Inoreg. Nucl. Chem.,* vol. 28, no. 10, pp. 2313-2324, 1966.

[207] G. F. Knoll, Radiation Detection and Measurement, Hoboken: John Wiley & Sons, Inc., 2010.

[208] S. Y. F. Chu, L. P. Ekström and R. B. Firestone, "WWW Table of Radioactive isotopes," Lawrence Berkeley National Laboratory, 28 February 1999. [Online]. Available: http://nucleardata.nuclear.lu.se/nucleardata/toi/. [Accessed 23 January 2014].

[209] H. R. Allcock, Inorganic Syntheses, Volume 25, New York: John Wiley & Sons, 2009.

[210] International Atomic Energy Agency, "Cyclotron Produced Radionuclides: Principles and Practice," International Atomic Energy Agency, Vienna, 2008.

[211] W. M. Gibson, "The Radiochemistry of Lead," Bell Telephone Laboratories, Murray Hill, NJ, 1961.

[212] N. Ramamoorthy, D. V. S. Narasimhan and R. S. Mani, "Studies on the Preparation of 113Sn-113mIn Generators," *Isotopenpraxis Isotopes in Environmental and Health Studies,* vol. 11, no. 7, pp. 246-249, 1975.

[213] H. Lundqvist, S. Scott-Robson, L. Einarsson and P. Malmborg, "110Sn/110In--A New Generator System for Positron Emission Tomography," *Appl. Radiat. Isot,* vol. 42, no. 5, pp. 447-450, 1991.

[214] D. Nayak and S. Lahiri, "Production of tracer packet of heavy and toxic elements," *J. Radioanal. Nucl Chem.,* vol. 254, no. 3, pp. 619-623, 2002.

[215] H. Thommen, H. R. Stohler, J. Wursch and J. R. Frey, "Chemotherapy of Experimental Schistosomiasis Mansoni: Distribution of Antimony-124 in mice and hamsters after a single dose of sodium antimony dimercaptosuccinate and antimony dimercaptosuccinic acid," *Annals of tropical medicine and parasitology,* vol. 58, no. 4, pp. 439-, 1964.

[216] E. P. Horwitz, M. L. Dietz, R. Chiarizia, H. Diamond, S. L. Maxwell III and M. R. Nelson, "Separation and preconcentration of actinides by extraction chromatography using a supported liquid anion exchanger: Application to the characterization of high-level nuclear waste solutions," *Anal. Chim. Acta,* vol. 310, no. 1, pp. 63-78, 1995.

[217] J. P. Faris and R. F. Buchanan, "Anion exchange characteristics of elements in nitric acid medium," *Anal. Chem.,* vol. 36, no. 6, pp. 1157-1158, 1964.

[218] F. Nelson, T. Murase and K. A. Kraus, "Ion Exchange Procedures I. Cation Exchange in Concentrated HCl and HClO4 Solutions," *J. Chrom. A,* vol. 13, pp. 503-535, 1963.

[219] K. A. Kraus, D. C. Michelson and F. Nelson, "Adsorption of Negatively Charged Complexes by Cation Exchangers," *J. Amer. Chem. Soc.,* vol. 81, no. 13, pp. 3204-3207, 1958.

[220] W. J. Maek, "The Radiochemistry of Antimony," Phillips Petroleum Company Atomic Energy Division, Idaho Falls, ID, 1961.

[221] K. A. Kraus and F. Nelson, "Distribution coefficients for adsorption of elements onto Dowex-A-1 anion exchange resin from hydrochloric acid," in *First U.N. Conf. on Peaceful Uses of At. Energy*, vol. 7, pp. 113-125, New York, 1955.

[222] J. P. Faris, "Adsorption of the elements from hydrofluoric acid by anion exchange," *Anal. Chem.,* vol. 32, no. 4, pp. 520-522, 1960.

[223] F. W. E. Strelow, "An ion exchange selectivity scale of cations based on equilibrium distribution coefficients," *Anal. Chem.,* vol. 32, no. 9, pp. 1185-1188, 1960.

[224] J. Roesmer, "The Radiochemistry of Mercury," Westinghouse Astronuclear Laboratory, Pittsburgh, PA, 1970.

[225] M. Seth, K. Faegri and P. Schwerdtfeger, "The stability of the oxidation state +4 in group 14 compounds from carbon to element 114," *Angew. Chem. Int. Ed.,* vol. 37, no. 18, pp. 2493-2496, 1998.

[226] T. Francis, "Liquid-liquid extraction and separation of mercury from industrial wastes," Ion-Specific Separation Science and Technology Group, Regional Research Laboratory (CSIR), India, 2002.

[227] N. K. Kulrestha, A. K. Dey and S. Ghosh, "Untersuchungen über hydratisiertes zinnoxyd," *Kolloid-Z,* vol. 141, no. 2, pp. 106-109, 1955.

[228] C. J. Pederson, "Crystalline salt complexes of macrocyclic polyethers," *J. Am. Chem. Soc.,* vol. 92, no. 2, pp. 386-391, 1970.

[229] C. J. Pederson, "Cyclic polyethers and their complexes with metal salts," *J. Am. Chem. Soc.,* vol. 89, no. 26, pp. 7017-7036, 1967.

[230] A. J. Blake and M. Schröder, "Chemistry of thoether macrocyclic complexes," *Adv. Inorg. Chem.,* vol. 35, pp. 1-80, 1990.

[231] R. G. Vibhute and S. M. Khopkar, "Solvent extraction of antimony(III) with 18-crown-6 from iodide media," *Talanta,* vol. 36, no. 9, pp. 957-959, 1989.

[232] K. S. Bhatki, "Radiochemistry of Bismuth," Teta Institute of Fundamental Research, Bombay, India, 1977.

[233] M. N. Gandhi and S. M. Khopkar, "Atomic absorption spectrophotometric analysis of lead(II) by ion pair extraction with cryptand 222B and eosin," *Ind. J. Chem.,* vol. 30A, p. 706, 1991.

[234] G. G. Talanova and H. -S. Hwang, "Calix[4]arenes with a novel proton-ionizable group: synthesis and metal ion separations," *J. Chem. Soc. Chem. Comm.,* no. 3, pp. 419-420, 1998.

[235] G. G. Talanova, V. S. Talanov and R. A. Bartsch, "Calix[4]arenes with hard donor groups as efficient soft cation extractants. Remarkable extraction selectivity of calix[4]arene N-(X)sulfonylcarboxamides for Hg(II)," *J. Chem. Soc. Chem. Comm.,* no. 13, pp. 1329-1330, 1998.

CURRICULUM VITAE

John D. Despotopulos

Graduate Student in the Radiochemistry Ph. D. Program at the University of Nevada, Las Vegas
Livermore Graduate Scholar
7000 East Ave, L-231
Livermore CA, 94551
Phone: (925) 432-7146 (work) / (541) 390-8667 (cell)
Email: despotopulos1@llnl.gov

RESEARCH HIGHLIGHTS

- Rapid separations of short-lived radionuclides and applications toward transactinide chemistry
- Production and isolation of carrier-free radionuclides
- Synthesis of macrocyclic organic molecules for use in radiochemical separations
- Preparation of electrodeposited osmium targets for experiments at the Omega Laser Facility
- Study of $^{19}F(\alpha,n)^{22}Na$ reaction rates from various PuF_x solids

LIVERMORE GRADUATE SCHOLAR

Lawrence Livermore National laboratory **February 2013 – Present**

Graduate student in the Radiochemistry Ph. D. Program at the University of Nevada, Las Vegas
Experimental Nuclear and Radiochemistry Group, Lawrence Livermore National Laboratory
Nuclear and Chemical Sciences Division
Physical and Life Sciences Directorate
Technical Advisor/Mentor: Dr. Dawn A. Shaughnessy
Ph. D. Advisor: Dr. Ralf Sudowe
Security Clearance: DOE

EDUCATION

University of Nevada Las Vegas, Las Vegas, NV **September 2010 — Present**

- Ph. D., Radiochemistry, expected May 2015
- Dissertation: "Investigation of flerovium and element 115 homologs with macrocyclic extractants"
- Advisor: Prof. Ralf Sudowe, Dr. Dawn A. Shaughnessy

University of Oregon, Eugene, OR **September 2006 – June 2010**

- B. S. in Chemistry with minor in Physics

- Magna Cum Laude

RESEARCH EXPERIENCE

Lawrence Livermore National Laboratory **July 2011 – Present**

Livermore Graduate Scholar February 2013 – Present

- Ph.D. Graduate Student:

    - Developed chemical systems for investigation of the chemistry of flerovium and element 115.
    - Developed rapid separation methods for the homologs and pseudo-homologs of flerovium (Pb, Sn and Hg) and element 115 (Bi and Sb) using macrocyclic extractants.
    - Investigated various macrocycles: crown ethers, thiacrowns, cryptands and calixarenes for their suitability to flerovium and element 115 chemistry.
    - Characterized Eichrom's Pb extraction chromatography resin for the homologs and pseudo-homologs of flerovium.
    - Established production methods for carrier-free radionuclides of the homologs and pseudo-homologs of flerovium and element 115 via proton reactions at the LLNL Center for Accelerator Mass Spectrometry (CAMS).
    - Established separation procedures for isolating carrier-free radionuclides from CAMS irradiated metal foils.
    - Developed a Pb generator for continual production of carrier-free ^{212}Pb through an elution of a ^{232}U loaded cation-exchange column.

- Independent Studies:

    - Developed method for dissolving enriched osmium metal samples and preparing electroplated osmium targets using titanium as the backing, for experiments at the Omega Laser Facility.
    - Participated in beam-line experiments through the TASCA collaboration that included the commissioning of the ALBEGA detector, chemical studies of seaborgium in the gas-phase and chemical studies of flerovium in the gas-phase.
    - Participated in Solid Radiochemistry nuclear diagnostic at the NIF.
    - Participated in first ever fission yield measurements at the NIF: 14 MeV neutron induced fission of ^{238}U.
    - Participated in experiments to study the fission yields from proton induced fission of ^{238}U at CAMS.
    - Characterized Eichrom's DGA resin for the dubnium homologs from nitric and hydrofluoric acid matrices.

Nuclear Forensic Summer Internship Summer 2012

- Continued development of suitable chemical systems to study the solution chemistry of elements with Z ≥ 114 (see Ph. D. Graduate Work above).

Student Academic Cooperation Program July 2011 – May 2012

- Investigated chemical systems for dubnium homologs using nitric and hydrofluoric acid matrices and Eichrom's DGA resin.
- Continued Ph. D. research (see Ph. D. Graduate Work above).

University of Nevada Las Vegas **September 2010 – Present**

Ph. D. Graduate Student September 2010 – Present

- See Ph.D. Graduate Student under Livermore Graduate Scholar above.
- Synthesis of hexathia-18-crown-6, a non-commercially available sulfur analog of 18-crown-6, for use in the study of flerovium and element 115.

Independent Studies June 2011 – Present

- Purified plutonium from americium, for preparation of Pu^{III} and Pu^{IV} solutions.
- Synthesized PuF_3, PuF_4, and $Pu(OH)_4 + ZrF_4$ solids for characterization of differences in $^{19}F(\alpha,n)^{22}Na$ reactions by HPGe gamma spectroscopy.
- Studied the homologs of rutherfordium (Zr and Hf) with Eichrom's Pb and Sr resin.

Lawrence Berkeley National laboratory , SULI Internship **Summer 2009**

- Studied ^{252}Cf spontaneous fission at the Berkeley Gas-filled Separator, to explore exotic neutron rich r-process nuclei.
- ^{252}Cf spontaneous fission decay chains were analyzed by new data analysis code based on ROOT.
- Data analysis code allowed for automatic calibration of the spectra and in-depth analysis of the decay chains.

HONORS, AWARDS AND FELLOWSHIPS

- Livermore Graduate Scholar, Lawrence Livermore National Laboratory, February 2013
- Certificate of APSORC13 Student Oral Presentation, JNRS, Japan, September 2013
- Nuclear Forensics Summer internship, Lawrence Livermore National Laboratory, June 2012
- Member Phi Beta Kappa Honor Society, University of Oregon, June 2010
- Invited to join Golden Key International Honour Society, December 2009
- SULI Internship, Lawrence Berkeley National Laboratory, June 2009

- Nuclear Chemistry Summer School, San Jose State University, June 2008
- Clarice Krieg Scholarship, University of Oregon, June 2008
- Invited to join National Honor Society, June 2006
- Valedictorian Ben Senior High School, June 2006

PUBLICATIONS

1. Despotopulos, J. D., Kmak, K. N., Kerlin, W. M., Gharibyan, N., Henderson, R. A., Moody, K. J., Shaughnessy, D. A., Sudowe, R. "Characterization of flerovium homologs with thiacrown ethers." *J. Radioanal. Nucl. Chem.* **2015**. (In preparation)
2. Despotopulos, J. D., Kmak, K. N., Gharibyan, N., Henderson, R. A., Moody, K. J., Shaughnessy, D. A., Sudowe, R. "Separations of lead and mercury by crown ether based extraction chromatography." *J. Radioanal. Nucl. Chem.* **2015.** (To be submitted)
3. Despotopulos, J. D., Kmak, K. N., Gharibyan, N., Henderson, R. A., Moody, K. J., Shaughnessy, D. A., Sudowe, R. "Production of carrier-free radionuclides at the Lawrence Livermore National Laboratory Center for Accelerator Mass Spectrometry." *J. Radioanal. Nucl. Chem.* **2015**. (Submitted)
4. Despotopulos, J. D., Gharibyan, N., Henderson, R. A., Moody, K. J., Shaughnessy, D. A., Sudowe, R. "Characterization of flerovium homologs on crown ether based extraction chromatography resins." *J. Radioanal. Nucl. Chem.* **2015**. (Submitted)
5. Grant, P. M., Moody, K. J., Gharibyan, N., Despotopulos, J. D., Shaughnessy, D. A. "Anomalous radiochemical recovery of post-detonation gold residues at the National Ignition Facility." *J. Radioanal. Nucl. Chem.* 303(3), 1851-1856, **2014.** DOI: 10.1007/s10967-014-3626-8
6. Gharbiyan, N., Moody, K. J., Brown, T. A., Despotopulos, J. D., Tumey, S. J., Shaughnessy, D. A. "Cumulative fission yield measurements for 10-15 MeV proton induced fission of ^{238}U." *J. Radioanal. Nucl. Chem.* **2014**. (In preparation)
7. Despotopulos, J. D., Gostic, J. M., Bennett, M. E., Gharibyan, N., Henderson, R. A., Moody, K. J., Sudowe, R., Shaughnessy, D. A. "Characterization of Group 5 dubnium homologs on diglycolomide extraction chromatography resins from nitric and hydrofluoric acid matrices." *J. Radioanal. Nucl. Chem.* 303(1), 485-494, **2014**. DOI: 10.1007/s10967-014-3398-1
8. Gharibyan, N., Moody, K. J., Despotopulos, J. D., Grant, P. M., Shaughnessy, D. A. "First fission yield measurements at the National Ignition Facility: 14 MeV neutron fission of ^{238}U." *J. Radioanal. Nucl. Chem.* 303(2), 1335-1338, **2014.** DOI: 10.1007/s10967-014-3474-6
9. Shaughnessy, D. A., Moody, K. J., Gharibyan, N., Grant, P. M.m Gostin, J. M., Torretto, P. C., Wooddy, P. T., Bandong, B. B., Despotopulos, J. D., Cerjan, D. J., Hagmann, C. A., Caggiano, J. A., Bernstein, L. A., Schneider, D. H., Henry, E. A., Fortner, R. J. "Radiochemical determination of Inertial Confinement Fusion capsule compression at the National ignition Facility." *Rev. Sci. Instrum.* 85(6), 063508, **2014.** DOI: 10.1063/1.4883186

REPORTS AND OTHERS

1. Despotopulos, J. D. "Investigation of flerovium and element 115 homologs with macrocyclic extractants." *Ph. D. Dissertation*. **2015.** (To be submitted)
2. Despotopulos, J. D., Sudowe, R., "Characterization of Group V dubnium homologs on DGA extraction chromatography resin from nitric and hydrofluoric acid matrices." *LLNL Tech. Rep.* **2012.** LLNL-SR-531417

PRESENTATIONS AND POSTERS

Presentations

1. Despotopulos, J. D., Kmak, K. N., Gharibyan, N., Henderson, R. A., Kerlin, W., Moody, K. J., Shaughnessy, D. A., Sudowe, R. "Studies of flerovium homologs with macrocyclic extractants." TASCA14, Darmstadt, Germany. **October 2015**.
2. Despotopulos, J. D., Gharibyan, N., Henderson, R. A., Kerlin, W., Moody, K. J., Tereshatov, E., Shaughnessy, D. A., Sudowe, R. "Studies of flerovium and element 115 homologs with macrocyclic extractants." APSORC13, Kanazawa, Japan. **September 2013**.
3. Despotopulos, J. D., Gharibyan, N., Henderson, R. A., Kerlin, W., Moody, K. J., Tereshatov, E., Shaughnessy, D. A., Sudowe, R. "Studies of flerovium and element 115 homologs with macrocycles" CHE8, Takayama, Japan. **September 2013.**
4. Despotopulos, J. D., Rofles, J., Shaughnessy, D. A., Sudowe, R. "Extraction chromatographic studies of element 114 and 115 homologs." American Nuclear Society Student Conference, Las Vegas, NV. **April 2012.**
5. Despotopulos, J. D., Shaughnessy, D. A., Sudowe, R. "Extraction chromatographic studies of element 114 and 115 homologs." American Chemical Society Fall 2011 Meeting, Denver, CO. **August 2011.**

Posters

1. Despotopulos, J., D., Kmak, K. N., Ghariyban, N., Henderson, R. A., Moody, K. J., Shaughnessy, D. A., Sudowe, R. "Studies of flerovium and element 115 homologs with macrocyclic extractants." LLNL Posdoctoral Poster Symposium, Livermore, CA. **June 2014.**
2. Despotopulos, J., D., Ghariyban, N., Henderson, R. A., Moody, K. J., Tereshatov, E., Shaughnessy, D. A., Sudowe, R. "Studies of flerovium homologs with macrocyclic extractants." LLNL Posdoctoral Poster Symposium, Livermore, CA. **June 2013.**
3. Despotopulos, J., D., Gostic, J. M., Ghariyban, N., Henderson, R. A., Moody, K. J., Tereshatov, E., Shaughnessy, D. A., Sudowe, R. "Extraction chromatographic studies of flerovium and element 115 homologs." LLNL Summer Student Poster Symposium, Livermore, CA. **August 2012**.
4. Despotopulos, J. D., Rolfes, J., Shaughnessy, D. A., Sudowe, R. "Extraction chromatographic studies of element 114 and 115 homologs.´Symposium Honoring the 100th Birthday of Glenn T. Seaborg, Berkeley, CA. **April 2012.**
5. Despotopulos, J., D., Gostic, J. M., Henderson, R. A., Moody, K. J., Tereshatov, E., Shaughnessy, D. A., Sudowe, R. "Extraction chromatographic studies of element 114 and 115 homologs." LLNL Summer Student Poster Symposium, Livermore, CA. **August 2011**.

OTHER INFORMATION

Professional Affiliations

- American Chemical Society, Nuclear Chemistry Division, 2008-2011
- American Nuclear Society, 2010-2011

Computer Skills and Programming

- Basic: JCHESS, KaleidaGraph
- Intermediate: C++, ROOT, MATLAB, HTML, Origin
- Advanced: MS Office, MAESTRO, Genie, System building

Other Contributions

- Instructor-Nuclear Science Merit Badge Workshop BSA, Las Vegas, NV, 2011-2012
- Student-ACS Nuclear Summer School, San Jose State University, San Jose, CA, 2008

REFERENCES

- **Dr. Ralf Sudowe**
  Radiochemistry Ph. D. program director at University of Nevada Las Vegas, Las Vegas, Nevada
  Phone: (702) 895-5964, Email: ralf.sudowe@unlv.edu
- **Dr. Dawn A. Shaughnessy**
  Group leader Experimental and Nuclear Radiochemistry Group, Lawrence Livermore National Laboratory, Livermore, California
  Phone: (925) 422-9574, Email: shaughnessy2@llnl.gov
- **Dr. Kenton J. Moody**
  Experimental and Nuclear Radiochemistry Group, Lawrence Livermore National Laboratory, Livermore, California
  Phone: (925) 432-4585, Email: moody3@llnl.gov
- **Additional references upon request**